DEVELOPMENT OF AN INTELLIGENT ELECTRONIC LOAD CONTROLLER FOR STAND-ALONE MICRO-HYDROPOWER SYSTEMS

By

GUILLIAM JOHANNES NEL

201106789

DISSERTATION FOR THE DEGREE:

MAGISTER OF PHILOSOPHIAE ELECTRICAL ENGINEERING

In

THE DEPARTMENT OF ELECTRICAL AND ELECTRONIC ENGINEERING

FACULTY OF ENGINEERING AND THE BUILT ENVIRONMENT

Supervisor:

Dr W Doorsamy

2019

DECLARATION

I, **Guilliam Johannes Nel** declare that this dissertation is a presentation of my own, unaided work, except where specifically acknowledged. It is submitted for the degree of Magister of Philosophiae to the Faculty of Engineering and the Built Environment at the University of Johannesburg. It has not been submitted before for any degree or examination at this or any other University.

Signed on this _____ day of _____ 2019

_____

Guilliam Johannes Nel

ABSTRACT

People living in rural and remote areas of Sub-Saharan Africa generally lack access to electricity due to their geographical location and the costs associated with connecting these areas to the national electrical grid. A viable technology to supply electricity to some of these areas are stand-alone micro-hydropower systems which harnesses energy from flowing water. Self-excited induction generators (SEIGs) are commonly used for the generation of electricity in stand-alone micro-hydropower systems. The electricity supplied by a SEIG to the demand side i.e. the load needs to be maintained stable under various consumer load conditions. This can be accomplished with the use of an Electronic Load Controller (ELC). This dissertation presents the design and development of an intelligent ELC that can maintain a stable voltage on the demand side of a 3-phase SEIG supplying varying single-phase consumer loads. The intelligent ELC consist of an uncontrolled bridge rectifier, filtering capacitor, chopper switch (IGBT), voltage sensor, current sensor, optocoupler, Arduino microcontrollers and a ballast load or storage, depending on site-specific requirements and economic viability. A fuzzy logic control method is implemented to maintain stable and reliable voltage supply. Hardware-in-the-loop simulations were carried out under various consumer load conditions using MATLAB/SIMULINK to analyse and test the efficiency of the system in real-time. Laboratory experiments were carried out and it was found that the Intelligent Electronic Load Controller was able to respond quickly and efficiently to changes in the consumer load to maintain the voltage on the demand side of the three-phase self-excited induction generator very stable and close to the set point voltage value. The intelligent ELC will contribute towards providing reliable and cost-effective means of enhancing the proliferation of micro-hydropower particularly in rural and remote applications in Sub-Saharan Africa.

DEDICATION

To my mother,

Henna Nel

ACKNOWLEDGEMENTS

I wish to express my most sincere gratitude and appreciation to the following people who made this Dissertation possible:

- God Almighty for the blessings He has bestowed upon me and for giving me the strength and wisdom throughout my research.

- My dad and sister for all their love, support and encouragement.

- Dr. Wesley Doorsamy for all his patience, guidance and support throughout my research.

- My friends and family for all their support and motivation.

- UJ staff members at the Department of Electrical and Electronic Engineering.

TABLE OF CONTENTS

LIST OF ABBREVIATIONS & SYMBOLS

- α Firing Angle
- a Maximum Value 1
- b Maximum Value 2
- B_s Stator Magnetic Field
- C_1 Capacitor 1
- C_2 Capacitor 2
- E_1 Induced Voltage
- Δe_k Change in Error
- e_k Error
- e_{k-1} Previous Error
- f_r Rotor Frequency
- $hgt(\underset{\sim}{C}_k)$ Largest Height in the Union
- I_{AC} AC Current
- I_{DC} DC Current
- I_{Line} Line Current
- I_m Magnetizing Current
- inf Infimum (Greatest lower bound)
- I_{Peak} AC Peak Current
- I_{Phase} Phase Current
- I_R Rotor Current
- I_S Stator Current
- k Fuzzy Set Number
- n Number of Fuzzy Sets
- NB Negative Big
- NM Negative Medium
- n_r Rotor Rotation Speed
- n_s Synchronous Rotation Speed
- NS Negative Small
- NVS Negative Very Small
- O Output

- P_B Ballast Load Power
- PB Positive Big
- P_C Consumer Load Power
- P_G Generated Power
- P_{in} Input Power
- P_{Iron} Iron Losses
- PM Positive Medium
- P_{Phase} Power per Phase
- PS Positive Small
- PVS Positive Very Small
- Q_{Phase} Reactive Power per Phase
- Q_{Total} Total Reactive Power
- R_1 Resistor 1
- R_2 Resistor 2
- R_B Ballast Load Resistance
- R_C Core Loss Resistance
- R_F Ripple Factor
- R_{Iron} Stator Core Resistance
- Rj Resistance
- R_R Rotor Resistance
- R_S Stator Resistance
- s Slip
- SEIG Self-Excited Induction Generator
- sup Supremum (Least Upper Bound)
- $\mu_{\tilde{C}}$ Membership Function
- $\mu_{\tilde{C}_k}$ Membership Function for the k-th Fuzzy Set
- $\mu_{\tilde{C}_m}$ Membership Function for the Convex Subregion that has the Largest Area Making Up $\tilde{C}_k$
- V_{DC} DC Voltage
- $V_{DC(10\%)}$ 10% DC Overvoltage
- V_L AC Input Voltage

- V_{Line} Line Voltage
- V_{MS} Actual Voltage Measured
- V_O Output Voltage
- V_{Phase} Phase Voltage
- V_S Supply Voltage
- V_{SP} Voltage Set Point
- x Input Variable
- X_1 Stator Reactance
- X_2 Rotor Reactance
- X_m Magnetizing Reactance
- y Output Variable
- z Element
- Z Universe of Discourse
- Z Zero
- z^* Defuzzified Value
- $\bar{z}$ Centroid of Each Symmetric Membership Function
- $\bar{z}$ Distance to the Centroid of Each of the Membership Functions
- Z_{Block} Impedance

LIST OF TABLES

LIST OF FIGURES

CHAPTER 1
INTRODUCTION

1.1. INTRODUCTION

This chapter presents an introduction and overview of the complete dissertation.

1.2. BACKGROUND INFORMATION

Electricity is an important factor in the economic development of a country. One of the major challenges in developing countries, especially in Sub-Saharan Africa, is the reliable supply of electricity to the people. According to the International Energy Agency an estimated 625 million people in Sub-Saharan Africa do not have access to electricity [1]. People living in rural and remote areas of Sub-Saharan Africa generally lack access to electricity due to their geographical location and the costs associated with connecting these areas to the national electrical grid. A viable technology to supply electricity to some of these areas are stand-alone micro-hydropower systems which harnesses energy from flowing water. Self-excited induction generators (SEIGs) are commonly used for the generation of electricity in stand-alone micro-hydropower systems due to its low cost, high reliability, less maintenance required, robust construction, no separate dc source required, brushless rotor operation and excellent resilience against overloads and short circuits [2]. The electricity supplied by a SEIG to the demand side i.e. the load needs to be maintained stable under various consumer load conditions. This can be accomplished with the use of an Electronic Load Controller (ELC). An ELC diverts surplus power to a ballast load or storage to keep the power generated by a SEIG constant. This system needs to contribute towards providing reliable and cost-effective means of enhancing the proliferation of micro-hydropower particularly in rural and remote applications in Sub-Saharan Africa.

1.3. PROBLEM STATEMENT

People living in rural and remote areas of Sub-Saharan Africa generally lack access to electricity due to their geographical location and the costs associated with connecting these areas to the national electrical grid. A viable technology to supply electricity to some of these areas are stand-alone micro-hydropower systems with the use of a self-excited induction generator. The electricity supplied by a self-excited induction generator to the demand side i.e. the load needs to be maintained stable under various consumer load conditions. This is accomplished with the use of an Electronic Load Controller. There is a great need for the design and development of a simple, reliable and cost-effective Intelligent Electronic Load Controller that will contribute towards providing reliable and cost-effective means of enhancing the proliferation of micro-hydropower particularly in rural and remote applications in Sub-Saharan Africa.

1.4. RESEARCH OBJECTIVES

The main objectives of this research are summarised as follow:

- Design and develop a simple, reliable and cost-effective Intelligent Electronic Load Controller for stand-alone micro-hydropower systems using a fuzzy logic control method.
- To maintain a stable voltage on the demand side of the three-phase self-excited induction generator, while supplying varying single-phase consumer loads.
- Reduce costs by using a low voltage three-phase self-excited induction generator system to supply single-phase consumer loads.

1.5. DISSERTATION OVERVIEW

This dissertation comprises of six chapters which are briefly described below:

- **Chapter 1 – Introduction:** Presents an introduction and overview of the complete dissertation.

- **Chapter 2 – Theoretical Background:** Presents an overview of hydropower systems together with some of its components and an in-depth discussion on the background of Electronic Load Control and fuzzy logic.

- **Chapter 3 – Self-Excited Induction Generator:** Presents the design and development of both the simulation model and experimental configuration of a self-excited induction generator.

- **Chapter 4 – Design of Electronic Load Controller:** Presents the design and development of both the hardware-in-the-loop simulation model and experimental configuration of an Intelligent Electronic Load Controller using a fuzzy logic control method.

- **Chapter 5 – Results and Discussion:** Presents the results from simulation and experimental testing conducted on the Intelligent Electronic Load Controller.

- **Chapter 6 – Conclusion and Recommendations:** Presents the summary of key findings of the research conducted together with recommendations for future work.

CHAPTER 2
THEORETICAL BACKGROUND

2.1. INTRODUCTION

This chapter presents an overview of hydropower systems together with some of its components and an in-depth discussion on the background of Electronic Load Control and fuzzy logic.

2.2. GENERAL DESCRIPTION OF HYDROPOWER

Hydropower is a form of power generation that converts the kinetic energy of flowing water into electricity. Hydropower is produced wherever water flows from a high elevation to a lower elevation. The difference between the two elevations is referred to as the head. To generate electricity both water flow and a head must be available. The flowing water causes the blades of a turbine to spin. The rotation of the turbine forces the generator to turn in order to generate electricity which is transmitted to a power grid or an area where it will be used [3].

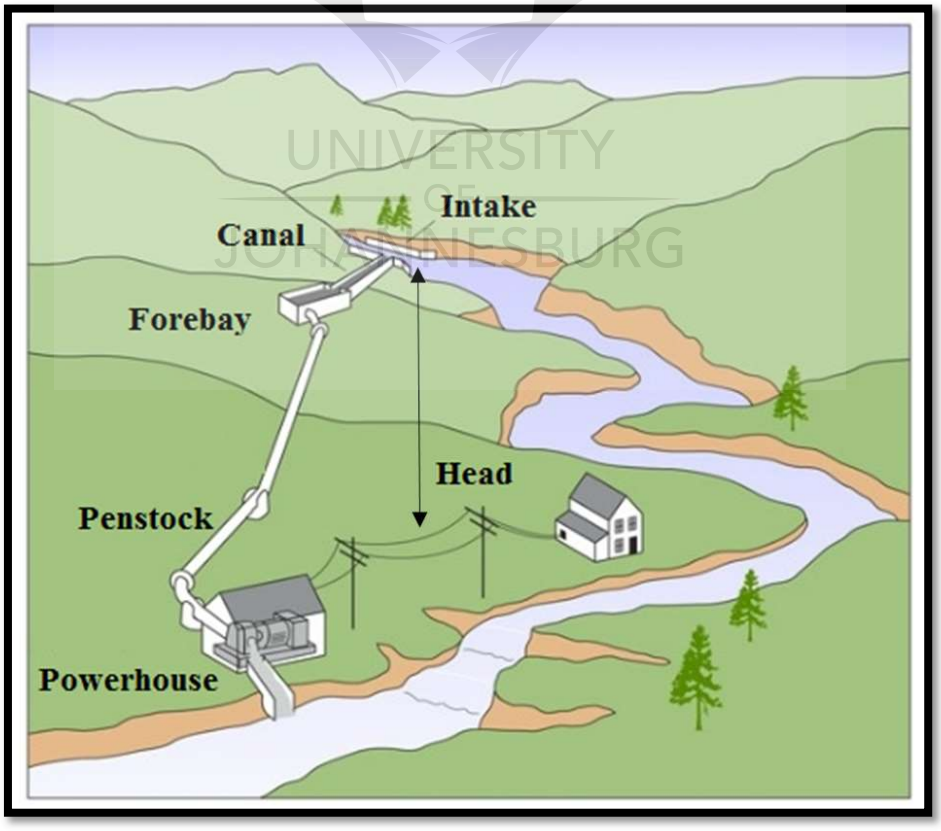

Figure 2.1: Example of micro-hydropower generation (Run-of-River) [4]

2.3. FACTORS AFFECTING HYDROPOWER SITE SELECTION

In order to select a site for a hydropower plant the following factors must be considered:

2.3.1. Water Resources

Water availability is the most important aspect when selecting a site for a hydropower plant. Data such as the amount of water available at the site and the amount of rainfall that occurs in the region throughout the year should be known in order to estimate the potential generation capacity of the plant [5 - 8].

2.3.2. Water Storage

Due to unpredictable rainfall during the year, water needs to be stored in a dam in order to generate and supply a constant power output. The storage capacity of a dam can be determined by using a mass curve [5 - 6]. A mass curve is the cumulative values of a hydrological quantity (such as precipitation or runoff) plotted against time [9].

2.3.3. Water Head

In order to generate and supply the amount of electricity that is required, a large quantity of water is required to flow from a high head. The quantity of water required to supply the powertrain is reduced when there is an increase in the head [5 - 8].

2.3.4. Distance from the Load Centre

The distance between the load centre and the power plant should be as short as possible to reduce the maintenance costs [7, 10].

2.3.5. Selection of Site

Access leading to and from the hydropower construction site should be easily accessible. At the ideal geological site, the constructed dam must able to store large quantities of water at a high head. The foundation rocks of the masonry dam must be strong and stable enough to withstand water thrust and other stresses exerted on it [5 - 8].

2.3.6. Environmental Impacts

The impact on the environment must be considered when selecting a hydropower site. Important considerations that needs to be considered are [5 - 8]:

- Deforestation
- Protection of fauna and flora
- Protection of historical, religious and cultural sites
- Degradation of catchment area
- Low oxygen levels in water
- Earthquake disasters

2.4. HYDROPOWER CLASSIFICATION

2.4.1. Run-of-River System

Run-of-River is one of the cheapest hydropower systems to implement since it does not require any significant water storage or the construction of a dam. Instead natural flowing water is diverted from a river into a channel and into a penstock where the water will flow down to the powerhouse where electricity will be generated. Run-of-River hydropower systems require a high head with a low flow rate or a low head with a high flow rate to generate electricity. If the flow rate of the water is insufficient due to a dry season, the Run-of-River hydropower system will be unable to generate electricity. The amount of electricity being generated is dependent on the head and flow rate of the system. One major advantage of this system is that it causes minimal environmental disruptions [7, 8, 11].

2.4.2. Impoundment System

An impoundment or storage system is the most commonly used type of operation for hydropower systems. In this system water gets stored in a large dam and only when there is high electricity demand or to maintain the dam level, the stored water gets released [7, 12]. During a high rainfall season water can be conserved in the dam, which provides some sort of security in the dry season [8]. One major advantage of this system is that the stored water (energy) can be used when necessary.

2.4.3. Pumped Storage System

A pumped storage hydropower system needs to be located between an upper and lower reservoir. During off-peak periods the water that is stored in the lower reservoir is pumped to the upper reservoir by the reversible pumping turbine to increase the volume of water in the upper reservoir for generating purposes during the peak demand periods. Around 70% of the power used during the pumping of water from the lower to upper reservoir can be recovered during the generating phase of electricity [7, 11, 12].

2.4.4. Tidal System

A tidal hydropower system needs to be located along the coastline. In a tidal system the energy obtained from the rise and fall of tides are converted into electricity. Tidal energy can be generated in the following ways [8, 11]:

- **Tidal Turbines:** Place a turbine below the water surface to harness the energy from the tidal streams [8].

- **Tidal Barrage:** A tidal barrage is a dam constructed across a suitable ocean inlet, river, bay or estuary. The barrage consists of sluice gates that are used to control water levels and water flow rates. As the tide rises, seawater flows into the reservoir to create a difference in the water levels. The sluice gates are closed at high tides. When the tides turn, the sluice gates are opened and the water flows back into the ocean through the turbine to create tidal energy [8].

2.4.5. Wave System

A wave hydropower system needs to be located at the coast. Large amounts of energy can be generated from waves [12]. There are three main wave energy systems used:

- **Float Ball System:** This system consists of a float ball device that is anchored to the ocean floor. The float ball moves up and down due to the rising and falling of waves. This movement drives a turbine [11 - 12].

- **Oscillating Water Column System:** This system consists of a chamber that has an opening beneath the ocean to allow seawater to flow in and out of the chamber. Air is compressed inside the chamber by the oscillation of the waves. Air is either forced out of the top opening of the chamber or drawn back into the chamber depending on the waves. A rising wave forces air out of the chamber and a falling wave draws air back into the chamber. This process drives a bi-directional turbine [11 - 12].

- **Tapered Channel System:** This system consists of an elevated reservoir and a tapered channel. The reservoir is filled with the water waves through the narrowing channel. By releasing water from the reservoir back into the ocean causes a turbine to turn [11 - 12].

2.5. GENERATORS

An electrical generator is a device that converts mechanical energy into electrical energy. In hydropower systems the following generators are commonly used:

- **Synchronous generators:** These generators are typically used for larger micro-hydropower systems.

- **Induction generators:** These generators are typically used for smaller micro-hydropower systems.

2.5.1. Basic Operation of an Induction Machine

An induction machine can be operated either as a generator or a motor. In order to understand the operating principle of an induction generator, the operating principle of an induction motor will be explained [13]: A three-phase AC voltage is applied to the stator of the induction motor and as soon as current starts to flow, a stator rotating magnetic field ($\mathbf{B_s}$) is produced. The rotating magnetic field cuts the rotor bars, inducing a voltage in the rotor. The induced voltage results in currents flowing in the rotor windings which lags behind the voltage. These currents interact with the rotating stator magnetic field and produces a torque. The induced torque resulting from the magnetic fields drag the rotor round with the field. In contrast to an induction motor whose rotor rotates slower than synchronous speed, an induction generator driven by a prime mover (turbine) produces electricity by rotating its rotor faster than synchronous speed, which is referred to as negative slip. Slip is the difference between the synchronous rotation speed and the rotor rotation speed. Slip can be calculated using equation 2.1:

$$\mathbf{s = \frac{n_s - n_r}{n_s}} \qquad \mathbf{(2.1)}$$

Where,

s	=	Slip
n_s	=	Synchronous Rotation Speed (RPM)
n_r	=	Rotor Rotation Speed (RPM)

The rotor frequency is related to the electric frequency and the slip and can be calculated using equation 2.2:

$$f_r = sf \tag{2.2}$$

Where,

f_r	=	Rotor Frequency (Hz)
s	=	Slip
f	=	Frequency (Hz)

The per-phase equivalent circuit of an induction generator is show in figure 2.2:

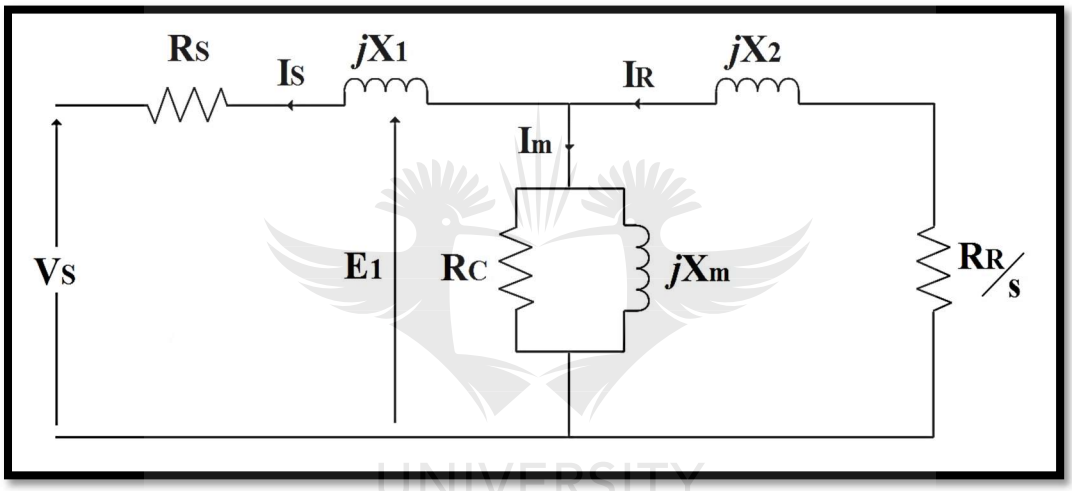

Figure 2.2: Induction generator per-phase equivalent circuit

Where,

V_S	=	Supply Voltage
R_S	=	Stator Resistance
I_S	=	Stator Current
X_1	=	Stator Reactance
I_m	=	Magnetizing Current
R_C	=	Core Loss Resistance
X_m	=	Magnetizing Reactance
E_1	=	Induced Voltage
I_R	=	Rotor Current
X_2	=	Rotor Reactance
R_R	=	Rotor Resistance

2.5.2. Self-Excited Induction Generator

In order for an induction machine to get started, reactive power is required. When an induction machine is connected to a grid, reactive power is automatically supplied at a fixed voltage and frequency. However, when an induction machine is not connected to a grid (stand-alone), an alternative method is required to supply the required reactive power. This is accomplished by connecting a capacitor bank to the stator terminals of an induction generator (self-excited induction generator). For a three-phase generation output, capacitors can be connected either in star or delta. For economical purposes the capacitor bank is connected in delta. If the capacitor bank is connected in star, the required capacitance to supply the same amount of reactive power is three times more in comparison to a delta connected capacitor bank. For a single-phase generation output, a three-phase induction generator is used as a single-phase induction generator. This is accomplished by connecting a three-phase induction generation in delta and instead of connecting a capacitor to each phase, the capacitors are connected in the C-2C configuration:

- Phase 1 - Capacitor 1
- Phase 2 - Capacitor 2 (Twice the size of Capacitor 1)
- Phase 3 - No capacitor

In stand-alone micro-hydropower systems, induction generators are often preferred for the generation of electricity due to [2]:

- Relatively low cost
- Less maintenance required
- High reliability
- Robust construction
- Brushless rotor operation
- No separate DC excitation required
- Excellent protection against overloads and short circuits

2.6. LOADS

2.6.1. Consumer Loads

Consumer loads used in a micro-hydropower system are typically small household appliances and electrical devices such as [14]: microwave ovens, toasters, fans, lights, radios, mobile phone chargers, televisions, laptops etc.

2.6.2. Ballast Load

A ballast load (also known as a dump load) is used to absorb any surplus energy that is not required or used by the consumers, so that, the total output power of the SEIG remains constant [15]. The surplus energy can be used for example to charge battery banks or for air/water heating purposes. The size of the ballast load is typically equal to or slightly greater than the rated output value of the generator [16].

2.6.3. Storage

A storage typically consists of a battery bank and is used to store any surplus energy that is not required or used by the consumer. When the demand for electricity increases beyond what the micro-hydropower system is generating, the battery bank is used to supply "extra" energy to keep the consumer loads running.

2.7. ELECTRONIC LOAD CONTROLLER

An Electronic Load Controller (ELC) is a device used to ensure that the generator output power remains constant under varying consumer loads. This is accomplished by diverting any surplus power to a ballast load or storage [17 - 18]. Equation 2.3 and figure 2.3 shows the following:

$$P_G = P_C + P_B \tag{2.3}$$

Where,

P_G = Generated Power (W)

P_C = Consumer Load Power (W)

P_B = Ballast Load Power (W)

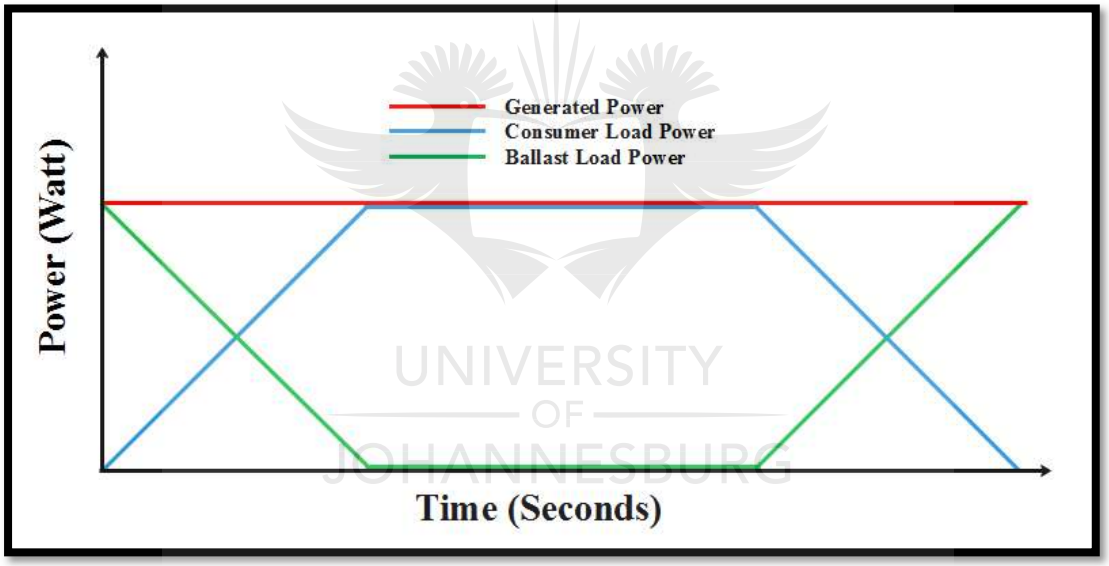

Figure 2.3: ELC principle of operation

The most commonly used methods to design an ELC are the following:

- Binary-Weighted Load Regulation
- Phase Angle Regulation
- Mark-Space Ratio Regulation
- Controlled Bridge Rectifier Regulation
- Uncontrolled Rectifier with a Chopper Regulation

2.7.1. Binary-Weighted Load Regulation

In a binary-weighted load regulation the ballast load comprises of multiple resistive loads. Each resistive load is twice the size of the previous resistive load. In order to keep the power output constant, a combination of resistive loads is either switched on or off (binary) according to changes in the consumer load [13]. The switching operation of resistive loads occur only during the transient period. Solid-state relays which include a zero-voltage switching circuit are used for the switching operation to reduce harmonic distortion [16]. During steady-state, no harmonic distortion is produced. The binary-weighted load regulation is very complex and expensive as it requires several resistive loads, each with its own connections, wires and solid-state relays [13].

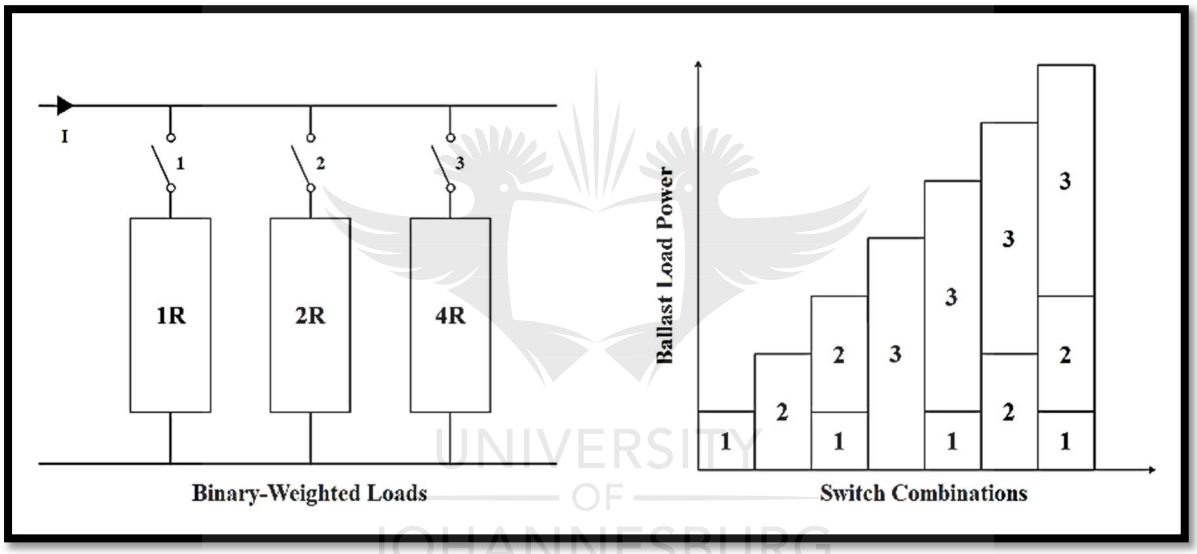

Figure 2.4: Binary-weighted load regulation

2.7.2. Phase Angle Regulation

A phase angle regulation comprises of a single resistive ballast load of magnitude equal to or slightly greater than the rated output value of the generator. Any change in the consumer load will result in the adjustment of the firing angle (α) of the switching device (thyristor or triac) and therefor current flowing through the ballast load is varied, thus maintaining a constant power output [16]. The delay in the firing angle (α) results in the demand for reactive power loading and produces harmonics, which can cause overheating in the generator windings [16], [18]. The phase angle regulation is generally used for synchronous generators and not for induction generators. When using an induction generator, the ballast load current can lag behind the voltage, effectively resulting in a variable lagging power factor [13].

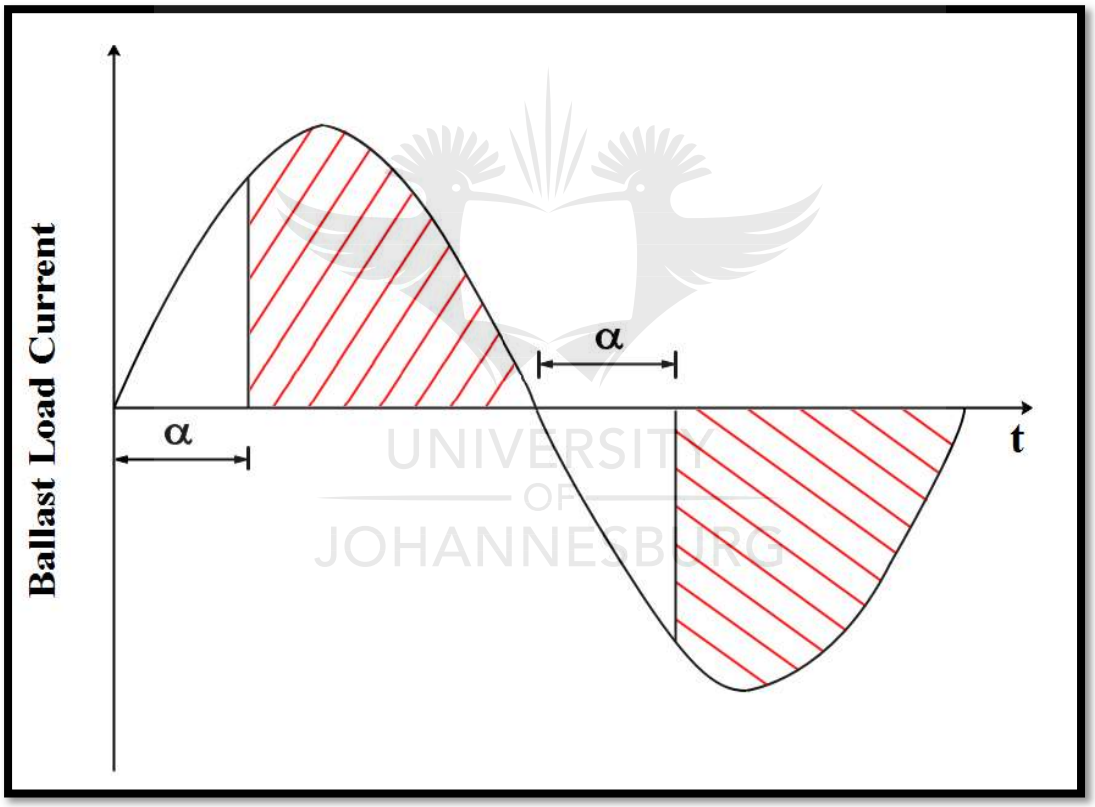

Figure 2.5: Phase angle regulation

2.7.3. Mark-Space Ratio Regulation

The Mark-Space ratio regulation comprises of only a single ballast load. The ballast load is connected across an uncontrolled bridge rectifier that converts AC voltage produced by the generator to DC voltage. A transistor is used to switch the ballast load on and off with variable duty cycle. Any change in the consumer load will result in the varying of the on and off times (duty cycle) of the PWM output in order to achieve a constant power output. The duty cycle can be varied from 0% to 100%. The Mark-Space ratio regulation is often favoured due to its good voltage and frequency regulation [13, 19].

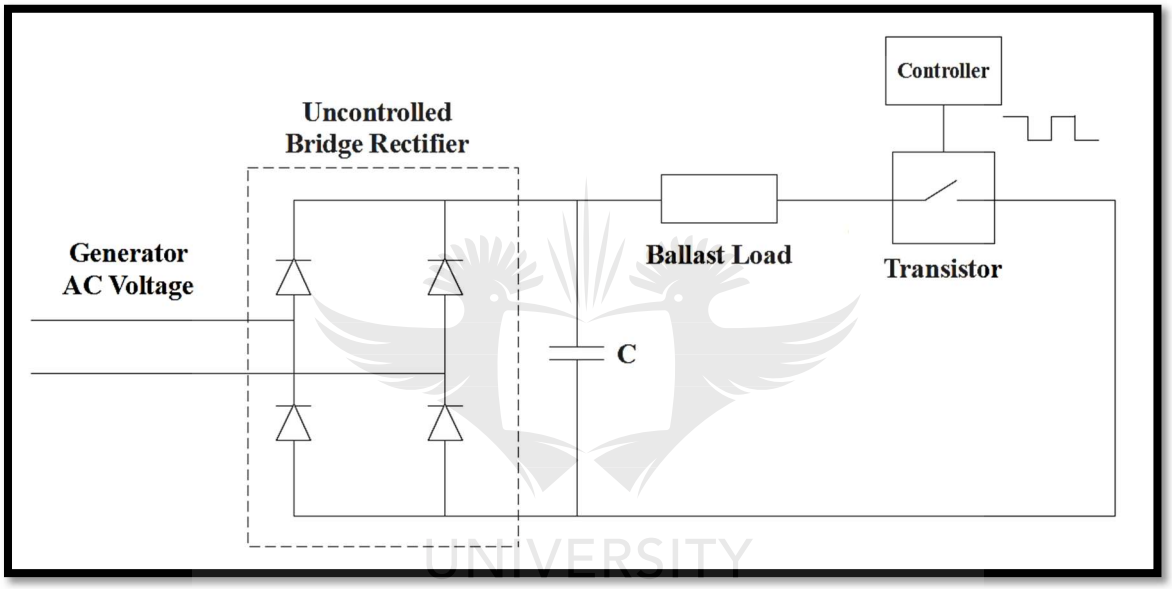

Figure 2.6: Single-phase Mark-Space ratio regulation

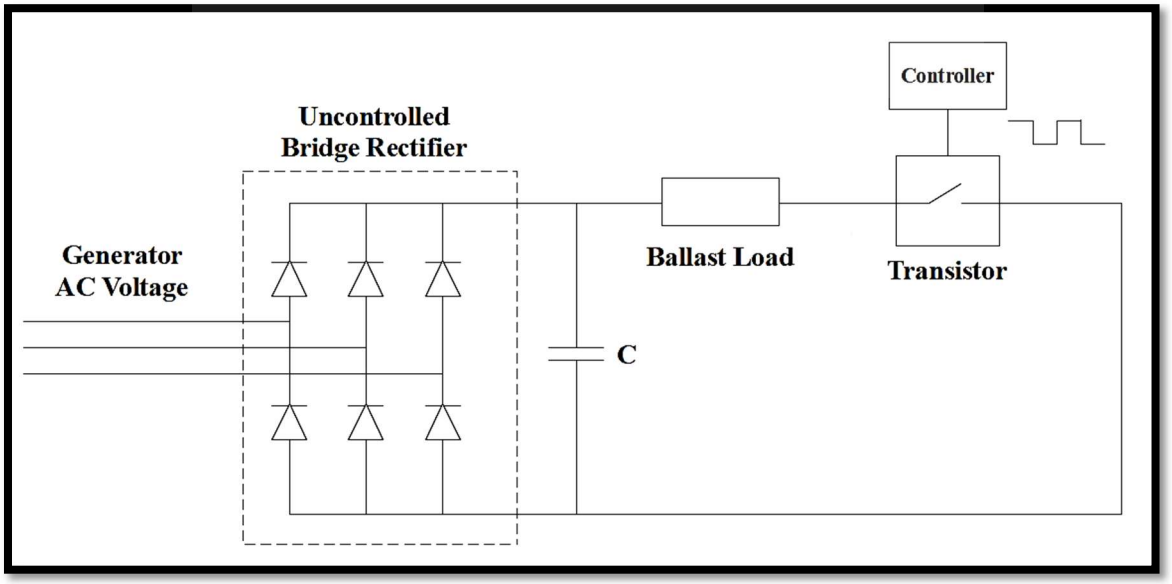

Figure 2.7: Three-phase Mark-Space ratio regulation

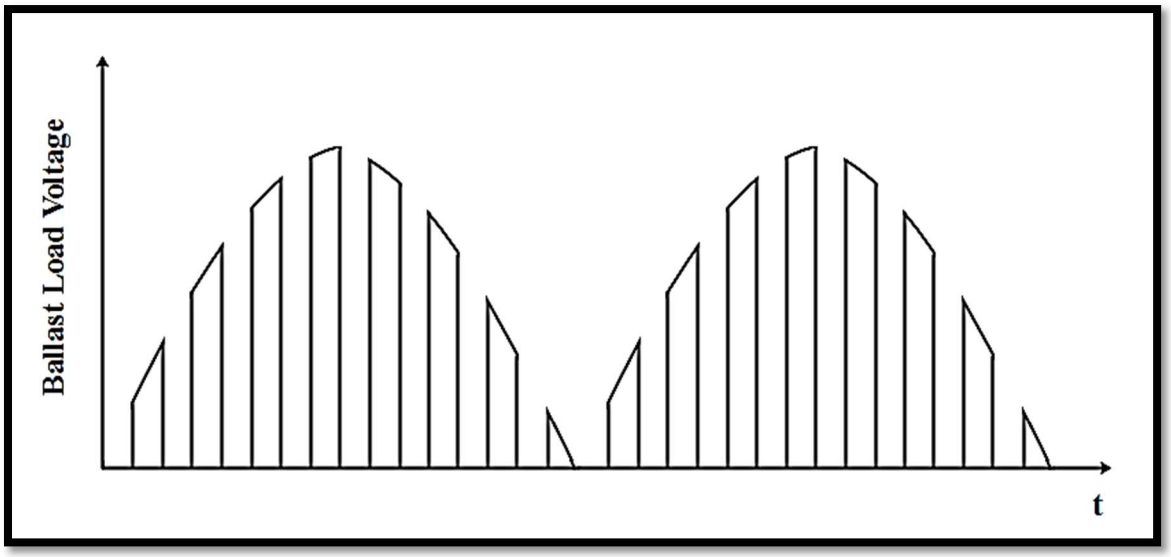

Figure 2.8: Mark-Space ratio regulation waveform

2.7.4. Controlled Bridge Rectifier Regulation

A controlled bridge rectifier regulation comprises of only a single ballast load. The ballast load is connected across a controlled bridge rectifier consisting of controllable thyristors that converts AC voltage produced by the generator to DC voltage. The thyristors are also used as control elements. Any change in the consumer load will result in the adjustment of the firing angle (α) of the thyristor and therefor current flowing through the ballast load is varied, thus maintaining a constant power output. The controlled bridge rectifier regulation is very complex, demands reactive power and inject harmonics onto the system [18].

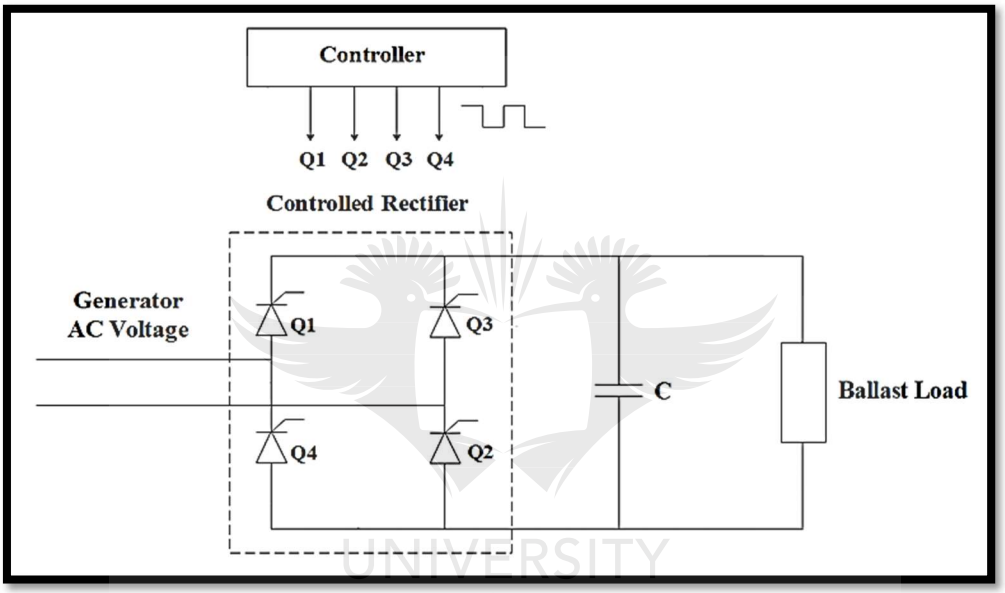

Figure 2.9: Single-phase controlled bridge rectifier regulation

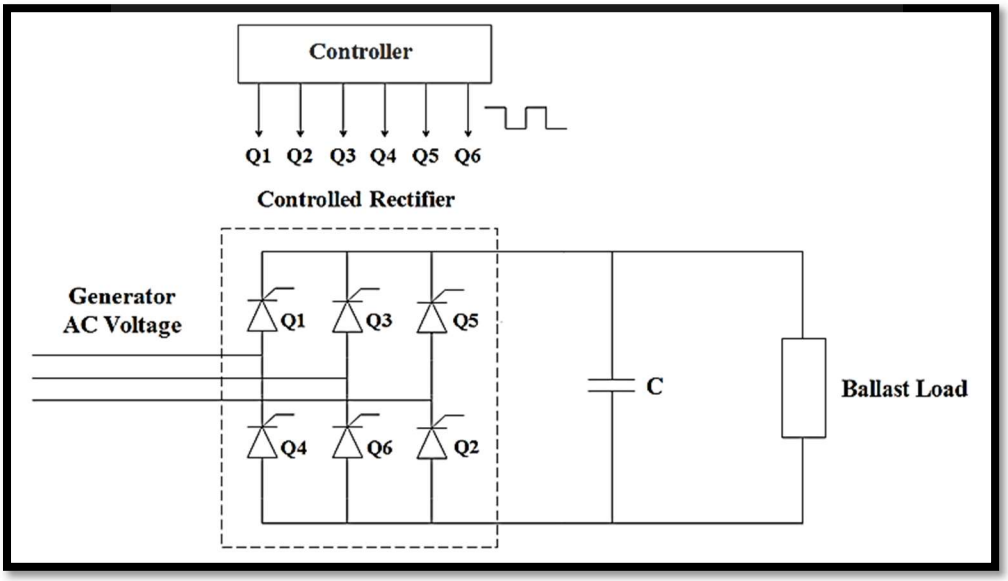

Figure 2.10: Three-phase controlled bridge rectifier regulation

2.7.5. Uncontrolled Bridge Rectifier with a Chopper Regulation

An uncontrolled bridge rectifier with a chopper regulation comprises of only a single ballast load. The ballast load is connected across an uncontrolled bridge rectifier that converts AC voltage produced by the generator to DC voltage. An IGBT/MOSFET is used as a chopper (self-commutating switching device) to switch the ballast load on and off with variable duty cycle. Any change in the consumer load will result in the varying of the on and off times (duty cycle) of the PWM output in order to achieve a constant power output. The duty cycle can be varied from 0% to 100%. The uncontrolled bridge rectifier with a chopper regulation is often favoured due to its good voltage and frequency regulation as well as a very cost-effective control method [18, 20].

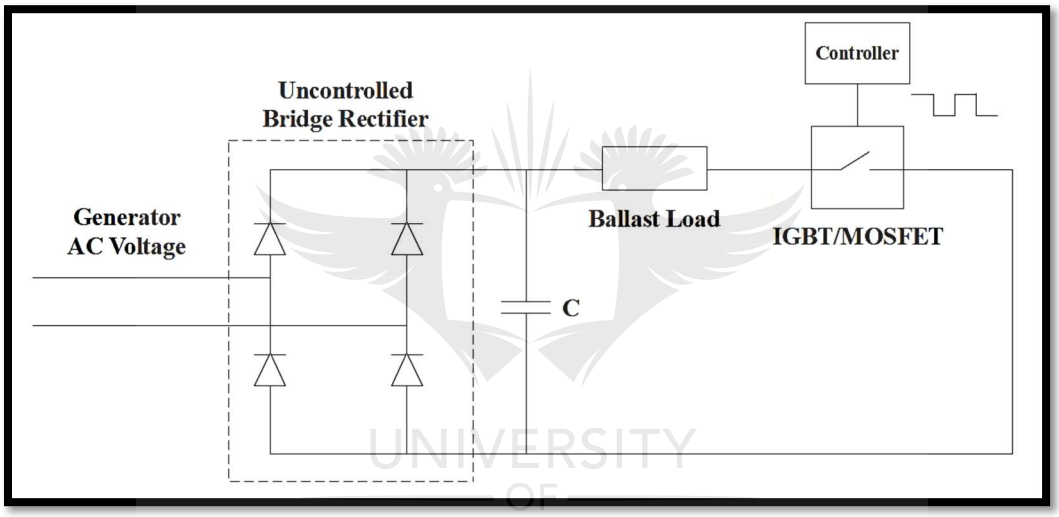

Figure 2.11: Single-phase uncontrolled bridge rectifier with a chopper regulation

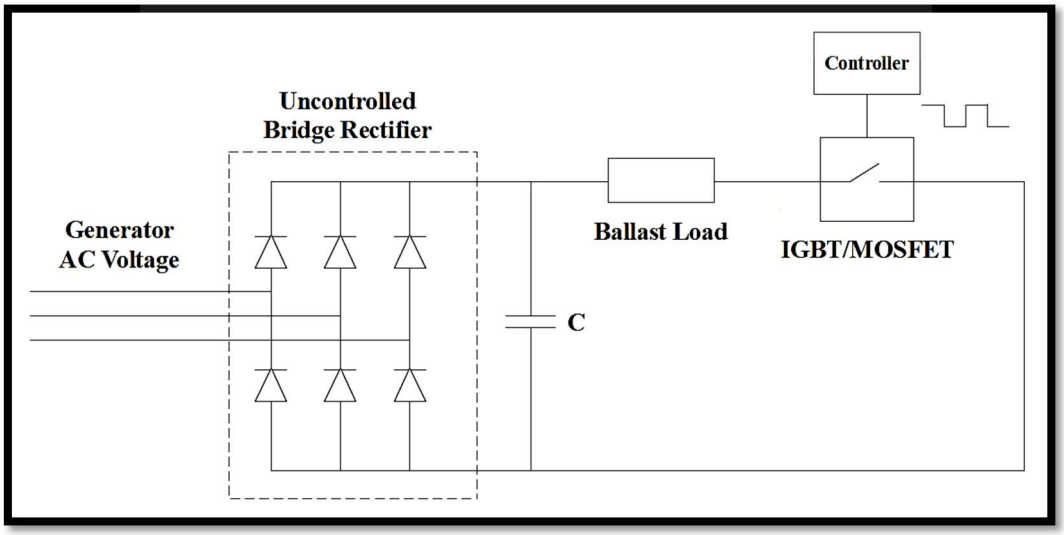

Figure 2.12: Three-phase uncontrolled bridge rectifier with a chopper regulation

2.8. FUZZY LOGIC CONTROL

In crisp logic, variables can only have true (1) values or false (0) values, no values in between. In fuzzy logic, variables can have values ranging between true (1) values and false values (0) [19]. An example of the difference between crisp logic and fuzzy logic is shown in table 2.1:

Table 2.1: Crisp logic vs Fuzzy logic

Crisp Logic	Fuzzy Logic
Cold	Cold
Hot	Cool
	Mild
	Warm
	Hot

Control systems use fuzzy logic due to the following reasons:

- Development is cheaper
- Cover a large selection of operating conditions
- Fast response times with virtually no overshoot
- Flexible in design and implementation

A block diagram of a typical fuzzy logic control system is shown in figure 2.13:

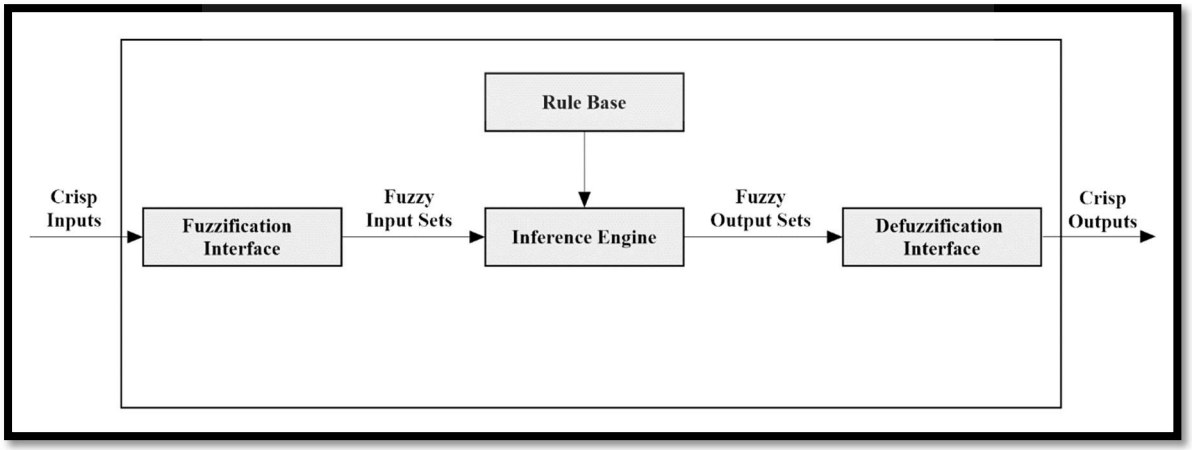

Figure 2.13: Fuzzy logic system

Each of the major components of the fuzzy logic controller, as shown in figure 2.13, are described in the subsequent sections.

2.8.1. Fuzzification Interface

The fuzzification interface is the process of converting crisp input values into fuzzy input values. Each crisp input value is assigned to its own group of membership functions. This group of membership functions exists within a universe of discourse that holds all relevant values that the crisp input can possess [21]. Figure 2.14 shows an example of a membership function curve:

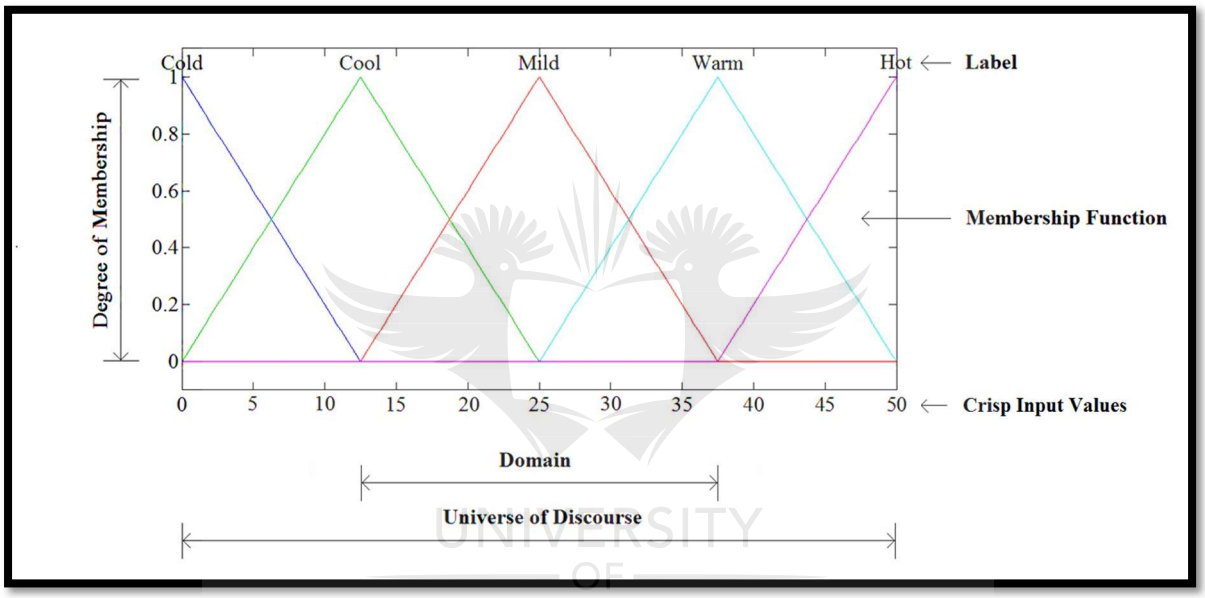

Figure 2.14: Membership function example [21]

- **Crisp Input Values:** Measurable variables such as voltage or temperature.

- **Domain:** Range/width over which a membership function is mapped.

- **Degree of Membership:** Expression of how true a membership function is between zero and one.

- **Labels:** Descriptive words used to identify different membership functions.

- **Membership Function:** A curve that defines how each point in the universe of discourse are assigned to a degree of membership. The most common shapes of a membership function are shown in figure 2.15:

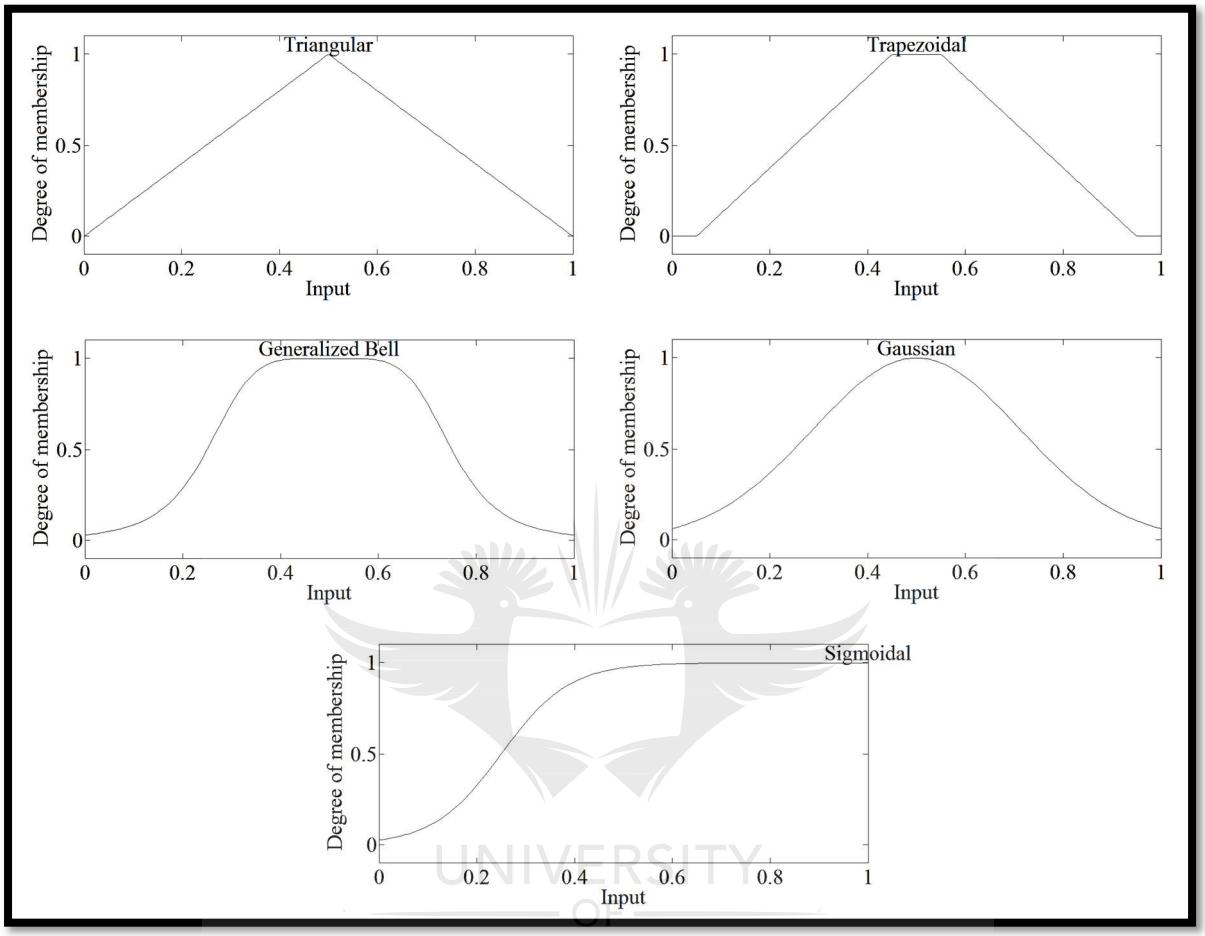

Figure 2.15: Membership function shapes

- **Universe of Discourse:** Range of all possible values that the crisp input can have.

2.8.2. Rule Base

The rule base consists of a collection of control rules that form the basis to obtain the fuzzy output values. The rules are expressed in "IF-THEN" format. An example of a simple fuzzy rule is expressed as [19]:

IF x is A, THEN y is B

Where x and y are defined as the input and output variables of a system, A and B are linguistic values defined by fuzzy sets on the universes of discourse. The IF-part (x is A) is called the "antecedent" and the THEN-part (y is B) is called the "consequent".

A fuzzy rule can also have multiple antecedents and consequents:

- Antecedents can be joined by logical operators such as AND or OR.
- Consequents can be joined by the logical operator AND.

All the rules get evaluated in order to control and obtain a fuzzy output value.

2.8.3. Inference Engine

The inference engine is the process of mapping input data to an output space via the rule base. There are primarily two types of inference engine methods used [22]:

- Mamdani fuzzy inference method
- Takagi-Sugeno-Kang fuzzy inference method

The operating procedure of the two fuzzy inference methods are very similar. The main difference between the two methods are the way in which the crisp output values are generated from the fuzzy input values. The Mamdani fuzzy inference method generates crisp output values by using different defuzzification methods. The output membership functions of this method are expected to be fuzzy sets. The Takagi-Sugeno-Kang fuzzy inference method differs in that it uses a weighted method for generating crisp output values. The output membership functions of this method are either linear or constant [19].

2.8.4. Defuzzification Interface

The defuzzification interface is the process of converting fuzzy output values into crisp output values. The following methods are commonly used for defuzzification [19]:

- **Max-membership method:** This method generates crisp output values by choosing the point at which membership functions reach their maximum values. The max-membership method is given by equation 2.4:

$$\mu_{\text{Ç}}(z^*) \geq \mu_{\text{Ç}}(z) \qquad \text{for all } z \in Z \tag{2.4}$$

Where,

$\mu_{\text{Ç}}$ = Membership Function

z^* = Defuzzified Value

z = Element

Z = Universe of Discourse

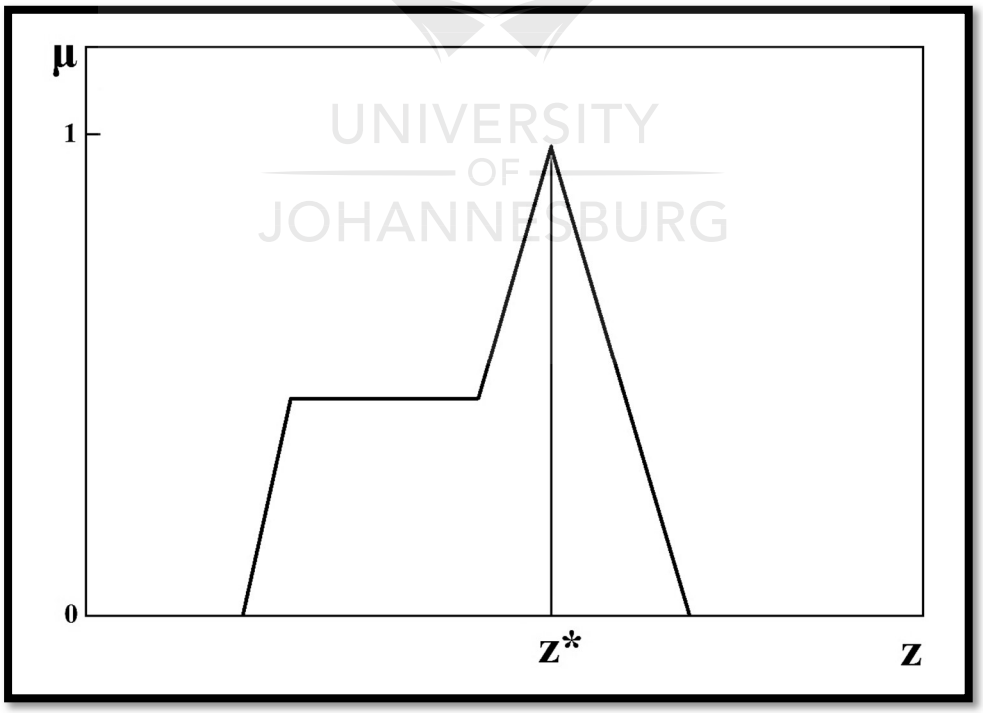

Figure 2.16: Max-membership method

- **Centroid method:** This method generates a crisp output value based on the centroid of a fuzzy set. For a discrete membership function, the centroid method is given by equation 2.5:

$$z^* = \frac{\sum \mu_{\tilde{C}}(z).z}{\sum \mu_{\tilde{C}}(z)} \tag{2.5}$$

Where,

z^* = Defuzzified Value

$\sum$ = Algebraic Sum

$\mu_{\tilde{C}}$ = Membership Function

z = Element

For a continuous membership function, the centroid method is given by equation 2.6:

$$z^* = \frac{\int \mu_{\tilde{C}}(z).z dz}{\int \mu_{\tilde{C}}(z) dz} \tag{2.6}$$

Where,

z^* = Defuzzified Value

$\int$ = Algebraic Integration

$\mu_{\tilde{C}}$ = Membership Function

z = Element

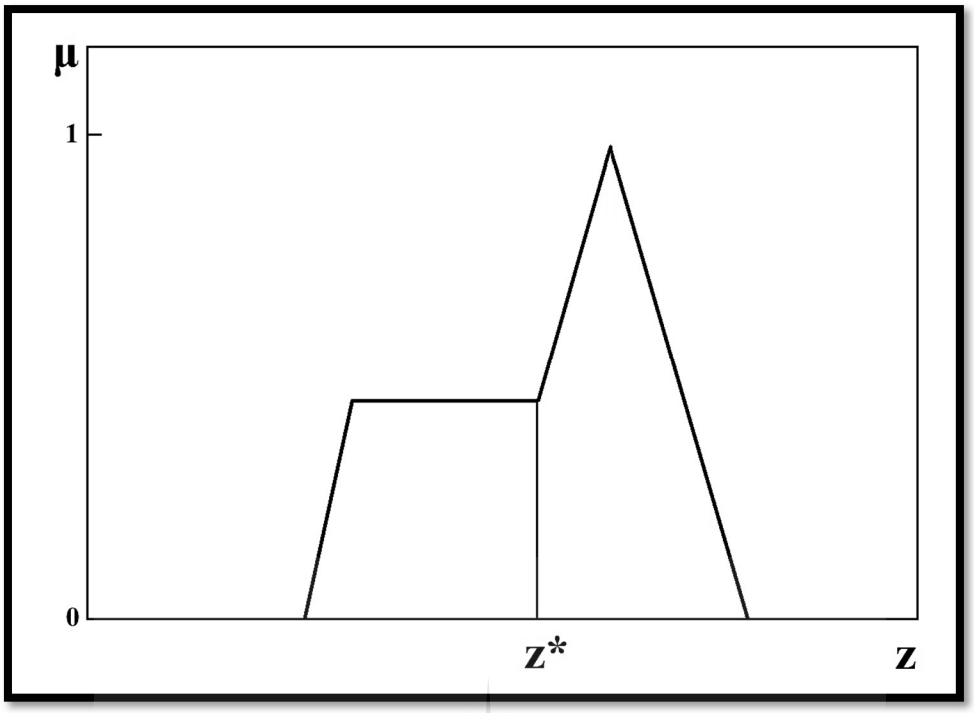

Figure 2.17: Centroid method

- **Weighted average method:** Each membership function in this method is weighted by its corresponding maximum membership function value and is only valid for symmetrical output membership functions. The weighted average method is given by equation 2.7:

$$z^* = \frac{\sum \mu_{\tilde{C}}(\bar{z}).\bar{z}}{\sum \mu_{\tilde{C}}(\bar{z})} \tag{2.7}$$

Where,

z^* = Defuzzified Value

$\sum$ = Algebraic Sum

$\mu_{\tilde{C}}$ = Membership Function

$\bar{z}$ = Centroid of Each Symmetric Membership Function

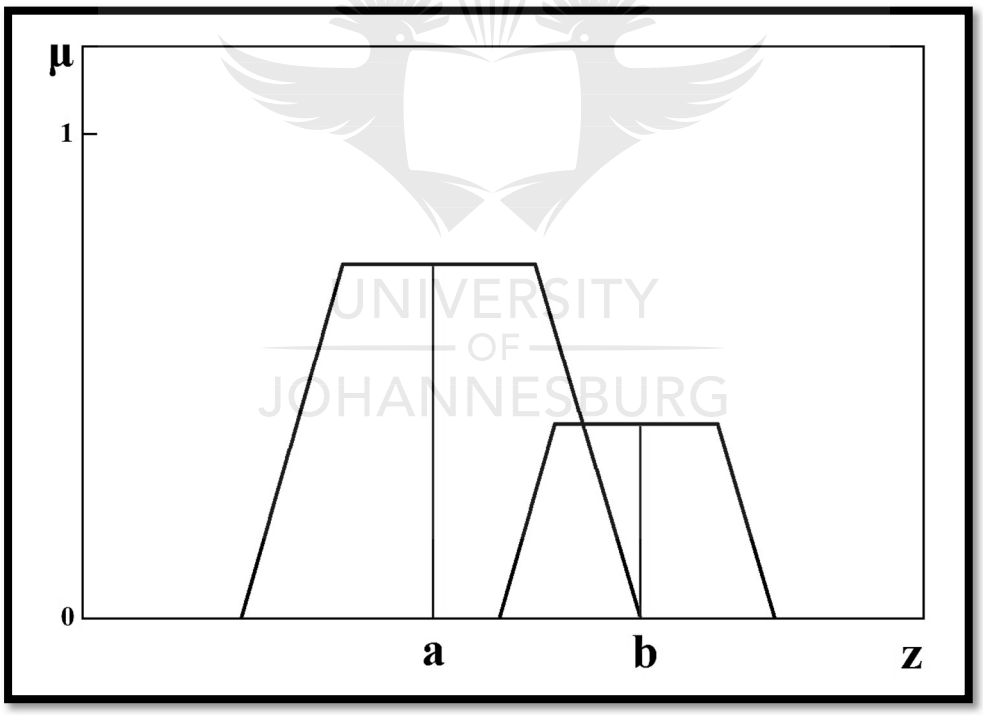

Figure 2.18: Weighted average method

- **Mean-max membership method:** This method generates crisp output values by choosing the point at which membership functions reach their maximum values. The mean value of the maxima is taken in cases where more than one of the membership functions have maximum membership values. The mean-max membership method is given by equation 2.8:

$$z^* = \frac{a + b}{2} \tag{2.8}$$

Where,

z^* = Defuzzified Value

a = Maximum Value 1

b = Maximum Value 2

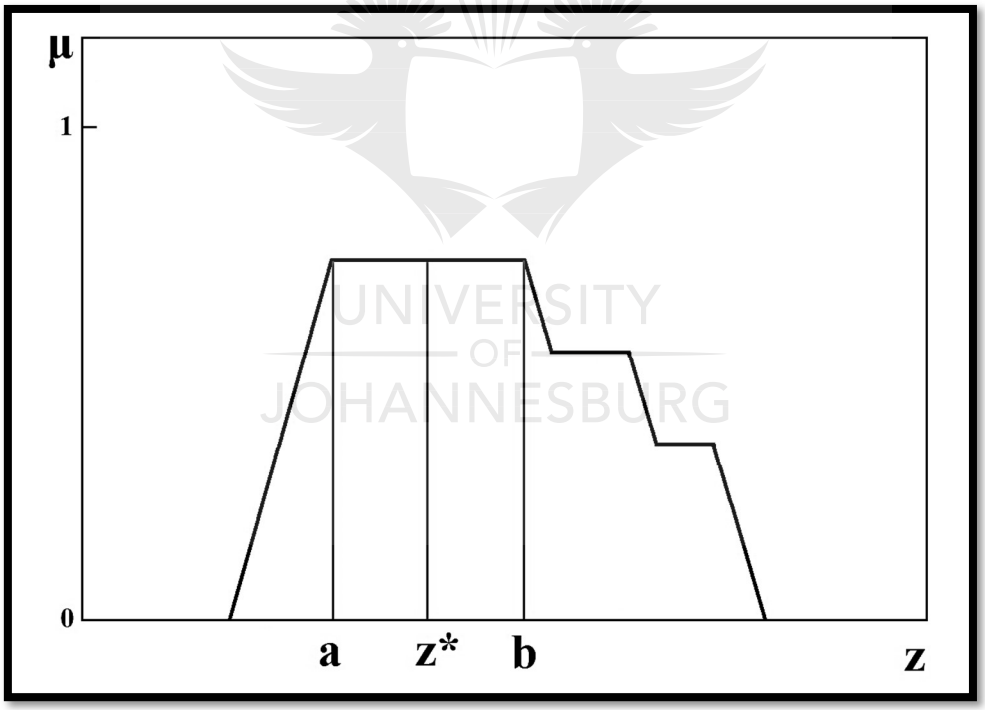

Figure 2.19: Mean-max membership method

- **Centre of sums method:** This method generates crisp output values by adding the intersecting area of membership functions twice. The centre of sums method is given by equation 2.9:

$$z^* = \frac{\sum_{k=1}^{n} \mu_{\underset{\sim}{C}_k}(z) \int_z \bar{z}\, dz}{\sum_{k=1}^{n} \mu_{\underset{\sim}{C}_k}(z) \int_z dz} \qquad (2.9)$$

Where,

z^* = Defuzzified Value

$\sum$ = Algebraic Sum

k = Fuzzy Set Number

n = Number of Fuzzy Sets

$\mu_{\underset{\sim}{C}_k}$ = Membership Function for the k-th Fuzzy Set

$\int$ = Algebraic Integration

$\bar{z}$ = Distance to the Centroid of Each of the Membership Functions

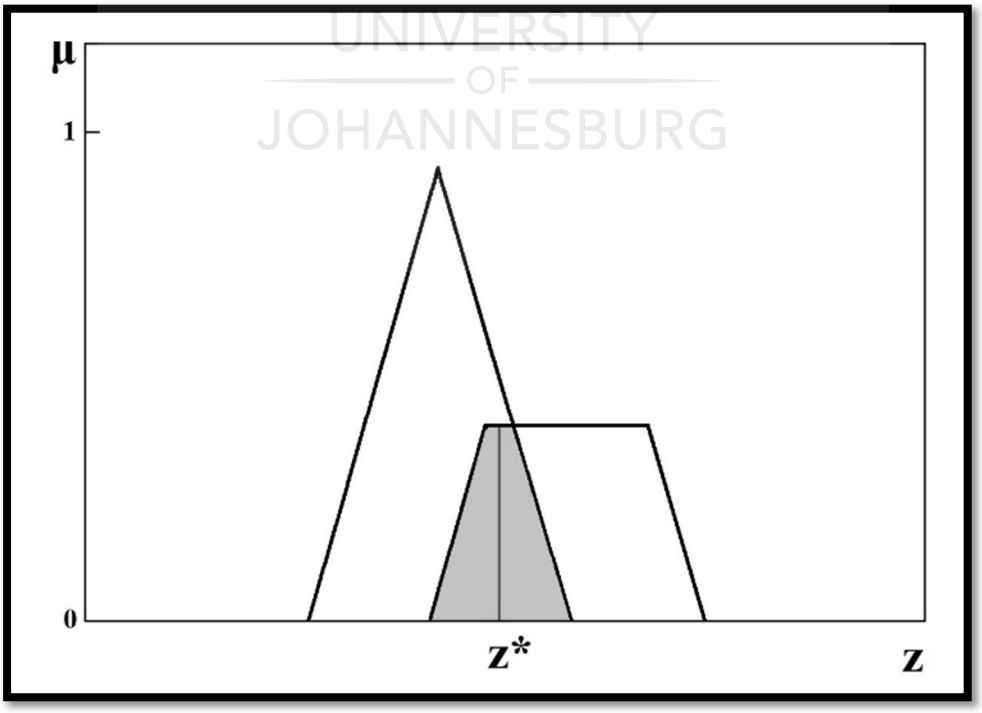

Figure 2.20: Centre of sums method

- **Centre of largest area method:** The output fuzzy set of this method requires at least two convex subregions. The centre of gravity of the subregion with the largest area is used to generate crisp output values. The centre of largest area method is given by equation 2.10:

$$z^* = \frac{\int \mu_{\tilde{C}_m}(z).z\,dz}{\int \mu_{\tilde{C}_m}(z)\,dz} \qquad \textbf{(2.10)}$$

Where,

z^* = Defuzzified Value

$\int$ = Algebraic Integration

$\mu_{\tilde{C}_m}$ = Membership Function for the Convex Subregion that has the Largest Area Making Up $\tilde{C}_k$

z = Element

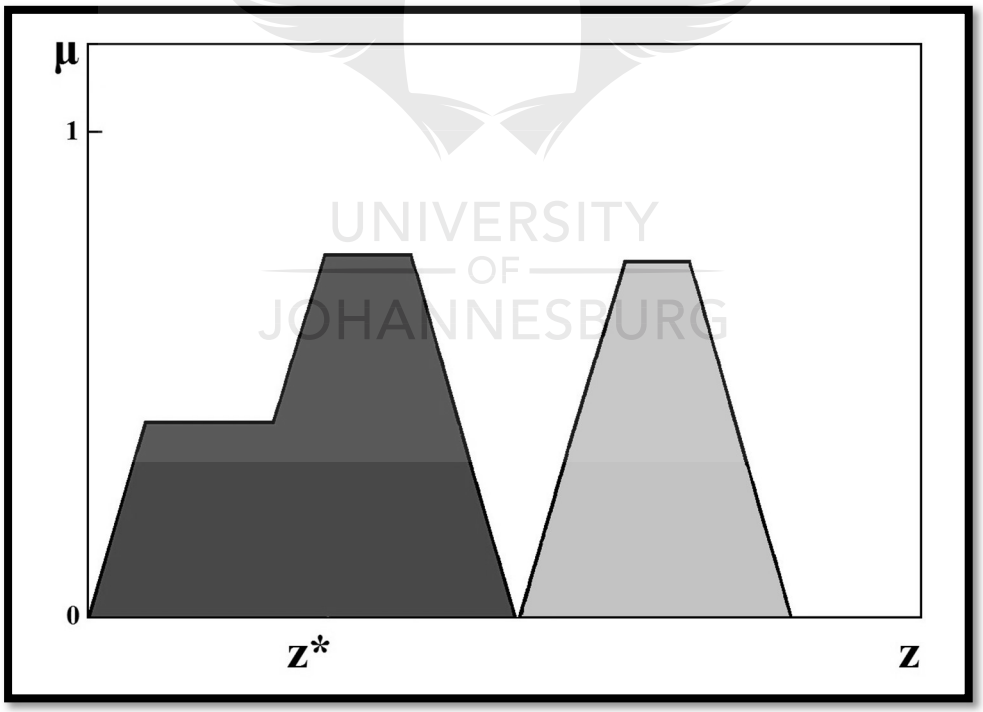

Figure 2.21: Centre of largest area method

- **First of maxima method:** This method determines the smallest value of the domain with maximum membership value. The largest height in the union is determined first before the first of maxima can be determined by using equation 2.11:

$$\mathbf{hgt}(\tilde{C}_k) = \sup \mu_{\tilde{C}_k}(z) \tag{2.11}$$

Where,

$hgt(\tilde{C}_k)$ = Largest Height in the Union

sup = Supremum (Least Upper Bound)

$\mu_{\tilde{C}_k}$ = Membership Function for the k-th Fuzzy Set

The first of maxima method is given by equation 2.12:

$$z^* = \inf \left\{ z \in Z \middle| \mu_{\tilde{C}_k}(z) = \mathbf{hgt}(\tilde{C}_k) \right\} \tag{2.12}$$

Where,

z^* = Defuzzified Value

inf = Infimum (Greatest lower bound)

z = Element

Z = Universe of Discourse

$\mu_{\tilde{C}_k}$ = Membership Function for the k-th Fuzzy Set

$hgt(\tilde{C}_k)$ = Largest Height in the Union

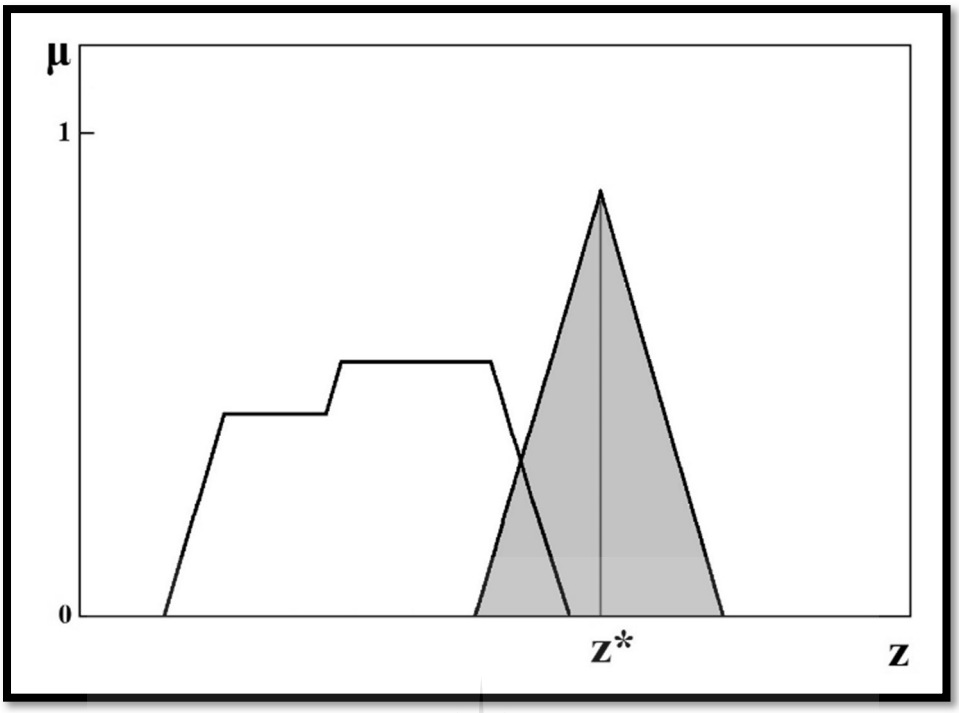

Figure 2.22: First of maxima method

- **Last of maxima method:** This method determines the largest value of the domain with maximum membership value. The largest height in the union is determined first before the last of maxima can be determined by using equation 2.13:

$$\mathbf{hgt}(\tilde{C}_k) = \sup \mu_{\tilde{C}_k}(z) \tag{2.13}$$

Where,

$hgt(\tilde{C}_k)$ = Largest Height in the Union

sup = Supremum (Least Upper Bound)

$\mu_{\tilde{C}_k}$ = Membership Function for the k-th Fuzzy Set

The last of maxima method is given by equation 2.14:

$$z^* = \sup \left\{ z \in Z \middle| \mu_{\tilde{C}_k}(z) = \mathbf{hgt}(\tilde{C}_k) \right\} \tag{2.14}$$

Where,

z^* = Defuzzified Value

sup = Supremum (Least Upper Bound)

z = Element

Z = Universe of Discourse

$\mu_{\tilde{C}_k}$ = Membership Function for the k-th Fuzzy Set

$hgt(\tilde{C}_k)$ = Largest Height in the Union

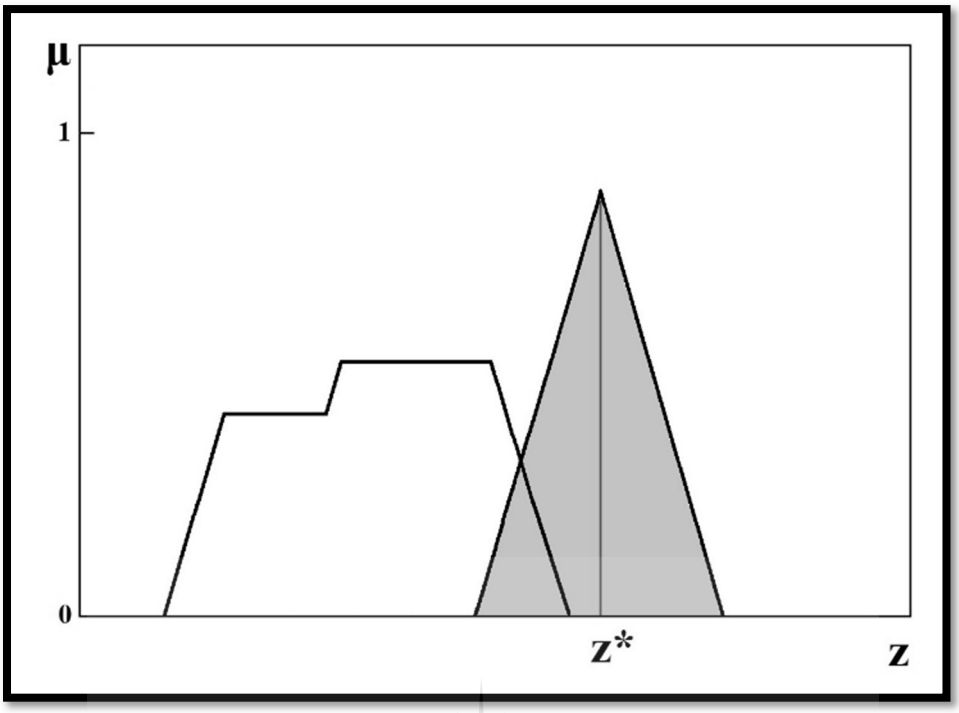

Figure 2.23: Last of maxima method

CHAPTER 3
SELF-EXCITED INDUCTION GENERATOR

3.1. INTRODUCTION

This chapter presents the design and development of both the simulation model and experimental configuration of a self-excited induction generator.

3.2. INDUCTION MACHINE TESTS

The following tests need to be performed on the induction machine in order to determine the parameters as well as the performance thereof [23]:

- DC test
- No-load test
- Blocked rotor test

These parameters and performance data assist with the design of the configuration of the induction machine as a self-excited induction generator. The induction machine nameplate parameters are listed in table 3.1:

Table 3.1: Experimental induction machine nameplate parameters

3-Phase Induction Machine		
	Y	**Δ**
Phase	3	3
Frequency (Hz)	50	50
Voltage (V)	400	230
Current (A)	1.45	2.5
Power (W)	550	550
Speed (RPM)	1395	1395
Power Factor	0.82	0.82

3.2.1. DC Test

The purpose of the DC test is to determine the stator resistance (R_S). To perform the DC test, a variable DC power supply is connected to the induction machine. The current flowing in the stator winding is adjusted to the rated value and the voltage between the terminals are measured. The results of the DC test are listed in table 3.2:

Table 3.2: Experimental DC test results

Parameter	Value
V_{DC}	35 V
I_{DC}	2.5 A

The stator resistance (R_S) is calculated as follow:

$$R_S = \frac{3V_{DC}}{2V_{DC}} \tag{3.1}$$

$$R_S = \frac{(3)(25)}{(2)(25)}$$

$$R_S = 21\ \Omega$$

Where,

R_S = Stator Resistance (Ω)

V_{DC} = DC Voltage (V)

I_{DC} = DC Current (A)

3.2.2. No-Load Test

The purpose of the no-load test is to determine the magnetizing reactance (X_m), iron loss (P_{Iron}) and stator core resistance (R_{Iron}). To perform the no-load test, the rated voltage is applied to the induction machine without any load connected. The results of the no-load test are listed in table 3.3:

Table 3.3: Experimental no-load test results

Parameter	Value
V_{Phase}	230 V
I_{Phase}	1.366 A
P_{in}	204 W
PF	0.217

The magnetizing reactance (X_m) is calculated as follow:

$$X_m = \frac{V_{Phase}\sqrt{1 - PF^2}}{I_{Phase}} - X_1 \quad (3.2)$$

$$X_m = \frac{(230)(\sqrt{1 - (0.217^2)})}{1.366} - 10.949$$

$$X_m = 154.009\ \Omega$$

Where,

X_m = Magnetizing Reactance (Ω)

V_{Phase} = Phase Voltage (V)

PF = Power Factor

I_{Phase} = Phase Current (A)

X_1 = Stator Reactance (Ω)

The iron loss (P_{Iron}) is calculated as follow:

$$\mathbf{P_{Iron} = P_{in} - 3R_S I_{Phase}^2} \quad \textbf{(3.3)}$$

$$\mathbf{P_{Iron} = 204 - (3)(21)(1.366)^2}$$

$$\mathbf{P_{Iron} = 86.376\ W}$$

Where,

P_{Iron} = Iron Losses (W)

P_{in} = Input Power (W)

R_S = Stator Resistance (Ω)

I_{Phase} = Phase Current (A)

The stator core resistance (R_{Iron}) is calculated as follow:

$$\mathbf{R_{Iron} = \frac{P_{Iron}}{3I_{Phase}^2}} \quad \textbf{(3.4)}$$

$$\mathbf{R_{Iron} = \frac{86.376}{(3)(1.366)^2}}$$

$$\mathbf{R_{Iron} = 15.421\ \Omega}$$

Where,

R_{Iron} = Stator Core Resistance (Ω)

P_{Iron} = Iron Losses (W)

I_{Phase} = Phase Current (A)

3.2.3. Blocked Rotor Test

The purpose of the blocked rotor test is to determine the rotor resistance (R_R) and the stator and rotor reactance (X_1 & X_2). To perform the blocked rotor test, the rotor of the induction machine is blocked so that it's unable to rotate when the rated current is applied. The results of the blocked rotor test are listed in table 3.4:

Table 3.4: Experimental blocked rotor test results

Parameter	Value
$\mathbf{V_{Phase}}$	57.8 V
$\mathbf{I_{Phase}}$	1.428 A
$\mathbf{P_{in}}$	208 W
PF	0.842

The rotor resistance (R_R) is calculated as follow:

$$\mathbf{Z_{Block}} = \frac{\mathbf{V_{Phase}}}{\mathbf{I_{Phase}}} \tag{3.5}$$

$$\mathbf{Z_{Block}} = \frac{\mathbf{57.8}}{\mathbf{1.428}}$$

$$\mathbf{Z_{Block}} = \mathbf{40.477\ \Omega}$$

Where,

Z_{Block} = Impedance (Ω)

V_{Phase} = Phase Voltage (V)

I_{Phase} = Phase Current (A)

$$\cos\theta = \frac{P_{in}}{3V_{Phase}I_{Phase}} \tag{3.6}$$

$$\cos\theta = \frac{208}{(3)(57.7)(1.428)}$$

$$\cos\theta = 0.841$$

Where,

$\cos\theta$ = Power Factor

P_{in} = Input Power (W)

V_{Phase} = Phase Voltage (V)

I_{Phase} = Phase Current (A)

$$R_S + R_R = (Z_{Block})\cos\theta \tag{3.7}$$

$$21 + R_R = (40.477)\,(0.841)$$

$$R_R = 13.04\ \Omega$$

Where,

R_S = Stator Resistance (Ω)

R_R = Rotor Resistance (Ω)

Z_{Block} = Impedance (Ω)

$\cos\theta$ = Power Factor

The stator and rotor reactance (X_1 & X_2) are calculated as follow:

$$\mathbf{Z_{Block}} = \frac{\mathbf{V_{Phase}}}{\mathbf{I_{Phase}}} \tag{3.8}$$

$$\mathbf{Z_{Block}} = \frac{\mathbf{57.8}}{\mathbf{1.2 - \mathit{j}0.773}}$$

$$\mathbf{Z_{Block} = 34.040 + \mathit{j}21.899\ \Omega}$$

Where,

Z_{Block} = Impedance (Ω)

V_{Phase} = Phase Voltage (V)

I_{Phase} = Phase Current (A)

j = Imaginary Number

$$\mathbf{X_1 = X_2 = \frac{R_\mathit{j}}{2}} \tag{3.9}$$

$$\mathbf{X_1 = X_2 = \frac{21.899}{2}}$$

$$\mathbf{X_1 = X_2 = 10.949\ \Omega}$$

Where,

X_1 = Stator Reactance (Ω)

X_2 = Rotor Reactance (Ω)

R*j* = Resistance

3.3. EXCITATION CAPACITORS

Excitation capacitors are used by the induction generator to generate the rated voltage under a specific load. The calculations for the required excitation capacitance for this system is shown below [13]:

$$\mathbf{Q_{Phase} = \frac{Q_{Total}}{3}} \tag{3.10}$$

$$\mathbf{Q_{Phase} = \frac{924}{3}}$$

$$\mathbf{Q_{Phase} = 308\ VAR}$$

Where,

Q_{Phase} = Reactive Power per Phase (VAR)

Q_{Total} = Total Reactive Power (VAR) - Obtained value from laboratory tests

$$\mathbf{I_{Phase} = \frac{Q_{Phase}}{V_{Phase}}} \tag{3.11}$$

$$\mathbf{I_{Phase} = \frac{308}{230}}$$

$$\mathbf{I_{Phase} = 1.333\ A}$$

Where,

I_{Phase} = Phase Current (A)

Q_{Phase} = Reactive Power per Phase (VAR)

V_{Phase} = Phase Voltage (V)

$$C_1 = \frac{I_{Phase}}{2\pi f V_{Phase}} \quad (3.12)$$

$$C_1 = \frac{1.333}{(2\pi)(50)(230)}$$

$$C_1 = 18.38\ \mu F$$

Where,

C_1 = Capacitor 1 (μF)

I_{Phase} = Phase Current (A)

f = Frequency (Hz)

V_{Phase} = Phase Voltage (V)

$$C_2 = 2C_1 \quad (3.13)$$

$$C_2 = (2)(18.38)$$

$$C_2 = 36.77\ \mu F$$

Where,

C_2 = Capacitor 2 (μF)

C_1 = Capacitor 1 (μF)

3.4. SEIG CONNECTION

A three-phase induction generator is connected in delta together with two capacitors in the C-2C configuration to supply single-phase loads as shown in figure 3.1. It is very important to connect capacitor C2 across phases b and c in order for the induction generator to run as a balanced system. By converting from a three-phase output to a single-phase output the induction generator will produce approximately 80% of its rating [24].

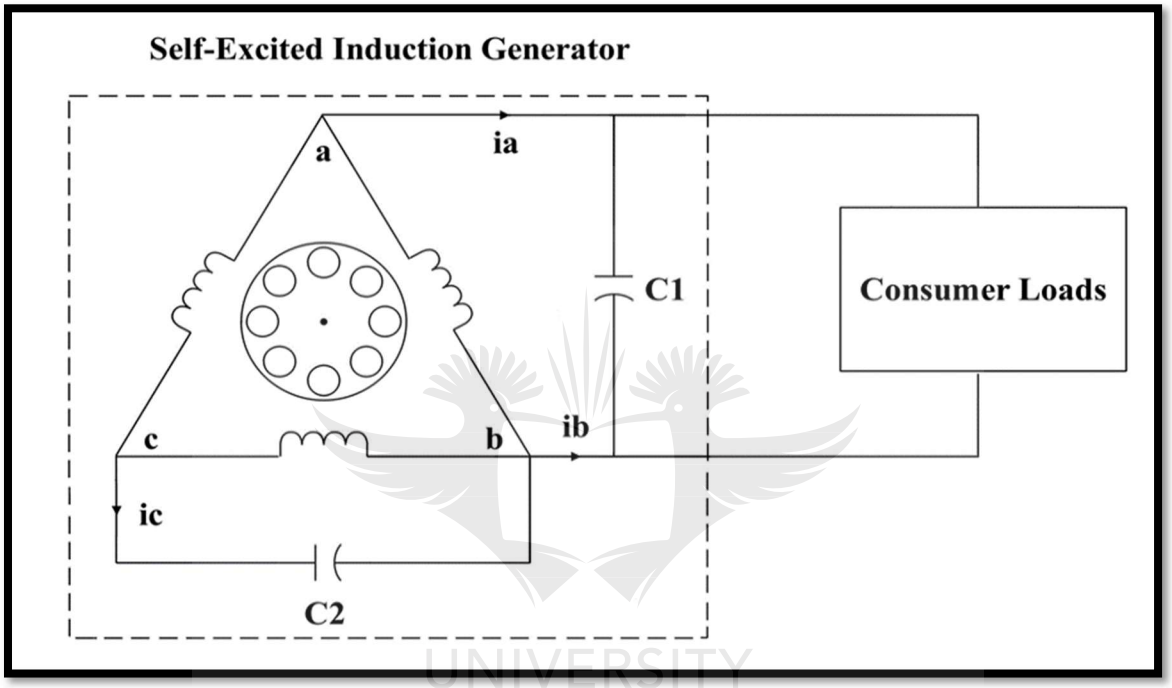

Figure 3.1: SEIG connection

3.5. SEIG SIMULATION MODEL

A SEIG simulation model as shown in figure 3.2 was developed using MATLAB/SIMULINK. The simulation model parameters of the SEIG are derived from the no-load and blocked rotor tests. This model was specifically developed to simulate and observe the voltage build-up of the induction generator at asynchronous speed.

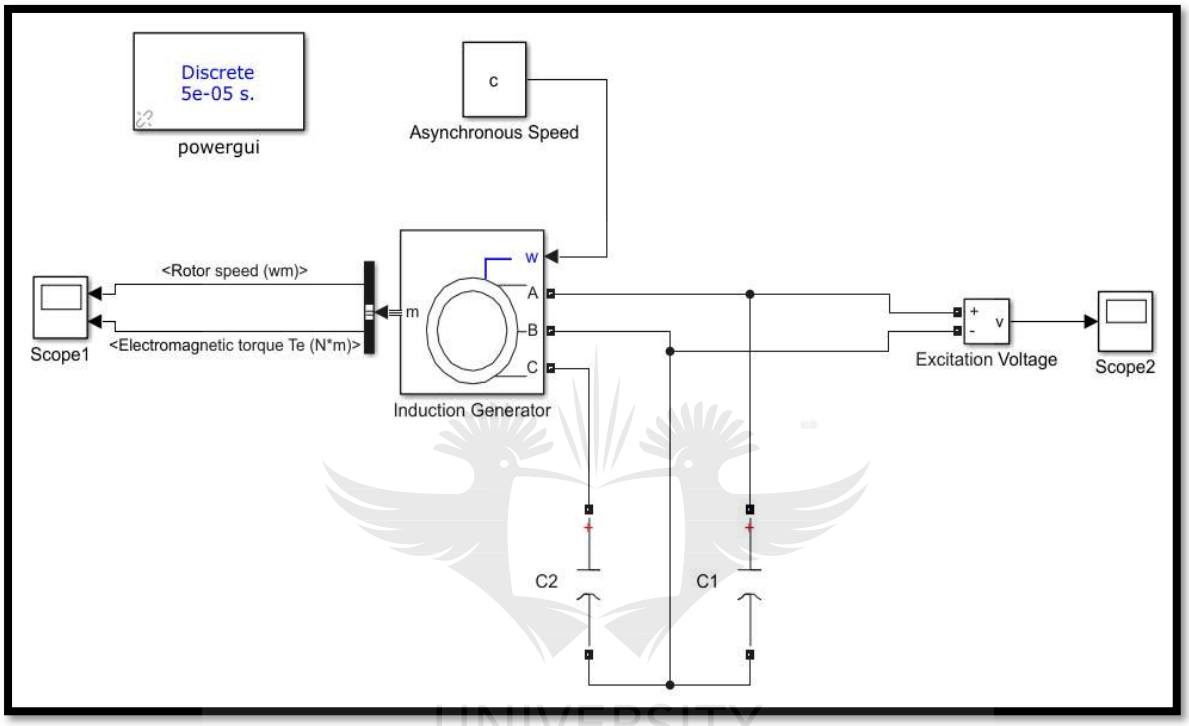

Figure 3.2: SEIG simulation model

The voltage build-up of the induction generator is shown in figure 3.3. A steady state voltage of 230 V is reached within 4 seconds.

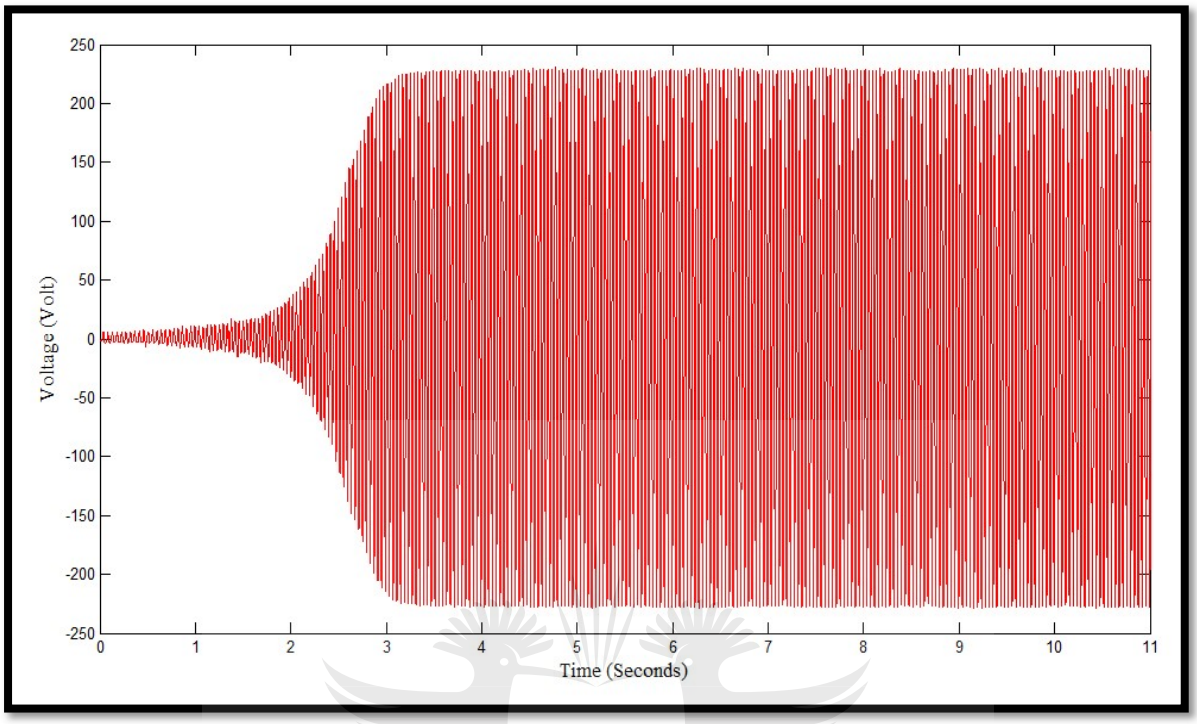

Figure 3.3: SEIG simulation voltage build-up

3.6. SEIG EXPERIMENTAL MODEL

The experimental setup is shown in figure 3.4 where the self-excited induction generator is driven by a prime mover. A variable speed drive (VSD) is used to control the speed of the prime mover. The experimental model is used to validate the results obtained from the simulation model.

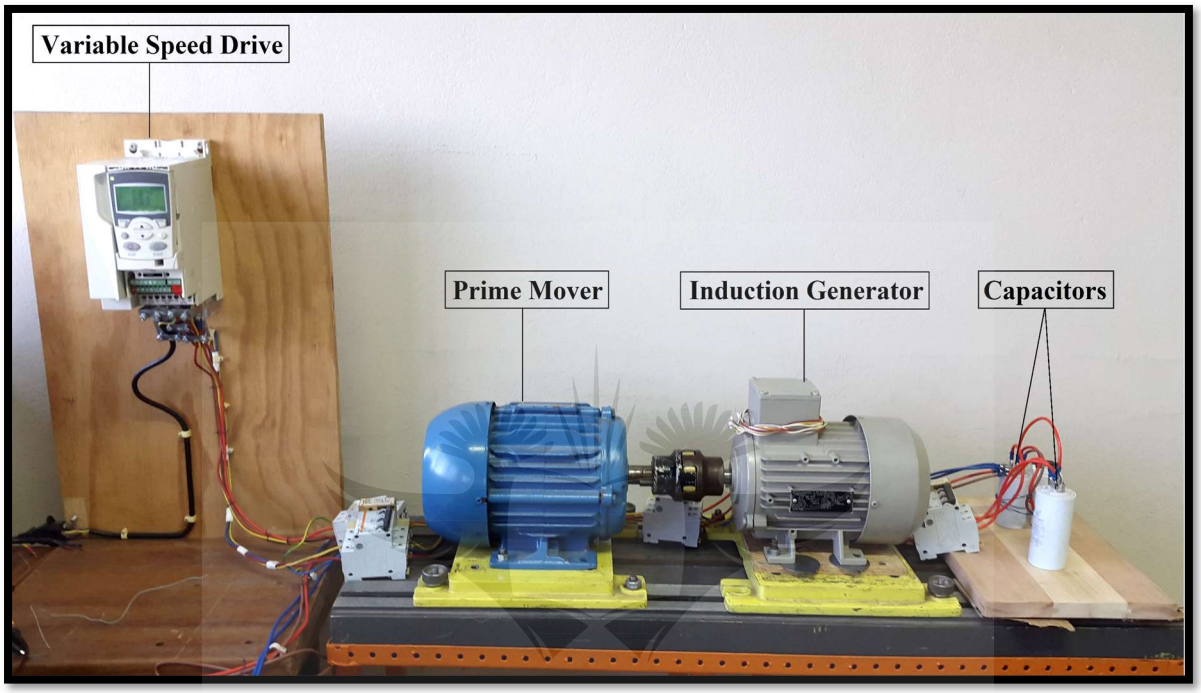

Figure 3.4: SEIG experimental model

The prime mover nameplate parameters are listed in table 3.5:

Table 3.5: Experimental prime mover nameplate parameters

3-Phase Induction Motor		
	Y	**Δ**
Phase	3	3
Frequency (Hz)	50	50
Voltage (V)	400	230
Current (A)	2.66	4.63
Power (W)	1100	1100
Speed (RPM)	1420	1420
Power Factor	0.79	0.79

The voltage build-up of the induction generator is shown in figure 3.5. A steady state voltage of 230 V is reached within 4 seconds.

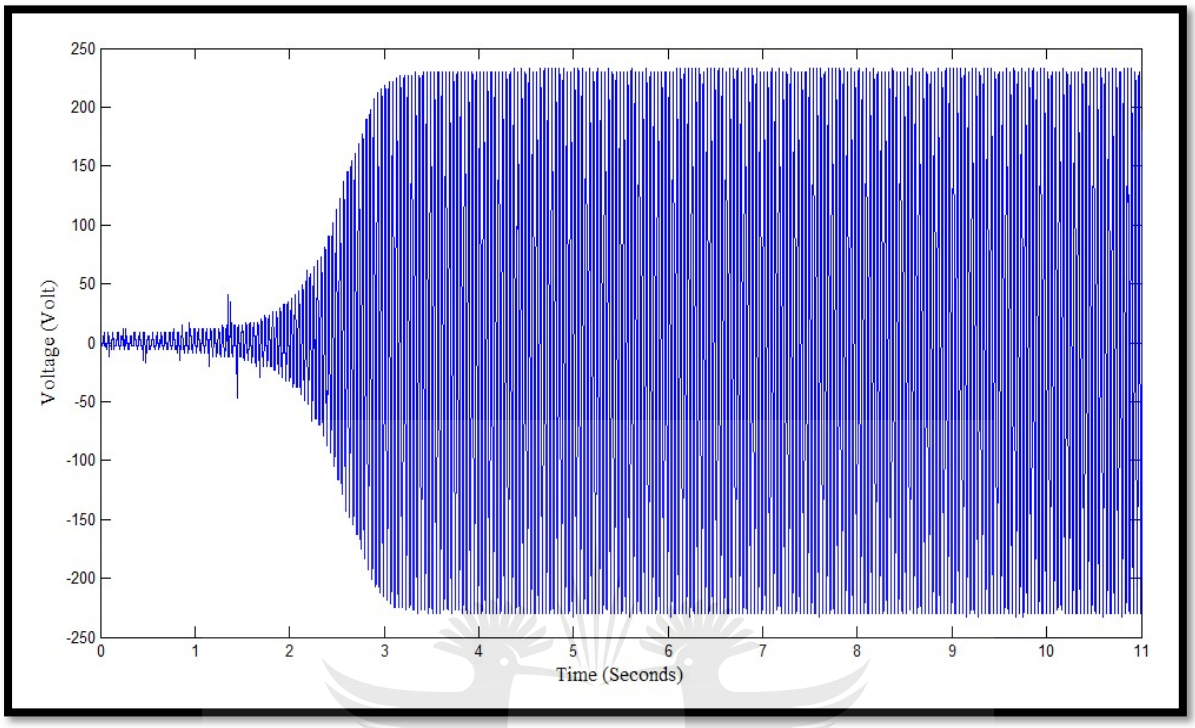

Figure 3.5: SEIG experimental voltage build-up

CHAPTER 4
DESIGN OF ELECTRONIC LOAD CONTROLLER

4.1. INTRODUCTION

This chapter presents the design and development of both the hardware-in-the-loop simulation model and experimental configuration of an Intelligent Electronic Load Controller using a fuzzy logic control method.

4.2. ELECTRONIC LOAD CONTROLLER COMPONENTS

The designed Electronic Load Controller consist of the following components as shown in figure 4.1:

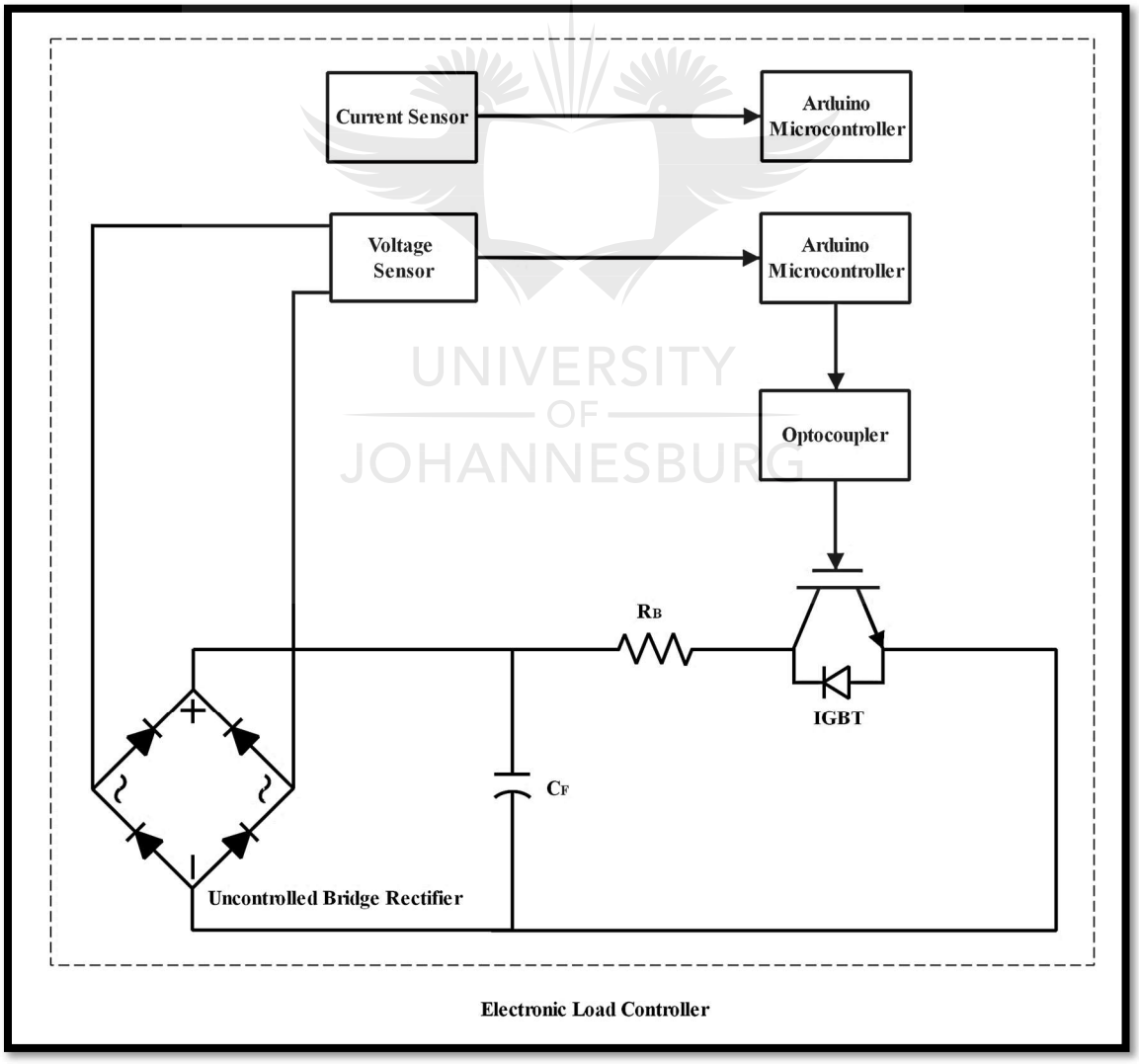

Figure 4.1: Electronic Load Controller

4.2.1. Voltage Sensor

The voltage sensor is connected to an Arduino microcontroller used to sense the terminal voltage produced by the self-excited induction generator and consist of the following components as shown in figure 4.2:

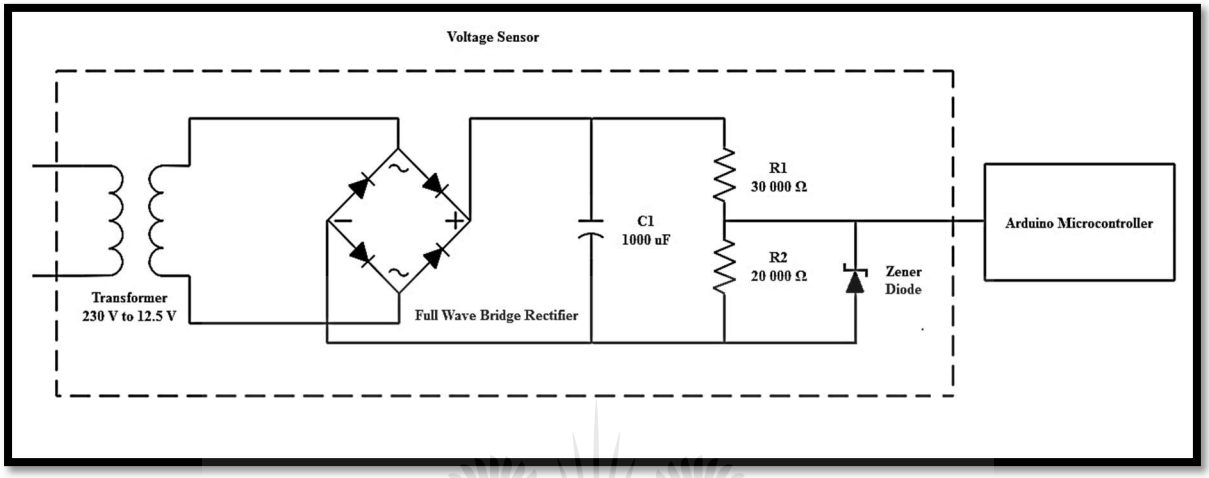

Figure 4.2: Voltage sensor

- **Step-Down Transformer:** A step-down transformer with a ratio of 92:5 is used to convert the 230 V AC produced by the SEIG to 12.5 V AC.
- **Full Wave Bridge Rectifier:** A full wave bridge rectifier is used to rectify the 12.5 V AC produced by the step-down transformer to 12.5 V DC.
- **Filtering Capacitor:** A 1000 µF 25 V electrolytic filtering capacitor is connected across the full wave bridge rectifier to filter out ripples that the output voltage contains in order to supply an almost constant DC voltage.

- **Voltage Divider:** A voltage divider consisting of two resistors R_1 and R_2 are connected in series across the output of the 12.5 V DC supply voltage. The 12.5 V DC supply voltage is divided between the two resistances to give a 5 V DC output across R_2, which is fed to the analog input of the Arduino microcontroller. Equation 4.1 is used for the voltage divider circuit:

$$\mathbf{V_O = \frac{V_S R_2}{(R_1+R_2)}} \qquad \textbf{(4.1)}$$

Where,

V_O = Output Voltage (V)

V_S = Supply Voltage (V)

R_1 = Resistor 1 (Ω)

R_2 = Resistor 2 (Ω)

- **Zener Diode:** A 5.1 V Zener diode (see Appendix A.1.) is connected after the voltage divider circuit in order to provide additional protection against overvoltage for the Arduino input pins.

4.2.2. Current Sensor

The current sensor (see Appendix A.2.) is connected to a second Arduino microcontroller used to sense the current of the system. The reason for using an additional Arduino microcontroller for measuring purposes is that the first Arduino microcontroller consumes a lot of memory for the measurement and control of the system. A Hall-Effect current sensor is used to measure the current of the system. A 5.1 V Zener diode (see Appendix A.1.) is connected to provide additional protection for the Arduino input pins. The Arduino microcontroller can only handle voltage inputs (0 V – 5 V). Due to this reason, the current being measured must be converted to a voltage, this is accomplished by adding in a burden resistor. A voltage divider is added to the current sensor circuit in order to measure negative voltage, as the Arduino microcontroller is unable to measure negative voltage directly. Both resistors are equal to each other in order to divide the 5 V from the Arduino microcontroller by 2. The Arduino microcontroller will sense the following:

- 0 V as the maximum negative AC voltage for maximum negative AC current
- 2.5 V as zero AC voltage for zero AC current
- 5 V as the maximum positive AC voltage for maximum AC current

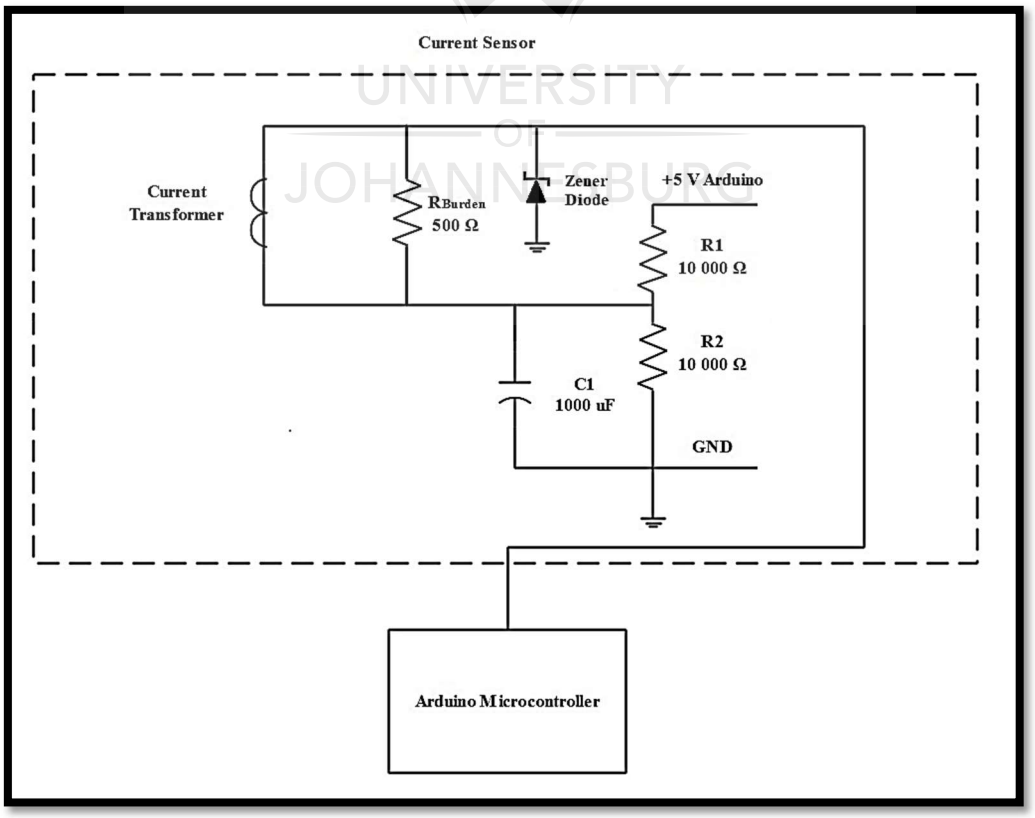

Figure 4.3: Current sensor

4.2.3. Arduino Microcontroller

An Arduino Mega 2560 microcontroller (see Appendix A.3.) is used to provide control to the system. The Arduino Mega 2560 microcontroller consist of the following important technical specifications [25]:

- Microcontroller — ATmega2560
- Operating Voltage — 5 V
- Input Voltage (recommended) — 7 – 12 V Input
- Voltage (limits) — 6 – 20 V
- Digital I/O Pins — 54 (of which 14 provide PWM output)
- Analog Input Pins — 16
- DC Current per I/O Pin — 40 mA
- DC Current for 3.3V Pin — 50 mA
- Flash Memory — 256 KB of which 8 KB is used by bootloader
- SRAM — 8 KB
- EEPROM — 4 KB
- Clock Speed — 16 MHz

The Arduino microcontroller used for this system is shown in figure 4.4:

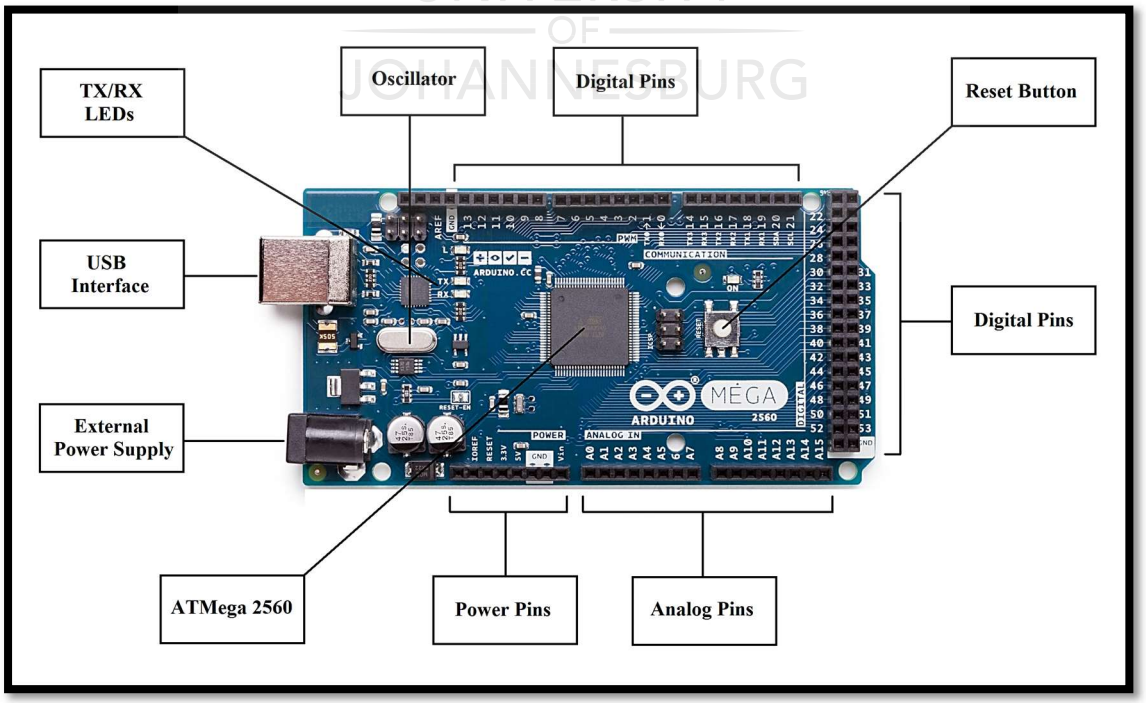

Figure 4.4: Arduino mega 2560 microcontroller [25]

4.2.4. Programming of Arduino Microcontroller – Voltage

MATLAB/SIMULINK was used to program the 1st Arduino microcontroller. The voltage of the system is fed to analog input pin 0 of the Arduino microcontroller. The analog values are converted into digital values by the Arduino microcontroller. The Arduino microcontroller generates a 10-bit value, ranging from 0 – 1023 for the analog inputs. This means that when the Arduino microcontroller senses 1023, the analog inputs equal 100% of the measured voltage. When the Arduino microcontroller senses 511.5, the analog inputs equal 50% of the measured voltage. When the Arduino microcontroller senses 0, the analog inputs equal 0% of the measured voltage. A gain function is used to scale down the 0 – 1023 values of the voltage input, in order to display the correct values being measured. The 1st gain function (Gain) is as follow: 0 – 1023 is scaled to 0 – 240 V. The actual measured voltage value is then compared with the reference voltage of 220 V. An error signal and change in error signal is generated after the comparison. These 2 signals are then multiplexed and fed to the fuzzy logic controller block. The fuzzy logic controller block generates an appropriate PWM output signal that is sent to the PWM output pin 8 of the Arduino microcontroller. A gain function is used to scale up the 0 – 1 values produced by the fuzzy logic controller block. The 2nd gain function (Gain1) is as follow: 0 – 1 is scaled to 0 – 255. The Arduino microcontroller generates an 8-bit value, ranging from 0 – 255 for the PWM output. This means that when the Arduino microcontroller generates a PWM output of 255, the PWM signal has a 100% duty cycle. When the Arduino microcontroller generates a PWM output of 127.5, the PWM signal has a 50% duty cycle. When the Arduino microcontroller generates a PWM output of 0, the PWM signal has a 0% duty cycle. The voltage programming model is shown in figure 4.5:

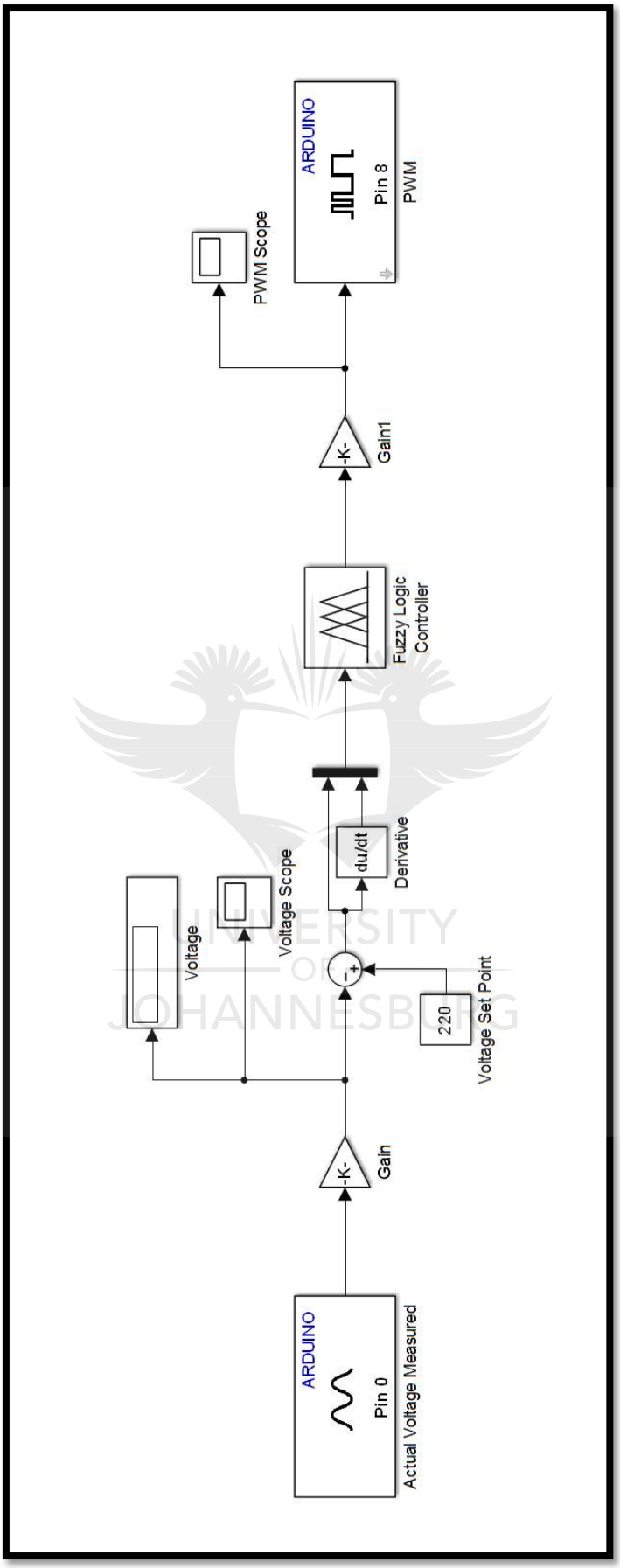

Figure 4.5: Arduino microcontroller programming model – Voltage

4.2.5. Programming of Arduino Microcontroller – Current

MATLAB/SIMULINK was used to program the 2nd Arduino microcontroller. The current of the system is fed to analog input pin 0 of the arduino microcontroller. The analog values are converted into digital values by the Arduino microcontroller. The Arduino microcontroller generates a 10-bit value, ranging from 0 – 1023 for the analog inputs. This means that when the Arduino microcontroller senses 1023, the analog inputs equal 100% of the measured current. When the Arduino microcontroller senses 511.5, the analog inputs equal 50% of the measured current. When the Arduino microcontroller senses 0, the analog inputs equal 0% of the measured current. A gain function is used to scale down the 0 – 1023 values of the current inputs, in order to display the correct values being measured. The gain function (Gain) is as follow: 0 – 1023 is scaled to 0 – 5 A. The current programming model is shown in figure 4.6:

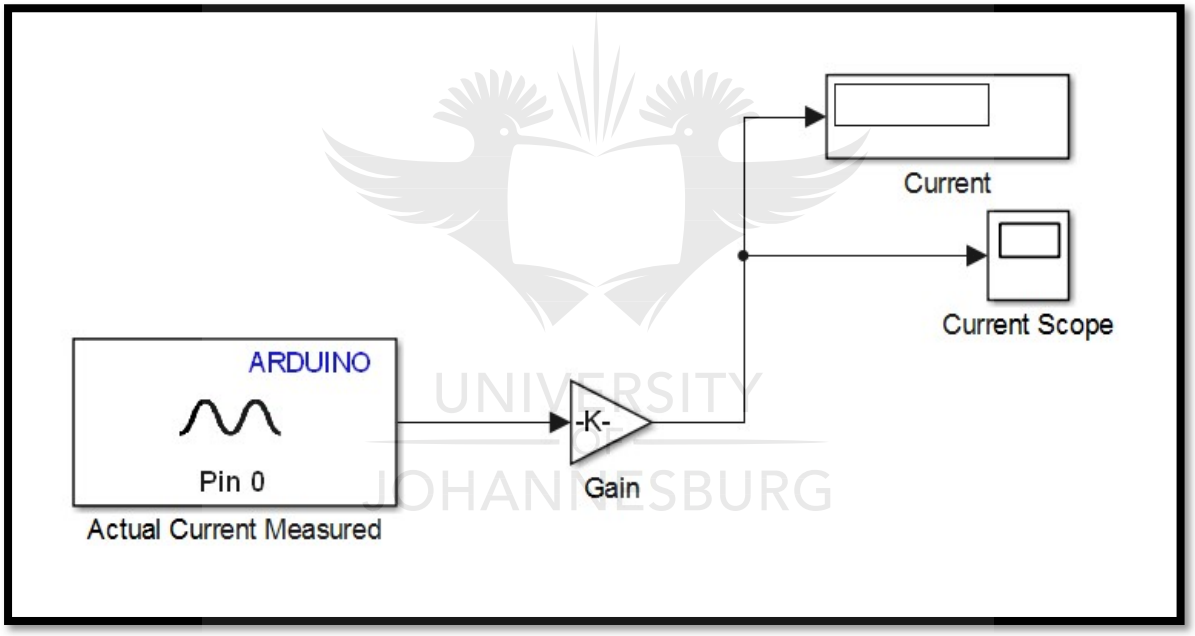

Figure 4.6: Arduino microcontroller programming model – Current

4.2.6. Optocoupler

A TLP250 optocoupler (see Appendix A.4.) is used as a gate driving circuit of the IGBT. An optocoupler is an electronic component that uses light to transfer electrical signals between two isolated circuits. The optocoupler consist of an input stage, an output stage and a power supply connection. The input stage consists of an infrared LED that is triggered by the Arduino microcontroller. The intensity of the infrared light being emitted is proportional to the PWM signal produced by the Arduino microcontroller. The output stage consists of a phototransistor. As soon as the LED starts to emit infrared light, a phototransistor switches on and produce the same voltage applied to its collector pin by the power supply. A ceramic capacitor (0.1 µF) must be connected across the power supply to stabilize the operation of the high gain linear amplifier. The ceramic capacitor must also be placed as close as possible to the optocoupler [26]. The ground of the input stage and the output stage must be different for isolation purposes.

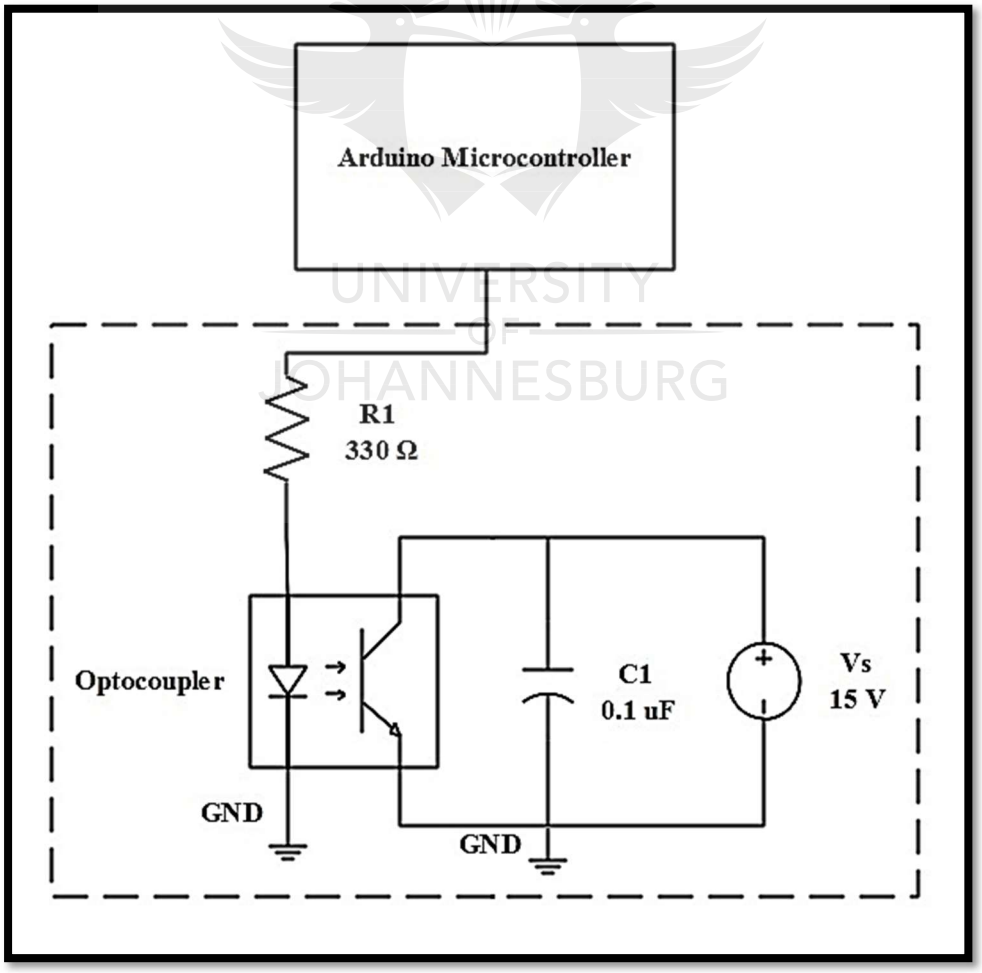

Figure 4.7: Optocoupler circuit

4.2.7. Insulated Gate Bipolar Transistor

An Insulated Gate Bipolar Transistor (IGBT) (see Appendix A.5.) is used as the chopper switch (switching device) of the system. The IGBT will switch the supply voltage (uncontrolled bridge rectifier) on and off according to the duty cycle of the PWM signal that the Arduino microcontroller generates.

4.2.8. Uncontrolled Bridge Rectifier

An uncontrolled bridge rectifier is used to rectify the 230 V AC produced by SEIG to 230 V DC.

4.2.9. Filtering Capacitor

A 330 μF 250 V electrolytic filtering capacitor (see equation 4.10) is connected across the uncontrolled bridge rectifier to filter out ripples that the output voltage contains in order to supply an almost constant DC voltage.

4.2.10. Ballast Load

A purely resistive ballast load is connected to the system to dump surplus power that is not required or used. By using a purely resistive ballast load, enables the self-excited induction generator to operate at a unity power factor.

4.3. FUZZY LOGIC DESIGN

A fuzzy logic system is designed using the MATLAB Fuzzy Logic Toolbox. A fuzzy logic system consists of the following four main parts used in the design procedure:

- Fuzzification
- Rule base
- Inference Engine
- Defuzzification

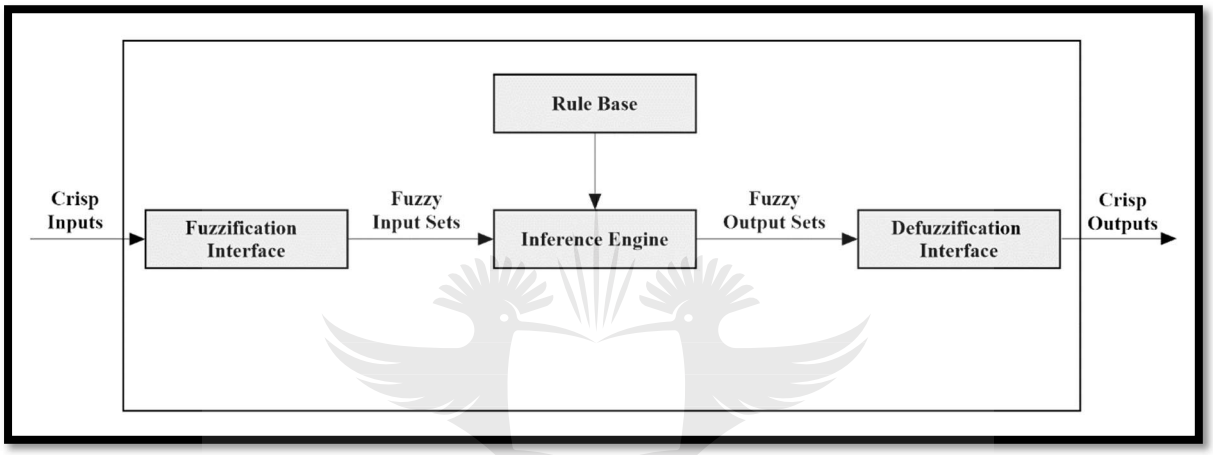

Figure 4.8: Fuzzy logic system

4.3.1. Fuzzification Design

This fuzzy logic system consists of two inputs. The 1st input is error (e_k), which is the difference between the voltage set point (V_{SP}) and the actual voltage measured (V_{MS}), the 2nd input is change in error (Δe_k), which is the difference between the current voltage error (e_k) and the previous voltage error (e_{k-1}). The following equations describes the two inputs:

$$e_k = V_{SP} - V_{MS} \quad (4.2)$$

$$\Delta e_k = e_k - e_{k-1} \quad (4.3)$$

Both inputs consist of nine triangular membership functions as shown in figure 4.9 and figure 4.10. A triangular membership function is a collection of 3 points forming a triangle using straight lines. Triangular membership functions are often used due to its simplicity, accuracy and efficiency.

For the two inputs these triangular membership functions are:

- Negative Big (NB)
- Negative Medium (NM)
- Negative Small (NS)
- Negative Very Small (NVS)
- Zero (Z)
- Positive Very Small (PVS)
- Positive Small (PS)
- Positive Medium (PM)
- Positive Big (PB)

The input range of the fuzzy logic system is between -20 and 20.

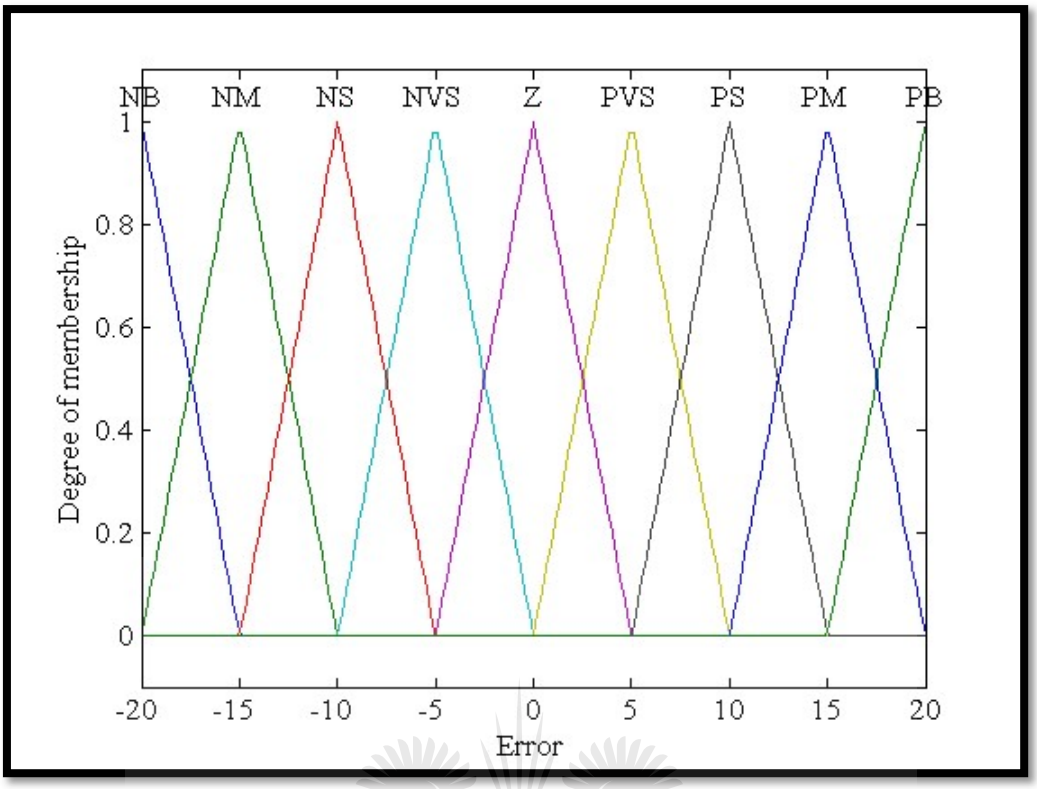

Figure 4.9: Error membership functions

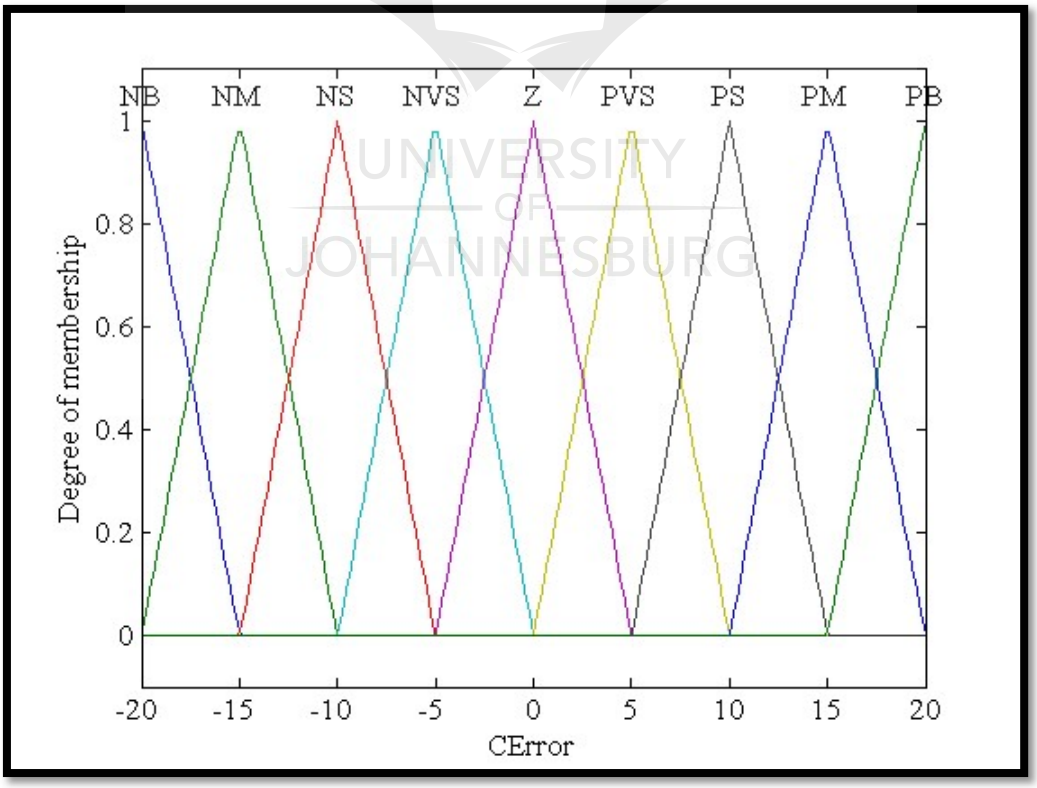

Figure 4.10: Change of error membership functions

4.3.2. Rule Base Design

The rule base for a fuzzy logic system is built upon IF-THEN statements. An example of these conditional statements used for control is if the error (e_k) is negative big (NB) and the change in error (Δe_k) is negative big (NB), then the controller should send a positive big (PB) output signal to bring the voltage of the system to the set point. If the error (e_k) is negative small (NS) and the change in error (Δe_k) is negative medium (NM), then the controller should send a positive medium (PM) output signal to bring the voltage of the system to the set point. If the error (e_k) is positive big (PB) and the change in error (Δe_k) is positive big (PB), then the controller should send a negative big (NB) output signal to bring the voltage of the system to the set point.

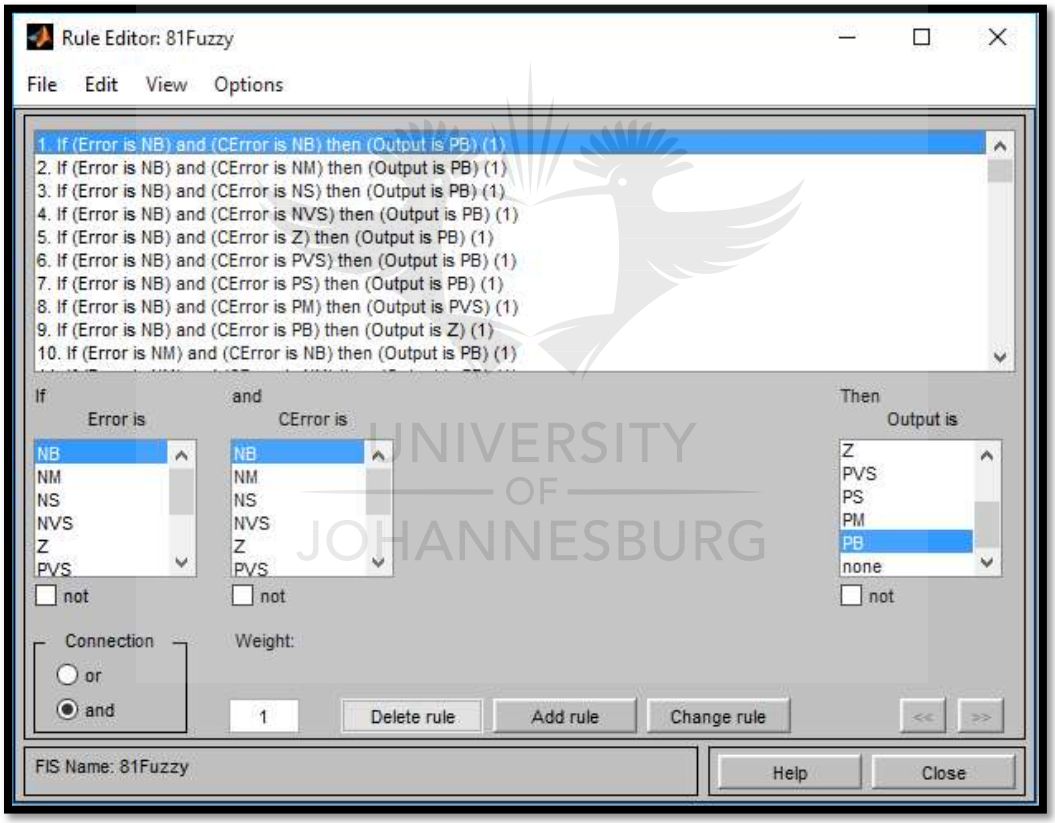

Figure 4.11: Fuzzy rule editor

The rule base design for the fuzzy logic system contains 81 fuzzy rules, as shown in table 4.1:

Table 4.1: Rule base design for fuzzy logic system

e_k / Δe_k	NB	NM	NS	NVS	Z	PVS	PS	PM	PB
NB	PB	PB	PB	PB	PB	PB	PB	PVS	Z
NM	PB	PB	PM	PM	PM	PS	PVS	Z	NVS
NS	PB	PM	PM	PM	PS	PVS	Z	NVS	NS
NVS	PB	PM	PM	PS	PVS	Z	NVS	NS	NB
Z	PB	PM	PS	PVS	Z	NVS	NS	NM	NB
PVS	PB	PS	PVS	Z	NVS	NS	NM	NM	NB
PS	PS	PVS	Z	NVS	NS	NM	NM	NM	NB
PM	PVS	Z	NVS	NS	NM	NM	NB	NB	NB
PB	Z	NVS	NS	NB	NB	NB	NB	NB	NB

4.3.3. Inference Engine

The Takagi-Sugeno-Kang inference system develops a systematic approach in order to generate fuzzy rules from the input-output data sets. This inference system is used in the design due to its computational efficiency, flexibility in design and improvement in response to fast-changing variables [27].

4.3.4. Defuzzification Design

The defuzzification method used to obtain crisp output values from the inference engine is the weighted average method. The weighted average method is chosen due to its computational efficiency. This fuzzy logic system consists of one output. The output (O) produces pulse width modulation (PWM) signals used for system control. The output consists of nine singleton membership functions as shown in figure 4.12. For the one output these membership functions are:

- Negative Big (NB)
- Negative Medium (NM)
- Negative Small (NS)
- Negative Very Small (NVS)
- Zero (Z)
- Positive Very Small (PVS)
- Positive Small (PS)
- Positive Medium (PM)
- Positive Big (PB)

The output range of the fuzzy logic system is between 0 and 255.

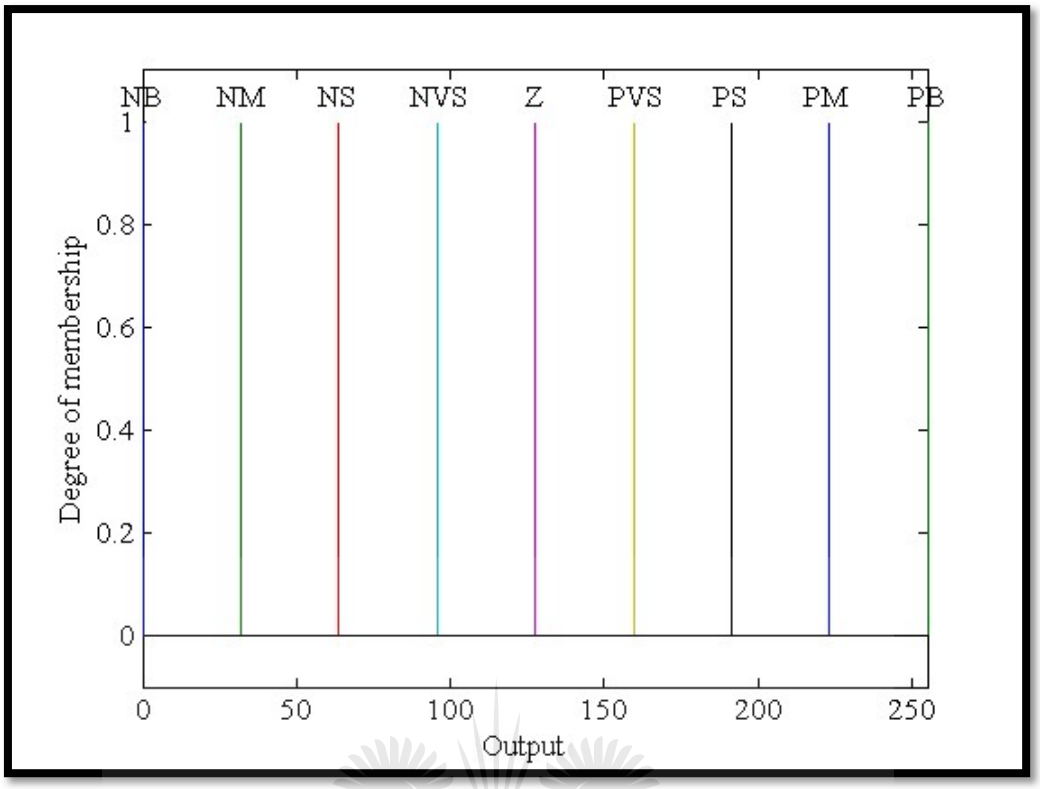

Figure 4.12: Output membership functions

4.4. FUZZY LOGIC CONTROL SURFACE

The control surface of the fuzzy logic system gives the two input membership functions and the output membership functions guided by the 81 fuzzy rules. The behaviour of the control surface matches the rule base design. The control surface of the fuzzy logic system is shown in figure 4.13:

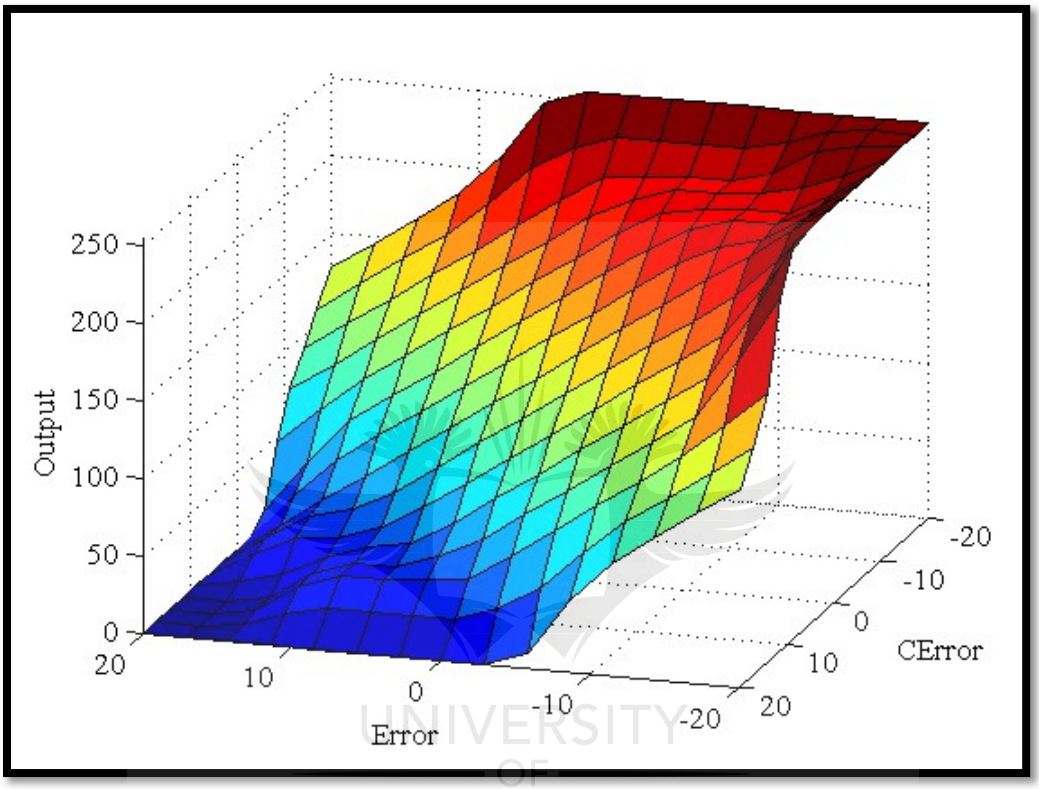

Figure 4.13: Control surface of the fuzzy logic system

4.5. ELECTRONIC LOAD CONTROLLER CALCULATIONS

The following calculations were performed to design the components of the Electronic Load Controller [18]:

4.5.1. Power Calculation

The power produced by the generator is kept constant by increasing the ballast load power to compensate for any drop in the consumer power.

$$\mathbf{P_G = P_B + P_C} \tag{4.4}$$

Where,

P_G = Generated Power (W)

P_B = Ballast Load Power (W)

P_C = Consumer Load Power (W)

4.5.2. Uncontrolled Rectifier and Chopper Switch Voltage Rating

The voltage rating of the uncontrolled bridge rectifier and chopper switch (IGBT) will be the same. The DC output voltage is calculated as:

$$\mathbf{V_{DC} = \frac{2\sqrt{2}V_L}{\pi}} \tag{4.5}$$

$$\mathbf{V_{DC} = \frac{(2)(\sqrt{2})(230)}{\pi}}$$

$$\mathbf{V_{DC} = 207.07\ V}$$

Where,

V_{DC} = DC Voltage (V)

V_L = AC Input Voltage (V)

An overvoltage of 10% of the rated voltage is considered for the transient state and is calculated as:

$$\mathbf{V_{DC(10\%)} = \sqrt{2}(V_L + (10\% \text{ of } V_L))} \quad \textbf{(4.6)}$$

$$\mathbf{V_{DC(10\%)} = \sqrt{2}(230 + (10\% \text{ of } 230))}$$

$$\mathbf{V_{DC(10\%)} = 367.80\ V}$$

Where,

$V_{DC(10\%)}$ = 10% DC Overvoltage (V)

V_L = AC Input Voltage (V)

4.5.3. Uncontrolled Rectifier and Chopper Switch Current Rating

The current rating of the uncontrolled bridge rectifier and chopper switch (IGBT) is calculated as:

$$\mathbf{I_{AC} = \frac{P}{V_L}} \quad \textbf{(4.7)}$$

$$\mathbf{I_{AC} = \frac{550}{230}}$$

$$\mathbf{I_{AC} = 2.39\ A}$$

Where,

I_{AC} = AC Current (A)

P = Power from SEIG (W)

V_L = AC Input Voltage (V)

$$I_{Peak} = \frac{2I_{AC}}{0.9} \quad (4.8)$$

$$I_{Peak} = \frac{(2)(2.39)}{0.9}$$

$$I_{Peak} = 5.31 \text{ A}$$

Where,

I_{Peak} = AC Peak Current (A)

I_{AC} = AC Current (A)

4.5.4. Ballast Load Resistance Calculation

The rating of the ballast load resistance is calculated as:

$$R_B = \frac{V_{DC}^2}{P} \quad (4.9)$$

$$R_B = \frac{207.07^2}{550}$$

$$R_B = 77.90\ \Omega$$

Where,

R_B = Ballast Load Resistance (Ω)

V_{DC} = DC Voltage (V)

P = Power from SEIG (W)

4.5.5. DC Filter Capacitor Calculation

The DC filter capacitor is calculated as:

$$C = \left(\frac{1}{4fR_B}\right)\left(1 + \frac{1}{\sqrt{2}R_F}\right) \quad (4.10)$$

$$C = \left(\frac{1}{(4)(50)(77.90)}\right)\left(1 + \frac{1}{(\sqrt{2})(0.2)}\right)$$

$$\mathbf{C = 291.09\ \mu F}$$

Where,

C	=	Filter Capacitor (μF)
f	=	Frequency (Hz)
R_B	=	Ballast Load Resistance (Ω)
R_F	=	Ripple Factor (20%)

The nearest commercially available value of 330 μF is selected for the filtering capacitor.

4.6. OPERATING PRINCIPLE OF ELC

A voltage sensor is used to sense the output voltage of the self-excited induction generator. An Arduino microcontroller is used to compare the sensed voltage with the reference voltage of 220 V. An error signal and change in error signal is generated after the comparison. These 2 signals are then multiplexed and fed to the fuzzy logic controller. The fuzzy logic control method is used to process these signals and generate an appropriate output signal. A PWM signal from the Arduino microcontroller is fed to the optocoupler and then to the IGBT. When the gate pulse to the IGBT is high, the current flows through the ballast load and consumes the difference in power, resulting in a constant load on the self-excited induction generator.

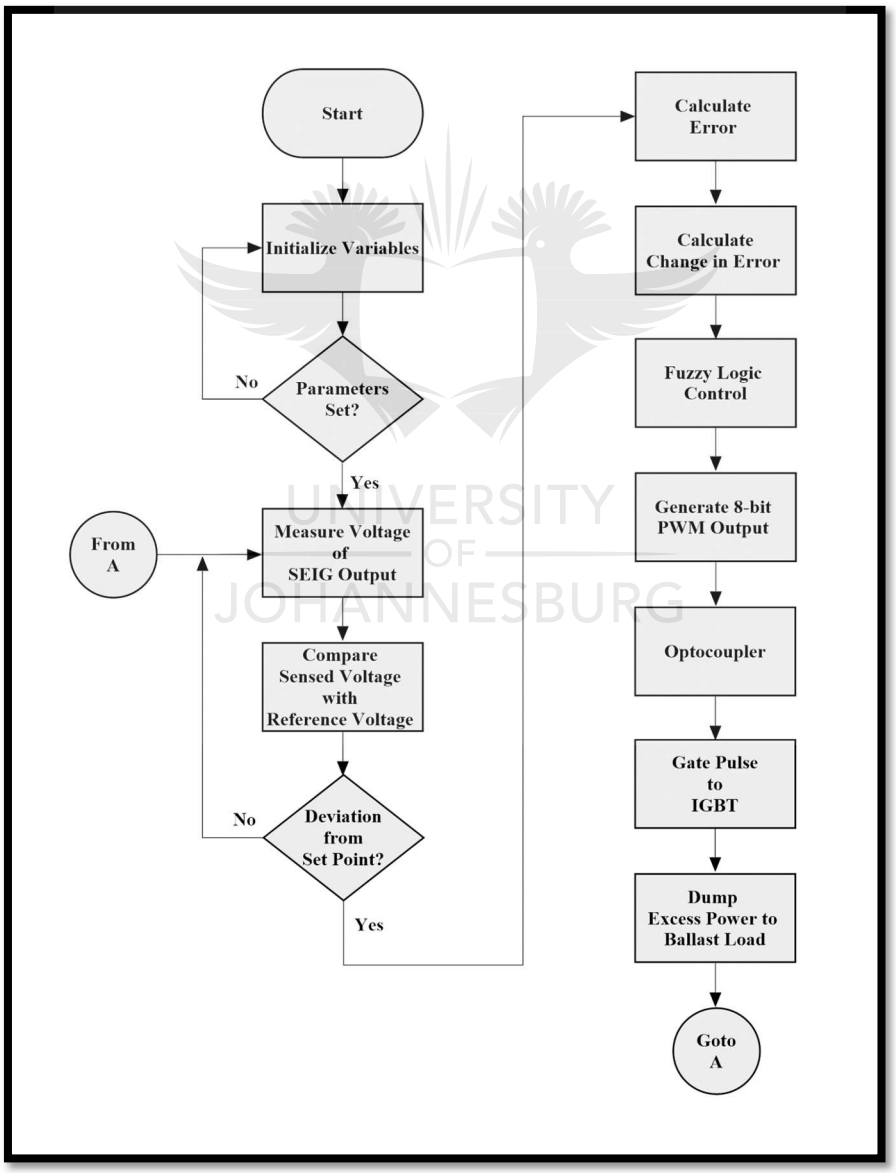

Figure 4.14: ELC operating principle flow chart

4.7. SIMULATION MODEL

A self-excited induction generator model generates voltage at asynchronous speed. Switch 1 and 2 are only switched in once the self-excited induction generator has generated a steady state voltage of 230 V. Various consumer loads were switched in and out in order to validate the operation and performance of the system. A voltage sensor is used to sense the output voltage of the self-excited induction generator. The sensed voltage is then compared with the reference voltage of 220 V. An error signal and change in error signal is generated after the comparison. These 2 signals are then multiplexed and fed to the fuzzy logic controller block. The fuzzy logic controller block generates an appropriate PWM output signal that is sent to the IGBT. When the gate pulse to the IGBT is high, the current flows through the ballast load and consumes the difference in power, resulting in a constant load on the self-excited induction generator. The current of the consumer load and ballast load is measured in order to calculate and monitor the power of these respective loads. The simulation model is shown in figure 4.15:

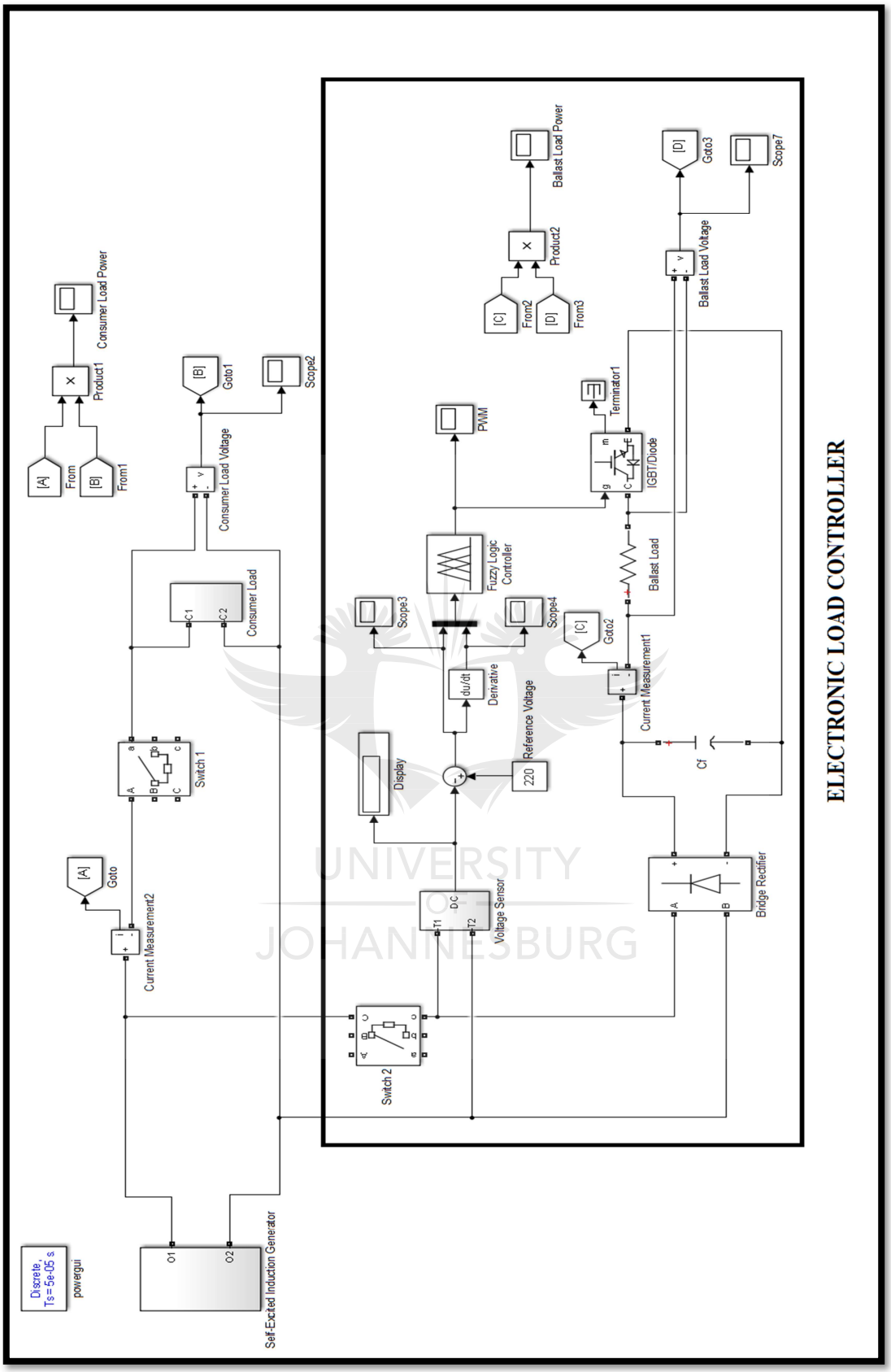

Figure 4.15: Simulation model

CHAPTER 5
RESULTS AND DISCUSSION

5.1. INTRODUCTION

This chapter presents the results from simulation and experimental testing conducted on the Intelligent Electronic Load Controller.

5.2. HARDWARE-IN-THE-LOOP SIMULATION RESULTS

A number of different simulation experiments have been carried out as given in table 5.1 in order to analyse and test the response of the Intelligent Electronic Load Controller to signal changes in real-time using the hardware-in-the-loop method. Hardware-in-the-loop simulation is a type of real-time simulation. In a hardware-in-the-loop simulation, a real-time computer is used as a virtual representation of a plant model (micro-hydropower model) and an actual version of the controller (Arduino microcontroller) to test and analyse the efficiency of the system in real-time.

Table 5.1: Different signal experiments

Different Signal Experiments	
Experiment No	**Signal**
1	210 V
2	230 V
3	240 V

MATLAB/SIMULINK was used to program the 1st Arduino microcontroller and to perform the hardware-in-the-loop simulation. A pre-determined voltage signal is fed to the Arduino microcontroller. The voltage signal value is then compared with the reference voltage of 220 V. An error signal and change in error signal is generated after the comparison. These 2 signals are then multiplexed and fed to the fuzzy logic controller block. The fuzzy logic controller block generates an appropriate output signal that is multiplied with a gain function of 255 and then sent to the PWM output pin 8 of the Arduino microcontroller. The hardware-in-the-loop simulation model is shown in figure 5.1:

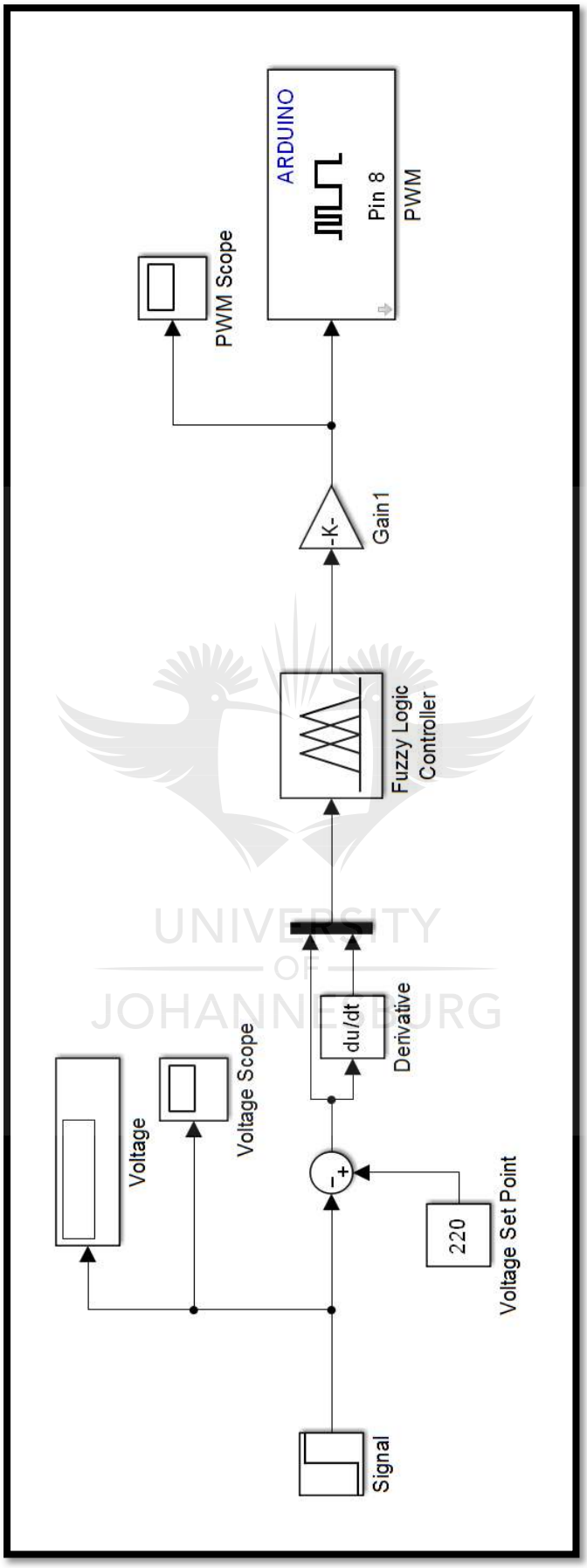

Figure 5.1: Hardware-in-the-loop simulation model

5.2.1. Experiment 1: 210 V Input Signal

The objective of experiment 1 was to send a 210 V signal to the Arduino microcontroller and observe how the ELC responds to the input signal. The experiment was divided into two time-periods as indicated on both figures. In figure 5.2 (input voltage signal), time-period A illustrates a constant voltage of 220 V. Time-period B illustrates a signal change at 5.60 seconds from 220 V to 210 V. The signal value of 210 V was reached at 5.65 seconds. In figure 5.3 (control output response), time-period A illustrates a constant control output signal of 127.5. Time-period B illustrates a change in the control output signal due to the change in the voltage. At 5.65 seconds the control output signal changes from 127.5 to 63.75. The control output signal value of 63.75 was reached at 5.70 seconds. It was observed that Intelligent Electronic Load Controller responds efficiently to changes in the voltage of the system.

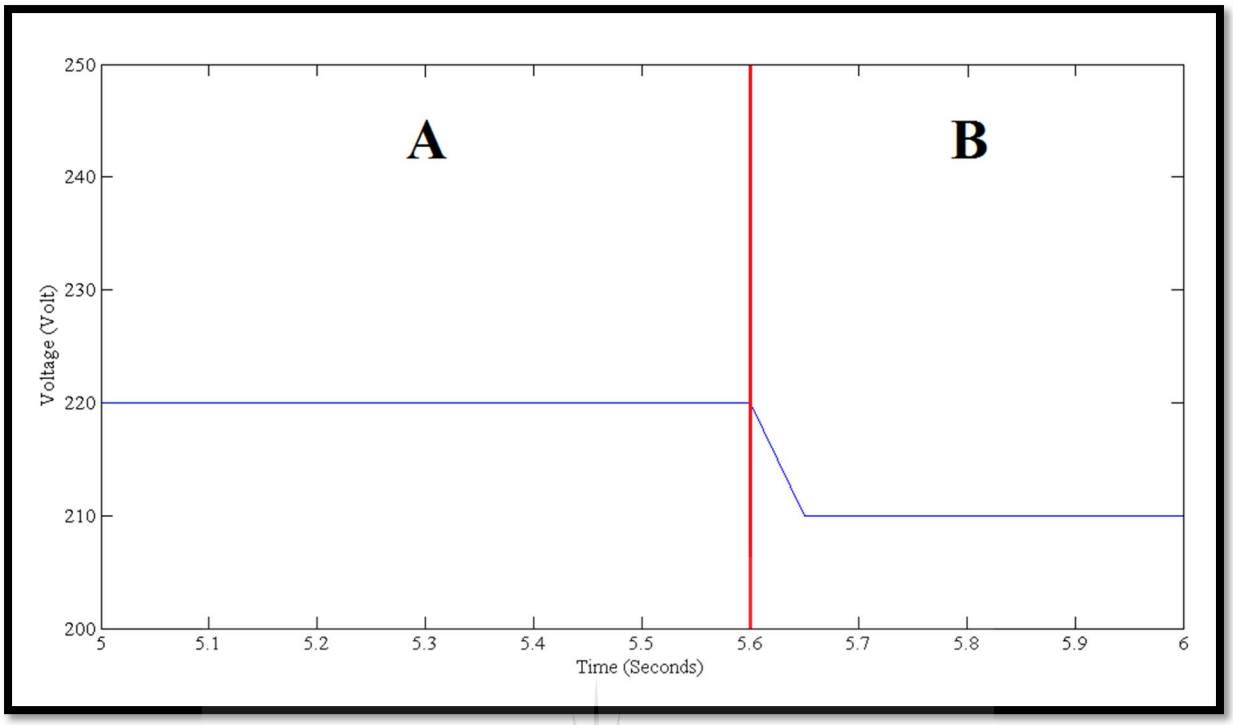

Figure 5.2: 210 V input signal

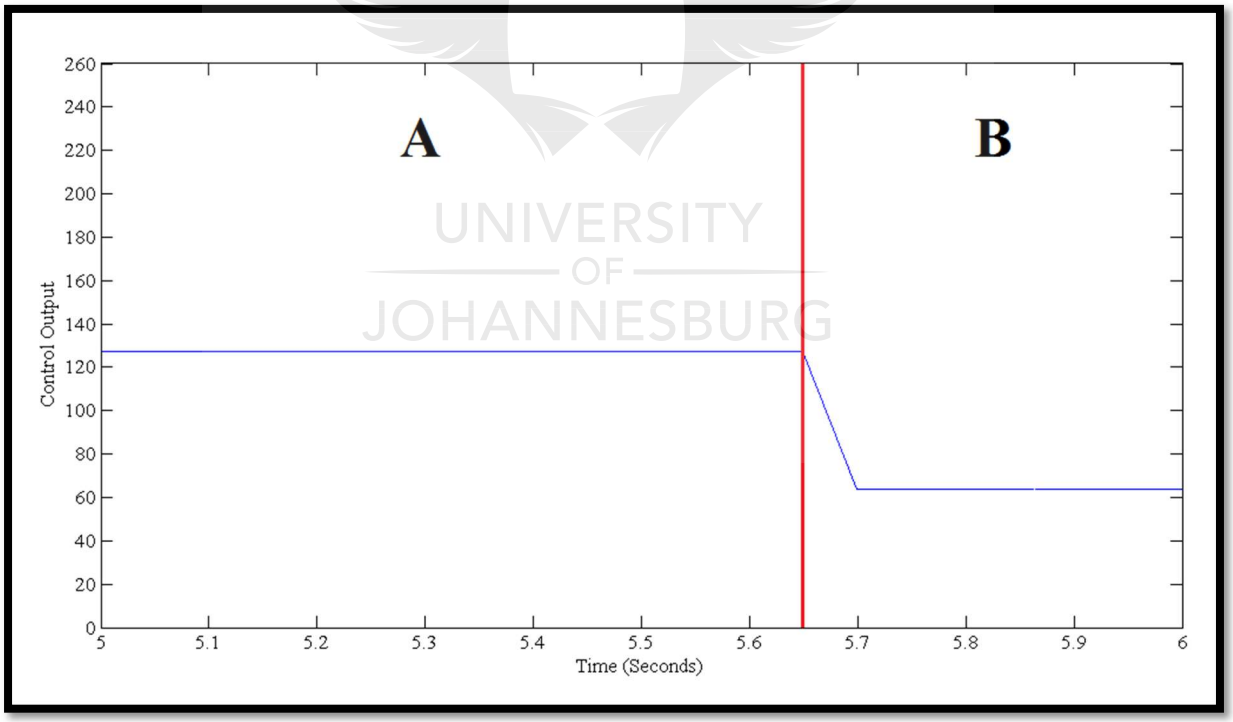

Figure 5.3: Control output response to 210 V input signal

5.2.2. Experiment 2: 230 V Input Signal

The objective of experiment 2 was to send a 230 V signal to the Arduino microcontroller and observe how the ELC responds to the input signal. The experiment was divided into two time-periods as indicated on both figures. In figure 5.4 (input voltage signal), time-period A illustrates a constant voltage of 220 V. Time-period B illustrates a signal change at 5.60 seconds from 220 V to 230 V. The signal value of 230 V was reached at 5.65 seconds. In figure 5.5 (control output response), time-period A illustrates a constant control output signal of 127.5. Time-period B illustrates a change in the control output signal due to the change in the voltage. At 5.65 seconds the control output signal changes from 127.5 to 191.25. The control output signal value of 191.25 was reached at 5.70 seconds. It was observed that Intelligent Electronic Load Controller responds efficiently to changes in the voltage of the system.

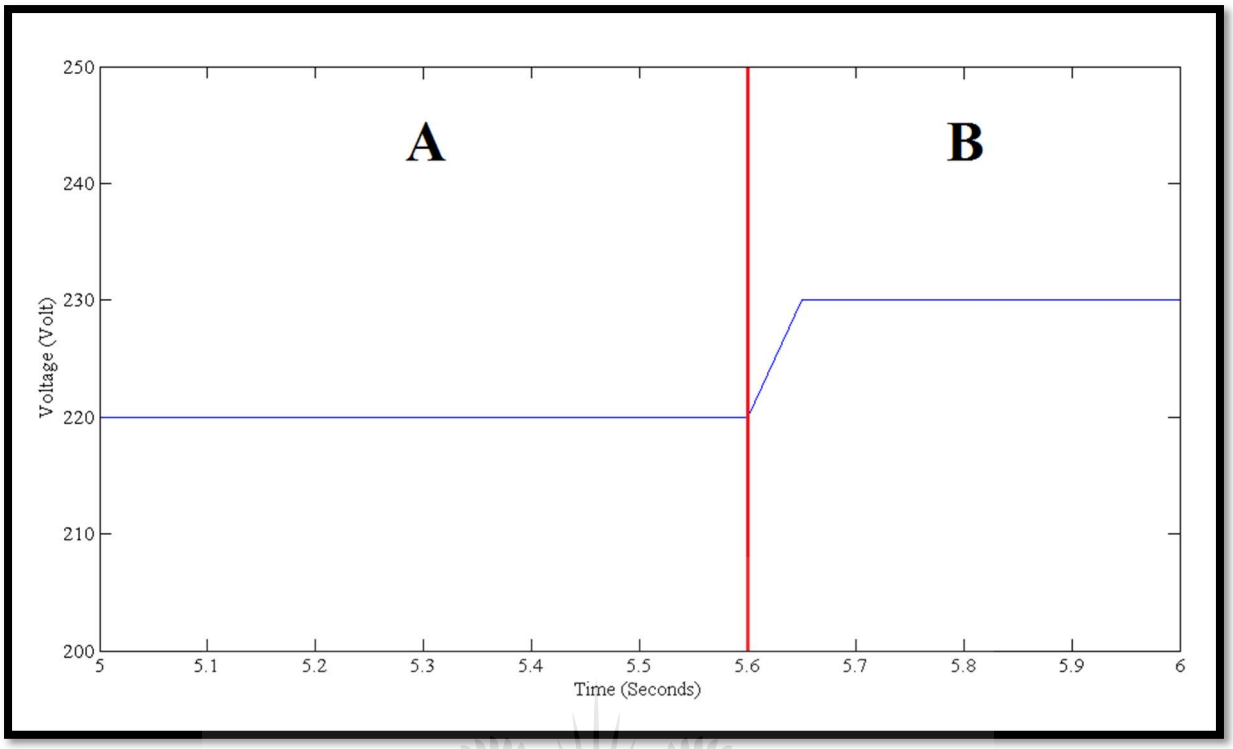

Figure 5.4: 230 V input signal

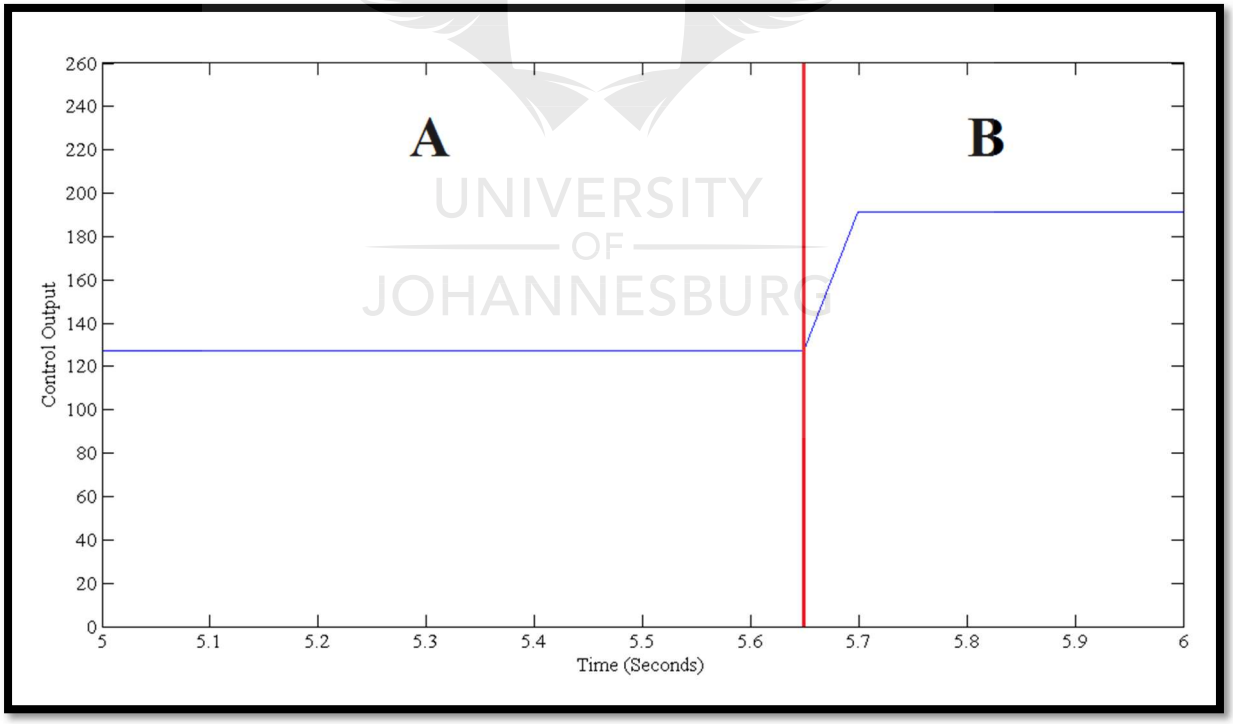

Figure 5.5: Control output response to 230 V input signal

5.2.3. Experiment 3: 240 V Input Signal

The objective of experiment 3 was to send a 240 V signal to the Arduino microcontroller and observe how the ELC responds to the input signal. The experiment was divided into two time-periods as indicated on both figures. In figure 5.6 (input voltage signal), time-period A illustrates a constant voltage of 220 V. Time-period B illustrates a signal change at 5.60 seconds from 220 V to 240 V. The signal value of 240 V was reached at 5.65 seconds. In figure 5.7 (control output response), time-period A illustrates a constant control output signal of 127.5. Time-period B illustrates a change in the control output signal due to the change in the voltage. At 5.65 seconds the control output signal changes from 127.5 to 255. The control output signal value of 255 was reached at 5.70 seconds. It was observed that Intelligent Electronic Load Controller responds efficiently to changes in the voltage of the system.

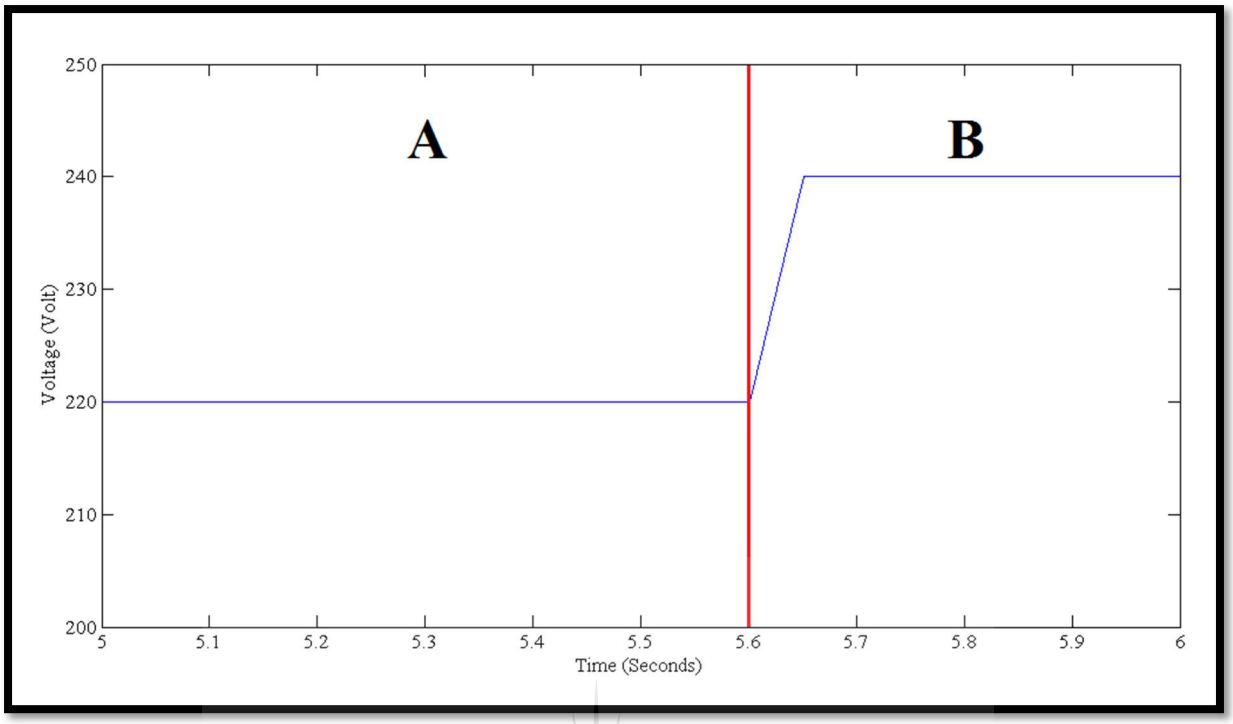

Figure 5.6: 240 V input signal

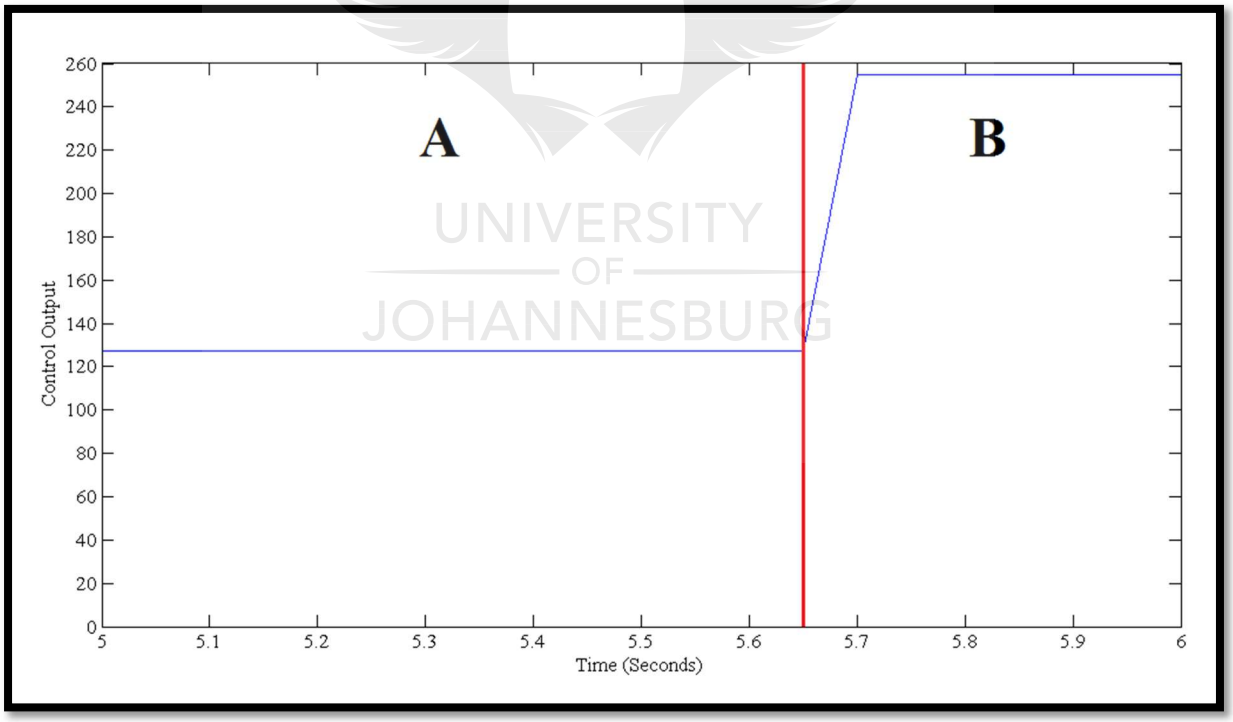

Figure 5.7: Control output response to 240 V input signal

5.3. EXPERIMENTAL RESULTS

Laboratory experiments were carried out on the system under various load conditions to validate the operation and performance of the Intelligent Electronic Load Controller. Figure 5.8 shows a schematic diagram of the system and figure 5.9 shows a complete experimental setup of the system in the laboratory:

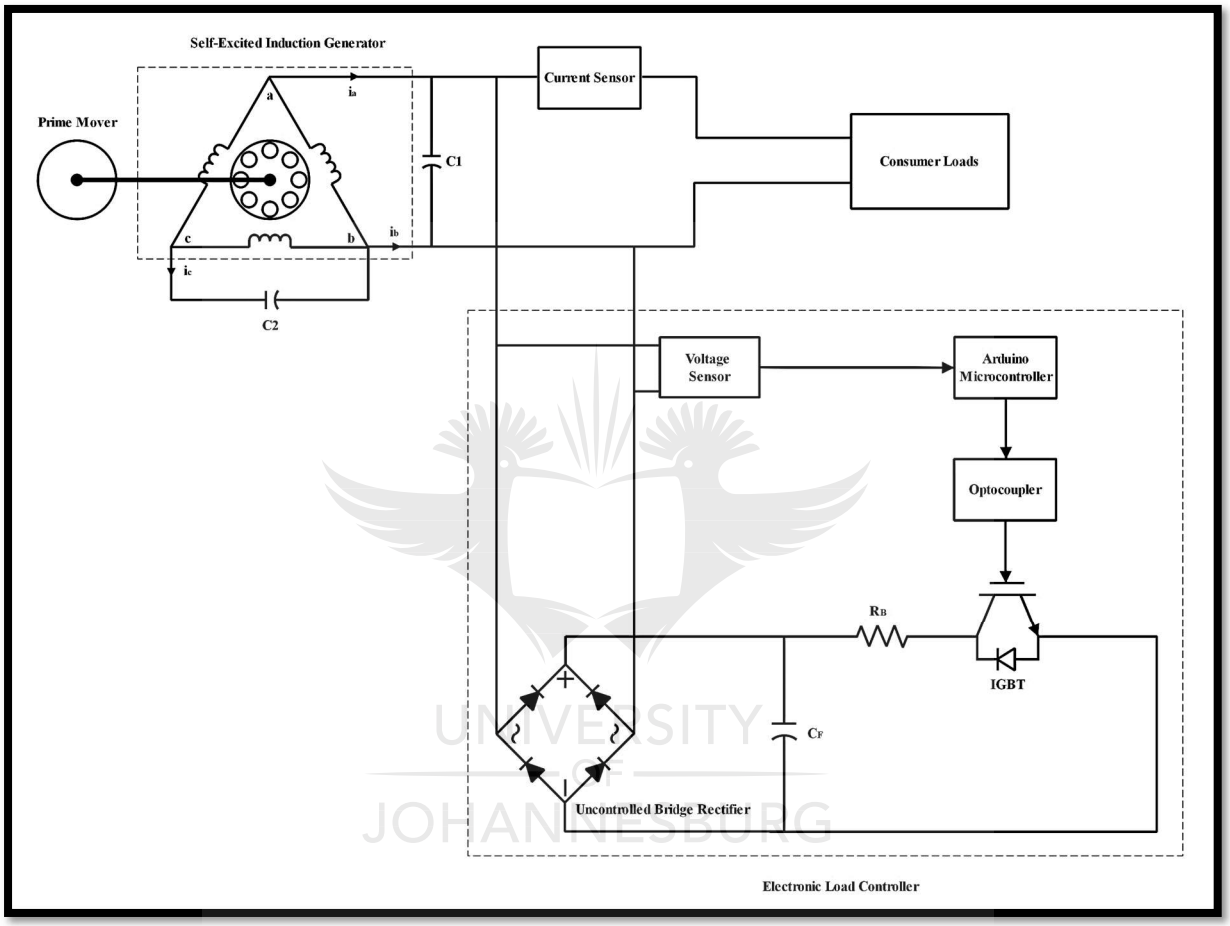

Figure 5.8: Schematic diagram

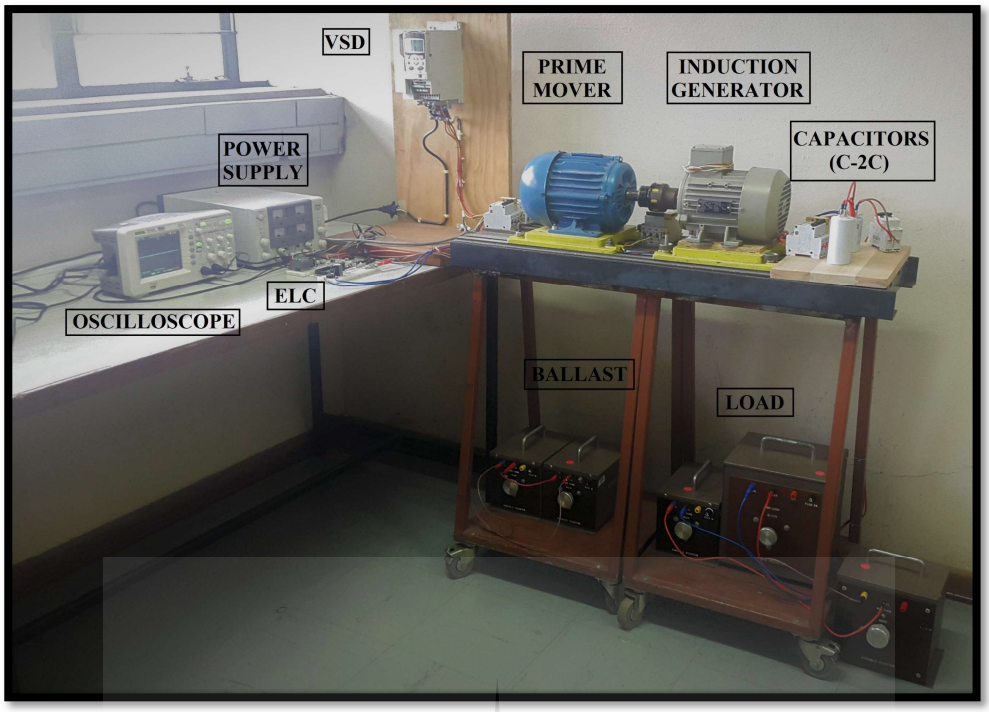

Figure 5.9: Laboratory experimental setup

A number of different experiments have been carried out in order to analyse and test the system as given in table 5.2 and table 5.3:

Table 5.2: Consumer load experiments

Consumer Load Experiments			
Experiment No	**Switching Consumer Load**	**Consumer Load**	**With/Without ELC**
1	Out	200 W	Without
2	Out	200 W	With
3	Out	400 W	Without
4	Out	400 W	With
5	In	200 W	With
6	In	0 W	With

Table 5.3: Power measurement

Power Measurement	
Experiment No	**Power**
7	Consumer Load/Ballast Load

MATLAB/SIMULINK was used to program the 1st Arduino microcontroller. The voltage of the system is fed to analog input pin 0 of the Arduino microcontroller. The analog values are converted into digital values by the Arduino microcontroller. The Arduino microcontroller generates a 10-bit value, ranging from 0 – 1023 for the analog inputs. A gain function is used to scale down the 0 – 1023 values of the voltage input, in order to display the correct values being measured. The 1st gain function (Gain) is as follow: 0 – 1023 is scaled to 0 – 240 V. The actual measured voltage value is then compared with the reference voltage of 220 V. An error signal and change in error signal is generated after the comparison. These 2 signals are then multiplexed and fed to the fuzzy logic controller block. The fuzzy logic controller block generates an appropriate PWM output signal that is sent to the PWM output pin 8 of the Arduino microcontroller. A gain function is used to scale up the 0 – 1 values produced by the fuzzy logic controller block. The 2nd gain function (Gain1) is as follow: 0 – 1 is scaled to 0 – 255. The Arduino microcontroller generates an 8-bit value, ranging from 0 – 255 for the PWM output. The experimental voltage measurement & control model is shown in figure 5.10:

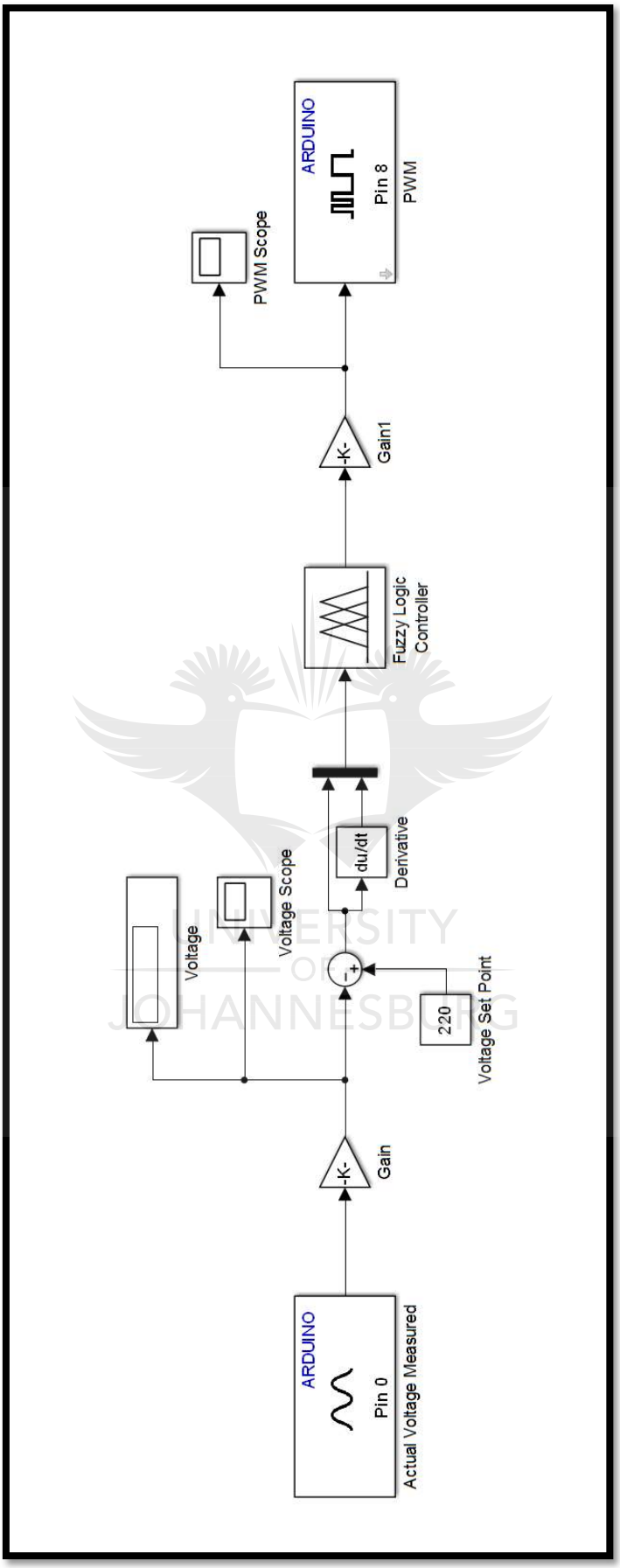

Figure 5.10: Experimental voltage measurement & control model

MATLAB/SIMULINK was used to program the 2nd Arduino microcontroller. The current of the system is fed to analog input pin 0 of the arduino microcontroller. The analog values are converted into digital values by the Arduino microcontroller. The Arduino microcontroller generates a 10-bit value, ranging from 0 – 1023 for the analog inputs. A gain function is used to scale down the 0 – 1023 values of the current inputs, in order to display the correct values being measured. The gain function (Gain) is as follow: 0 – 1023 is scaled to 0 – 5 A. The experimental current measurement model is shown in figure 5.11:

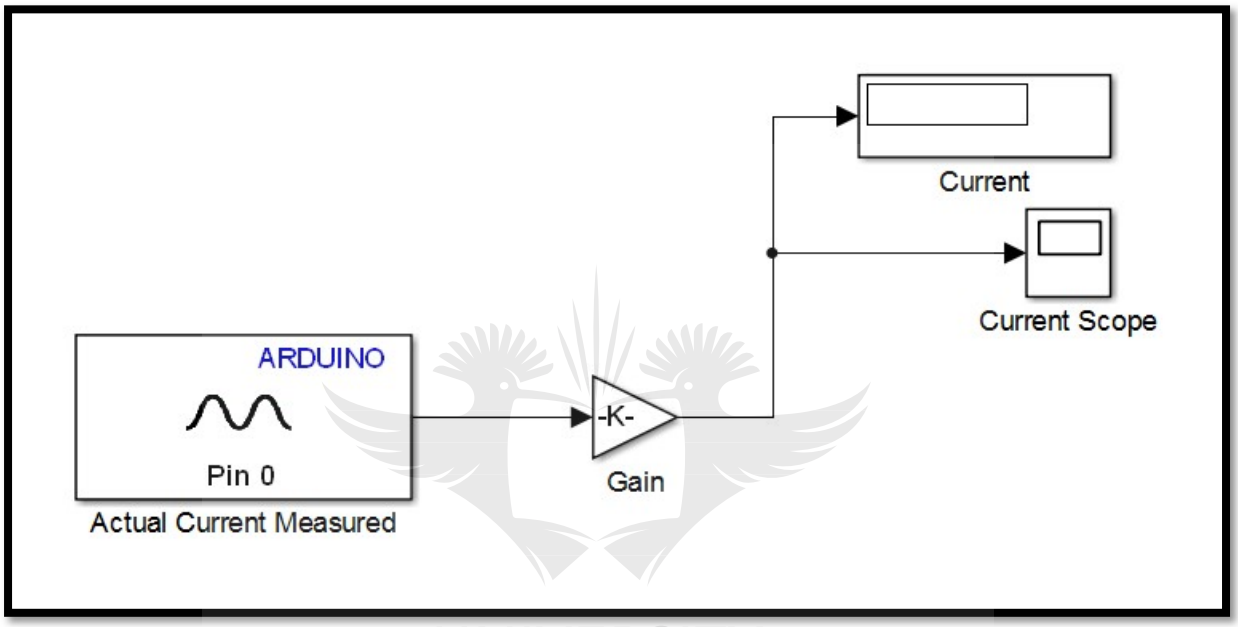

Figure 5.11: Experimental current measurement model

5.3.1. Experiment 1: Switching out 200 W Consumer Load without ELC

The objective of experiment 1 as shown in figure 5.12 was to switch out 200 W consumer and observe what happens to system without using an ELC. The experiment was divided into two time-periods. Time-period A illustrates a stable voltage of 220 V with 400 W consumer load switched in. Time-period B illustrates the switching out of 200 W without an ELC. At 8.00 seconds the 200 W consumer load was switched out and the voltage increased to 224 V. It was observed that there was no response from the ELC to adjust the power flow in order to maintain the reference voltage of 220 V. Thus, the voltage remained at 224 V.

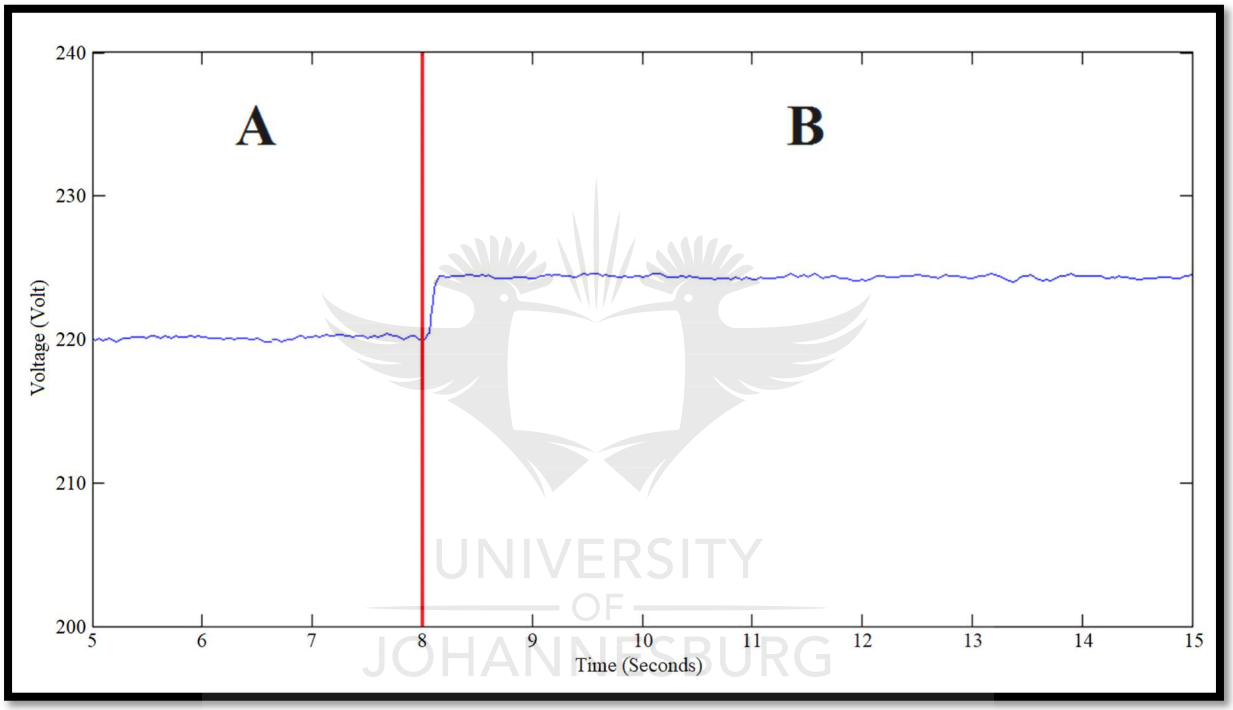

Figure 5.12: Switching out 200 W consumer load without ELC

5.3.2. Experiment 2: Switching out 200 W Consumer Load with ELC

The objective of experiment 2 as shown in figure 5.13 was to switch out 200 W consumer load and to observe how the ELC responds to this specific change. The experiment was divided into three time-periods. Time-period A illustrates the control of voltage at 220 V with 400 W consumer load switched in. Time-period B illustrates the switching out of 200 W consumer load and the response of the ELC. At 8.00 seconds the 200 W consumer load was switched out and the voltage increased to 224 V. At 8.50 seconds the ELC started to respond to the change in the voltage. It was observed that the ELC adjusted the power flow to the ballast load in such a manner that the reference voltage of 220 V was reached at 9.05 seconds. Time-period C illustrates that the ELC maintains a stable voltage of 220 V from 9.05 seconds until 15.00 seconds.

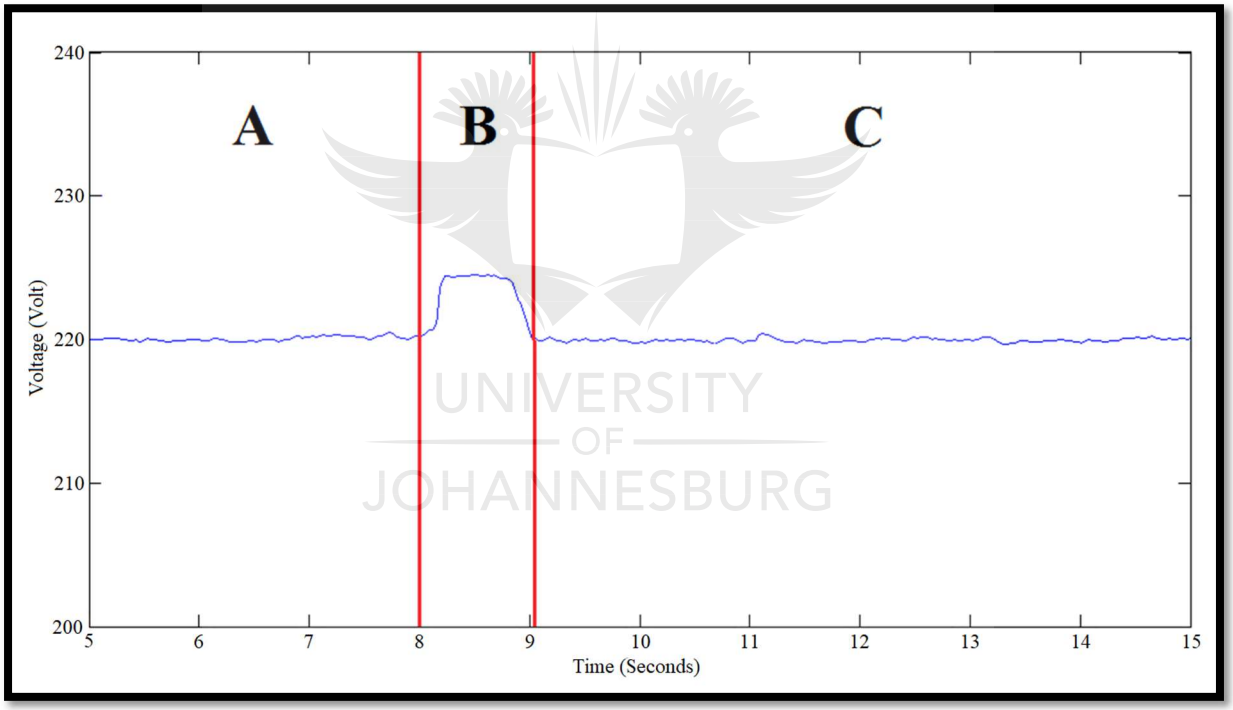

Figure 5.13: Switching out 200 W consumer load with ELC

5.3.3. Experiment 3: Switching out 400 W Consumer Load without ELC

The objective of experiment 3 as shown in figure 5.14 was to switch out 400 W consumer and observe what happens to system without using an ELC. The experiment was divided into two time-periods. Time-period A illustrates a stable voltage of 220 V with 400 W consumer load switched in. Time-period B illustrates the switching out of 400 W without an ELC. At 8.00 seconds the 400 W consumer load was switched out and the voltage increased to 230 V. It was observed that there was no response from the ELC to adjust the power flow in order to maintain the reference voltage of 220 V. Thus, the voltage remained at 230 V.

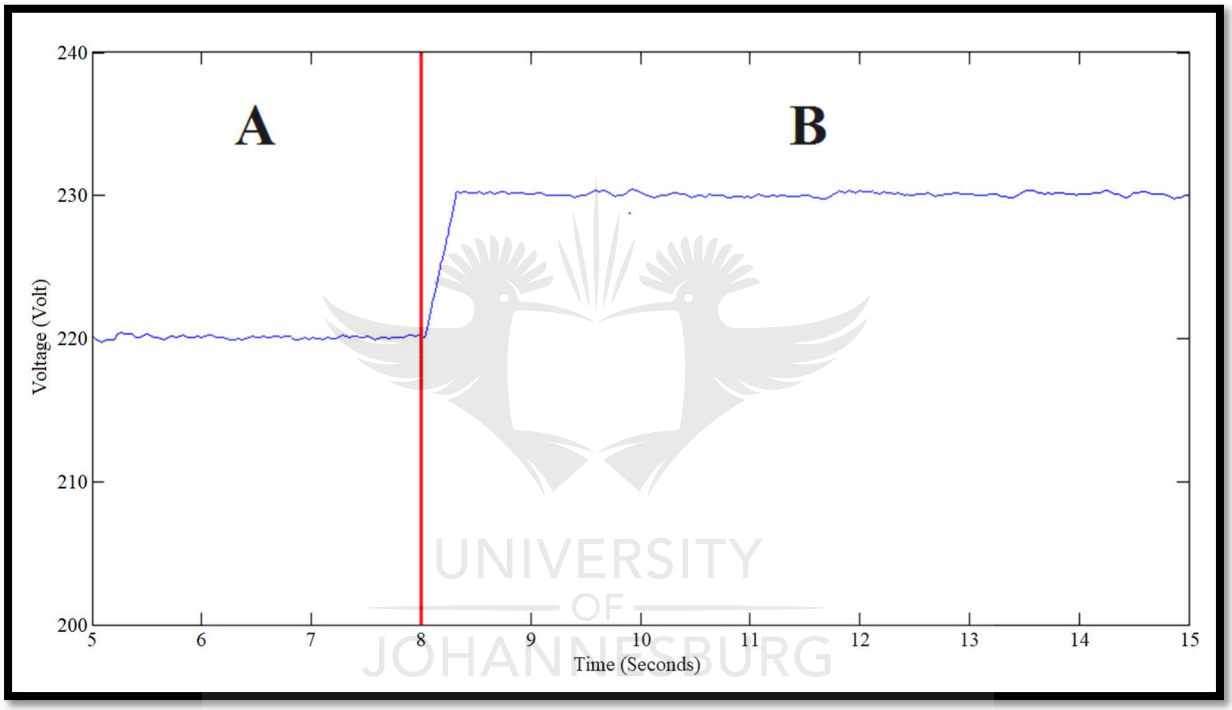

Figure 5.14: Switching out 400 W consumer load without ELC

5.3.4. Experiment 4: Switching out 400 W Consumer Load with ELC

The objective of experiment 4 as shown in figure 5.15 was to switch out 400 W consumer load and to observe how the ELC responds to this specific change. The experiment was divided into three time-periods. Time-period A illustrates the control of voltage at 220 V with 400 W consumer load switched in. Time-period B illustrates the switching out of 400 W consumer load and the response of the ELC. At 8.00 seconds the 400 W consumer load was switched out and the voltage increased to 230 V. At 8.50 seconds the ELC started to respond to the change in the voltage. It was observed that the ELC adjusted the power flow to the ballast load in such a manner that the reference voltage of 220 V was reached at 9.20 seconds. Time-period C illustrates that the ELC maintains a stable voltage of 220 V from 9.20 seconds until 15.00 seconds.

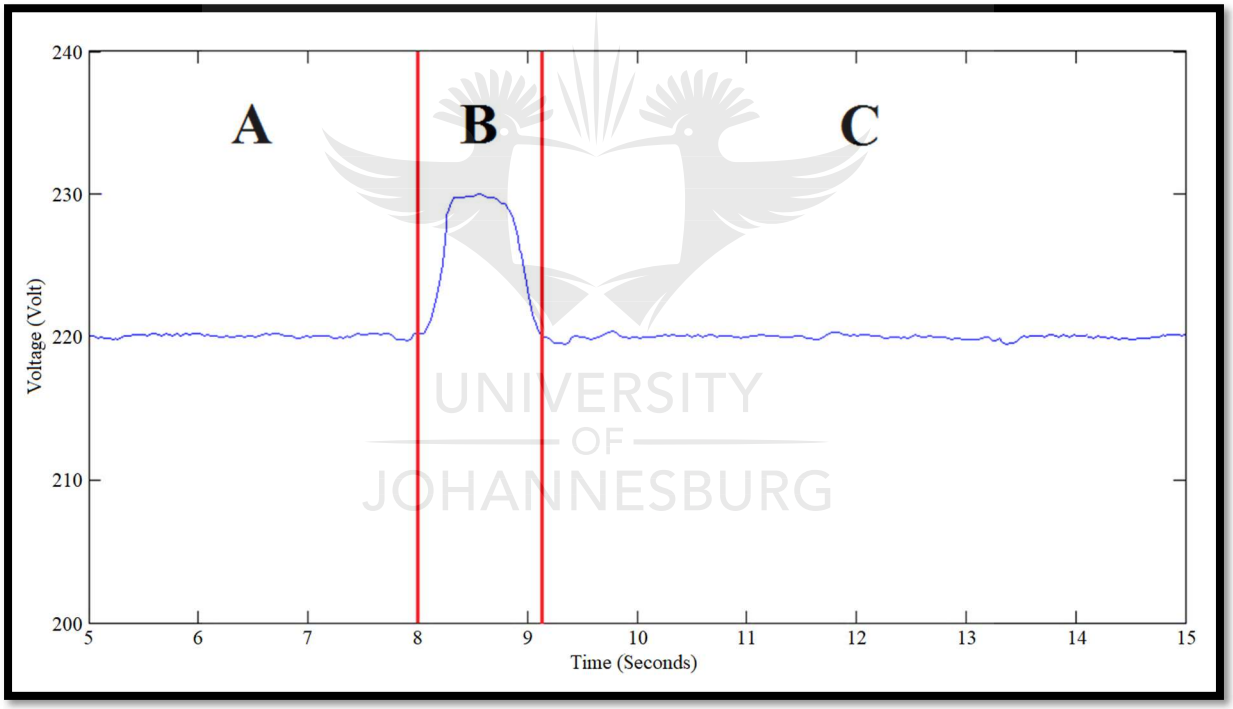

Figure 5.15: Switching out 400 W consumer load with ELC

5.3.5. Experiment 5: Switching in 200 W Consumer Load with ELC

The objective of experiment 5 as shown in figure 5.16 was to switch in 200 W consumer load and to observe how the ELC responds to this specific change. The experiment was divided into three time-periods. Time-period A illustrates the control of voltage at 220 V with 0 W consumer load switched in. Time-period B illustrates the switching in of 200 W consumer load and the response of the ELC. At 8.00 seconds the 200 W consumer load was switched in and the voltage decreased to 216 V. At 8.50 seconds the ELC started to respond to the change in the voltage. It was observed that the ELC adjusted the power flow to the ballast load in such a manner that the reference voltage of 220 V was reached at 9.15 seconds. Time-period C illustrates that the ELC maintains a stable voltage of 220 V from 9.15 seconds until 15.00 seconds.

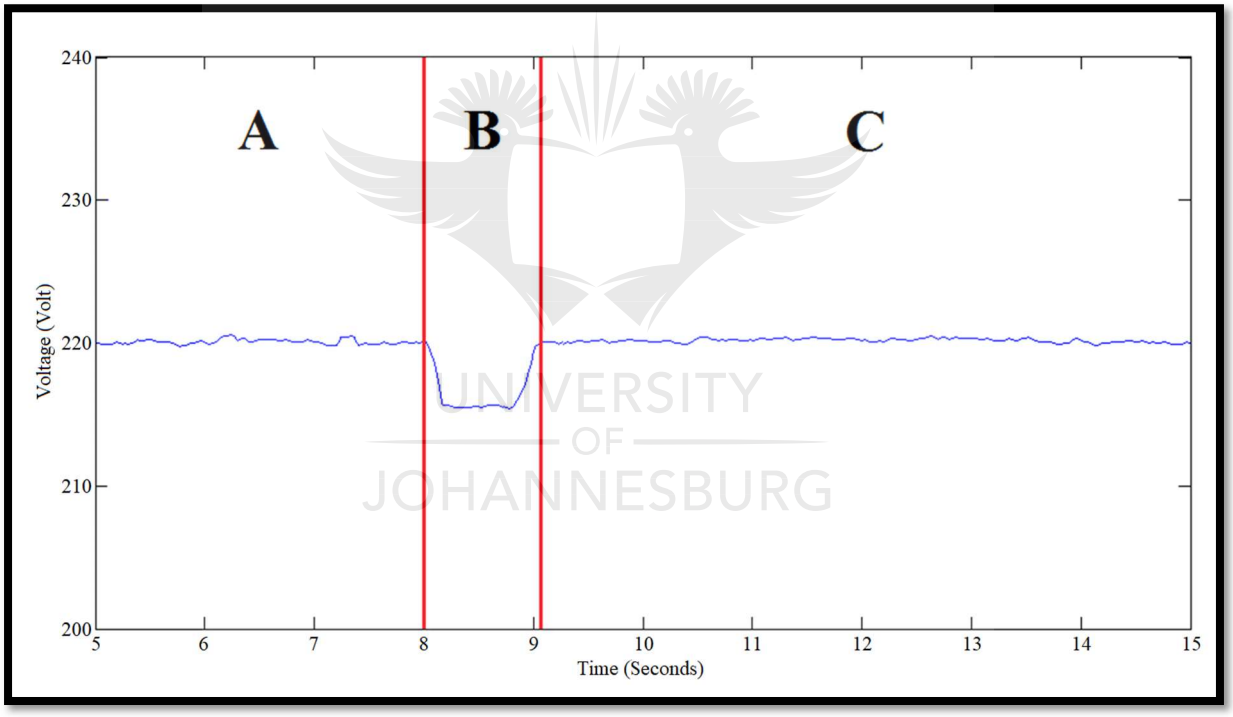

Figure 5.16: Switching in 200 W consumer load with ELC

5.3.6. Experiment 6: Switching in 0 W Consumer Load with ELC

The objective of experiment 6 as shown in figure 5.17 was to switch in 0 W consumer load and to observe how the ELC responds to this specific change. The experiment was divided into two time-periods. Time-period A illustrates the generation of 230 V by the SEIG under no-load conditions. Time-period B illustrates the switching in of 0 W consumer load and the response of the ELC. At 8.00 seconds the ELC was switched on and it was observed that the ELC adjusts the power flow to the ballast load in such a manner that the reference voltage of 220 V was reached at 8.75 seconds and maintained stable until 15.00 seconds.

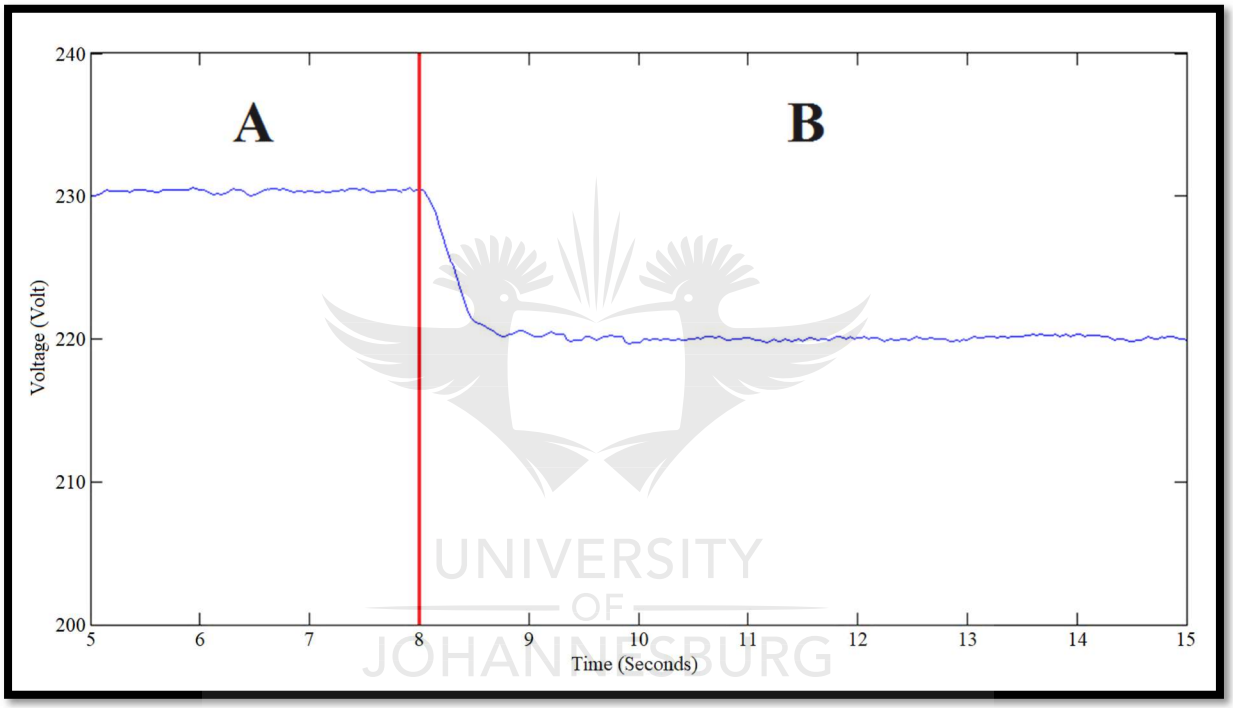

Figure 5.17: Switching in 0 W consumer load with ELC

5.3.7. Experiment 7: Power Measurement

The objective of experiment 7 was to combine the voltage and current measurements to obtain the power measurements for both the consumer load and ballast load as shown in figure 5.18. It was observed that as the consumer load power decreases the amount of surplus power being diverted to the ballast load increases.

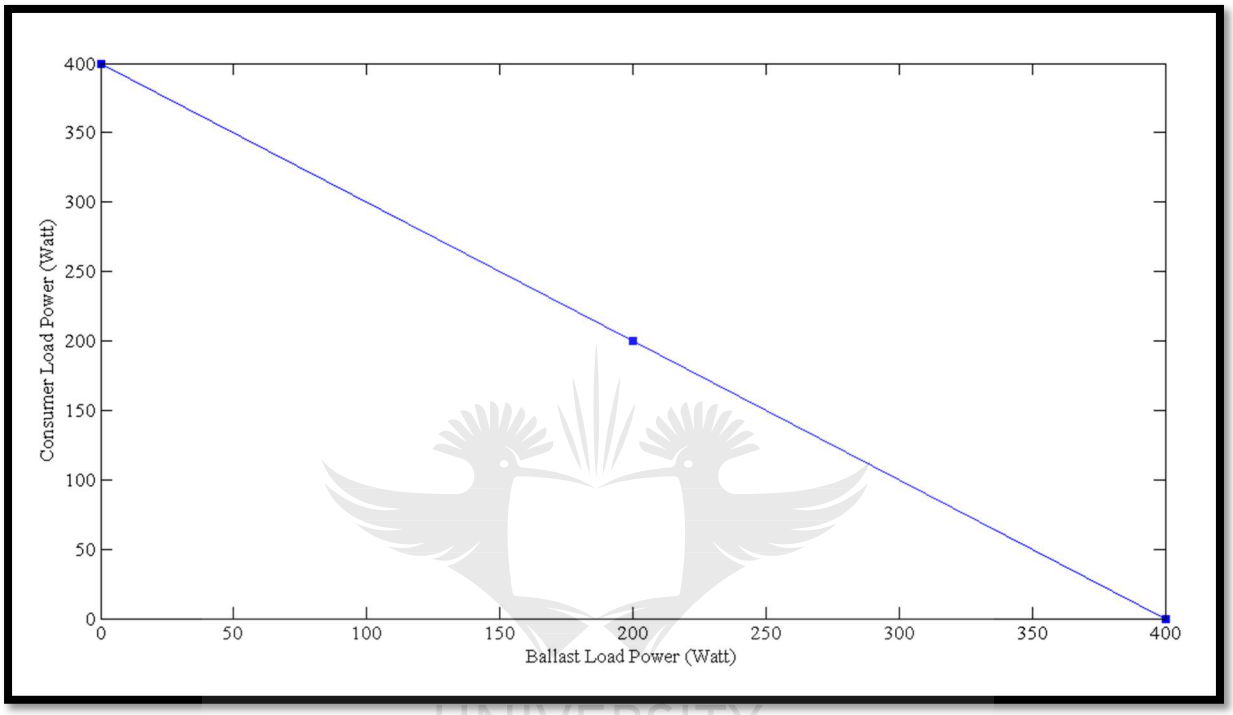

Figure 5.18: Power measurement

CHAPTER 6
CONCLUSION AND RECOMMENDATIONS

6.1. CONCLUSION

The purpose of this research was to design and develop a simple, reliable and cost-effective Intelligent Electronic Load Controller for stand-alone micro-hydropower systems. A lot of research has been done on the controlling of the three-phase self-excited induction generator, however, this research focused on how the Intelligent Electronic Load Controller will be able to maintain a stable voltage on the demand side of the three-phase self-excited induction generator, while supplying varying single-phase consumer loads. The following major findings were made during this research:

- The Intelligent Electronic Load Controller used a fuzzy logic control method. An assessment of the other control methods was carried out and a fuzzy logic control method was chosen due to cheaper development, faster response times with virtually no overshoot and the flexibility in design and implementation.
- A three-phase self-excited induction generator was used to supply single-phase consumer loads instead of a single-phase self-excited induction generator. It was found that a three-phase self-excited induction generator is much more reliable and cost-effective. The self-excited induction generator used in the experiment produced approximately 80% of its rating due to the conversion from a three-phase output to a single-phase output.
- A simple open platform microcontroller like the Arduino was used with advance control intelligence to make the system cost-effective. Two Arduino microcontrollers had to be used for the control and measurement of the system due to insufficient memory.
- Hardware-in-the-loop simulations were carried out under various consumer load conditions using MATLAB/SIMULINK and an Arduino microcontroller to analyse and test the efficiency of the system in real-time.
- Laboratory experiments were carried out and it was found that the Intelligent Electronic Load Controller was able to respond quickly and efficiently to changes in the consumer load to maintain the voltage on the demand side of the three-phase self-excited induction generator very stable and close to the set point voltage value.

The Intelligent Electronic Load Controller will contribute towards providing reliable and cost-effective means of enhancing the proliferation of micro-hydropower particularly in rural and remote applications in Sub-Saharan Africa.

6.2. RECOMMENDATIONS

To enhance the system, it is recommended to amalgamate previous work done on the control side of the generator and the presented load control on the demand side in order to achieve a harmonious stand-alone micro-hydropower control system. Further testing needs to be conducted on imbalance loads and what effects it will have on the system. Potential operation of the system at non-unity power factor could be achieved through testing the system with inductive and capacitive consumer loads. The system could also be implemented and experimentally verified on a larger power capacity scale.

REFERENCES

[1] International Energy Agency, "World Energy Outlook 2016," 16 November 2016. [Online]. Available: http://www.iea.org/Textbase/npsum/WEO2016SUM.pdf. [Accessed 19 April 2017].

[2] R. C. Bansal, "Three-phase self-excited induction generators: an overview," *IEEE Transactions on Energy Conversion,* vol. 20, no. 2, pp. 292-299, 2005.

[3] H. -J. Wagner and J. Mathur, Introduction to Hydro Energy Systems: Basics, Technology and Operation, Berlin: Springer-Verlag, 2011.

[4] U.S. Department of Energy, "Microhydropower Systems," Department of Energy, [Online]. Available: https://energy.gov/energysaver/microhydropower-systems. [Accessed 8 March 2017].

[5] M. K. Gupta, "Hydroelectric Power Plant," in *Power Plant Engineering*, New Delhi, PHI Learning, 2012, pp. 119-120.

[6] P. K. Nag, "Hydroelectric Power Plant," in *Power Plant Engineering (3rd ed.)*, New Delhi, Tata McGraw-Hill, 2008, pp. 657-734.

[7] Fichtner, "IFC - International Finance Corporation," February 2015. [Online]. Available: http://www.ifc.org/wps/wcm/connect/06b2df8047420bb4a4f7ec57143498e5/Hydropower_Report.pdf?MOD=AJPERES. [Accessed 15 March 2017].

[8] P. Breeze, Hydropower (1st ed.), Oxford: Academic Press - Elsevier, 2018.

[9] K. Subramanya, "Precipitation," in *Engineering Hydrology (4th ed.)*, New Delhi, McGraw-Hill Education, 2013, p. 37.

[10] B. Pandey and A. Karki, Hydroelectric Energy: Renewable Energy and the Environment, Boca Raton: CRC Press - Taylor & Francis Group, 2016.

[11] M. Kaltschmitt, W. Streicher and A. Wiese, Renewable Energy: Technology, Economics and Environment, Berlin: Springer, 2007.

[12] V. Quaschning, “Hydropower Plants - Wet Energy,” in *Renewable Energy and Climate Change*, West Sussex, Wiley-IEEE Press, 2010, pp. 198-202.

[13] N. Smith, Motors as Generators for Micro-hydro Power (2nd ed.), London: Practical Action, 2008.

[14] S. K. Jha , P. Stoa and K. Uhlen, “Socio-economic Impact of a Rural Microgrid,” in *4th International Conference on the Development in the in Renewable Energy Technology*, Dhaka, 2016.

[15] S. Kumar Rai, O. P. Rahi and S. Kumar, “Implementation of electronic load controller for control of micro hydro power plant,” in *International Conference on Energy Economics and Environment (ICEEE)*, Noida, 2015.

[16] D. Henderson, “An advanced electronic load governor for control of micro hydroelectric generation,” *IEEE Transactions on Energy Conversion,* vol. 13, no. 3, pp. 300-304, 1998.

[17] Y. Sofian and M. Iyas, “Design of electronic load controller for a self excited induction generator using fuzzy logic method based microcontroller,” in *International Conference on Electrical Engineering and Informatics (ICEEI)*, Bandung, 2011.

[18] B. Singh, S. S. Murthy and S. Gupta, “Analysis and Design of Electronic Load Controller for Self-Excited Induction Generators,” *IEEE Transactions on Energy Conversion,* vol. 21, no. 1, pp. 285-293, 2006.

[19] T. J. Ross, Fuzzy Logic with Engineering Applications (3rd ed.), West Sussex: John Wiley & Sons, Ltd, 2010.

[20] S. S. Murthy, R. K. Ahuja and J. K. Chaudhary, “Design and fabrication of a low cost analog electronic load controller for a self excited induction generator supplying single-phase loads,” in *International Conference on Power and Energy Systems (ICPS)*, Chennai, 2011.

[21] C. Grosan and A. Abraham, “Fuzzy Expert Systems,” in *Intelligent Systems: A Modern Approach*, Berlin, Springer-Verlag, 2011, pp. 219-260.

[22] C. C. Lee, “Fuzzy Logic in Control Systems: Fuzzy Logic Controller - Part 1,” *IEEE Transactions on Systems, Man, and Cybernetics,* vol. 20, no. 2, pp. 404-418, 1990.

[23] M. Godoy Simões and F. A. Farret, Modeling and Analysis with Induction Generators (3rd ed.), Boca Raton: CRC Press - Taylor & Francis Group, 2014.

[24] J. B. Ekanayake, “Induction generators for small hydro schemes,” *Power Engineering Journal,* vol. 16, no. 2, pp. 61-67, 2002.

[25] Arduino, “ArduinoBoardMega,” Arduino, [Online]. Available: https://www.arduino.cc/en/Main/arduinoBoardMega. [Accessed 4 October 2017].

[26] Toshiba, “Toshiba Electronic Components,” 27 May 2017. [Online]. Available: https://toshiba.semicon-storage.com/ap-en/product/opto/photocoupler/detail.TLP250.html. [Accessed 10 October 2017].

[27] T. Takagi and M. Sugeno, “Fuzzy identification of systems and its applications to modeling and control,” *IEEE Transactions on Systems, Man, and Cybernetics,* vol. 15, no. 1, pp. 116-132, 1985.

APPENDIX A
DATASHEETS

A.1. ZENER DIODE

FAIRCHILD SEMICONDUCTOR®

June 2007

1N5221B - 1N5263B
Zener Diodes

Tolerance = 5%

DO-35 Glass case
COLOR BAND DENOTES CATHODE

Absolute Maximum Ratings * T_A = 25°C unless otherwise noted

Symbol	Parameter	Value	Units
P_D	Power Dissipation Derate above 50°C	500 4.0	mW mW/°C
T_{STG}	Storage Temperature Range	-65 to +200	°C
T_J	Maximum Junction Operating Temperature	+200	°C
	Lead Temperature (1/16" from case for 10 seconds)	+230	°C

* These ratings are limiting values above which the serviceability of the diode may be impaired.
** Non-recurrent square wave PW = 8.3ms, Ta = 50 degrees C.

Electrical Characteristics T_A=25°C unless otherwise noted

Device	V_Z (V) @ I_Z (Note 1)			Z_Z (Ω) @ I_Z (mA)		Z_{ZK} (Ω) @ I_{ZK} (mA)		I_R (μA) @ V_R (V)		T_C (%/°C)
	Min.	Typ.	Max.							
1N5221B	2.28	2.4	2.52	30	20	1,200	0.25	100	1.0	-0.085
1N5222B	2.375	2.5	2.625	30	20	1,250	0.25	100	1.0	-0.085
1N5223B	2.565	2.7	2.835	30	20	1,300	0.25	75	1.0	-0.080
1N5224B	2.66	2.8	2.94	30	20	1,400	0.25	75	1.0	-0.080
1N5225B	2.85	3	3.15	29	20	1,600	0.25	50	1.0	-0.075
1N5226B	3.135	3.3	3.465	28	20	1,600	0.25	25	1.0	-0.07
1N5227B	3.42	3.6	3.78	24	20	1,700	0.25	15	1.0	-0.065
1N5228B	3.705	3.9	4.095	23	20	1,900	0.25	10	1.0	-0.06
1N5229B	4.085	4.3	4.515	22	20	2,000	0.25	5.0	1.0	+/-0.055
1N5230B	4.465	4.7	4.935	19	20	1,900	0.25	2.0	1.0	+/-0.03
1N5231B	4.845	5.1	5.355	17	20	1,600	0.25	5.0	2.0	+/-0.03
1N5232B	5.32	5.6	5.88	11	20	1,600	0.25	5.0	3.0	0.038
1N5233B	5.7	6	6.3	7.0	20	1,600	0.25	5.0	3.5	0.038
1N5234B	5.89	6.2	6.51	7.0	20	1,000	0.25	5.0	4.0	0.045
1N5235B	6.46	6.8	7.14	5.0	20	750	0.25	3.0	5.0	0.05
1N5236B	7.125	7.5	7.875	6.0	20	500	0.25	3.0	6.0	0.058
1N5237B	7.79	8.2	8.61	8.0	20	500	0.25	3.0	6.5	0.062
1N5238B	8.265	8.7	9.135	8.0	20	600	0.25	3.0	6.5	0.065
1N5239B	8.645	9.1	9.555	10	20	600	0.25	3.0	7.0	0.068
1N5240B	9.5	10	10.5	17	20	600	0.25	3.0	8.0	0.075

Device	V_Z (V) @ I_Z (Note 1)			Z_Z (Ω) @ I_Z (mA)		Z_{ZK} (Ω) @ I_{ZK} (mA)		I_R (μA) @ V_R (V)		T_C (%/°C)
	Min.	Typ.	Max.							
1N5241B	10.45	11	11.55	22	20	600	0.25	2.0	8.4	0.076
1N5242B	11.4	12	12.6	30	20	600	0.25	0.1	9.1	0.077
1N5243B	12.35	13	13.65	13	9.5	600	0.25	0.1	9.9	0.079
1N5244B	13.3	14	14.7	15	9.0	600	0.25	0.1	10	0.080
1N5245B	14.25	15	15.75	16	8.5	600	0.25	0.1	11	0.082
1N5246B	15.2	16	16.8	17	7.8	600	0.25	0.1	12	0.083
1N5247B	16.15	17	17.85	19	7.4	600	0.25	0.1	13	0.084
1N5248B	17.1	18	18.9	21	7.0	600	0.25	0.1	14	0.085
1N5247B	18.05	19	19.95	23	6.6	600	0.25	0.1	14	0.085
1N5250B	19	20	21	25	6.2	600	0.25	0.1	15	0.086
1N5251B	20.9	22	23.1	29	5.6	600	0.25	0.1	17	0.087
1N5252B	22.8	24	25.2	33	5.2	600	0.25	0.1	18	0.088
1N5253B	23.75	25	26.25	35	5.0	600	0.25	0.1	19	0.088
1N5254B	25.65	27	28.35	41	4.6	600	0.25	0.1	21	0.089
1N5255B	26.6	28	29.4	44	4.5	600	0.25	0.1	21	0.090
1N5256B	28.5	30	31.5	49	4.2	600	0.25	0.1	23	0.09
1N5257B	31.35	33	34.65	58	3.8	700	0.25	0.1	25	0.092
1N5258B	34.2	36	37.8	70	3.4	700	0.25	0.1	27	0.093
1N5259B	37.05	39	40.95	80	3.2	800	0.25	0.1	30	0.094
1N5260B	40.85	43	45.15	93	3.0	900	0.25	0.1	33	0.095
1N5261B	44.65	47	49.35	105	2.7	1000	0.25	0.1	36	0.095
1N5262B	48.45	51	53.55	125	2.5	1100	0.25	0.1	39	0.096
1N5263B	53.2	56	58.8	150	2.2	1300	0.25	0.1	43	0.096
V_F Forward Voltage = 1.2V Max. @ I_F = 200mA										

Notes:

1.Zener Voltage (V_Z)
The zener voltage is measured with the device junction in the thermal equilibrium at the lead temperature (T_L) at 30°C ± 1°C and 3/8" lead length

Top Mark Information

Device	Line 1	Line 2	Line 3
1N5221B	LOGO	22	1B
1N5222B	LOGO	22	2B
1N5223B	LOGO	22	3B
1N5224B	LOGO	22	4B
1N5225B	LOGO	22	5B
1N5226B	LOGO	22	6B
1N5227B	LOGO	22	7B
1N5228B	LOGO	22	8B
1N5229B	LOGO	22	9B
1N5230B	LOGO	23	0B
1N5231B	LOGO	23	1B
1N5232B	LOGO	23	2B
1N5233B	LOGO	23	3B
1N5234B	LOGO	23	4B
1N5235B	LOGO	23	5B
1N5236B	LOGO	23	6B
1N5237B	LOGO	23	7B
1N5238B	LOGO	23	8B
1N5239B	LOGO	23	9B
1N5240B	LOGO	24	0B
1N5241B	LOGO	24	1B
1N5242B	LOGO	24	2B
1N5243B	LOGO	24	3B
1N5244B	LOGO	24	4B
1N5245B	LOGO	24	5B

1N5246B	LOGO	24	6B
1N5247B	LOGO	24	7B
1N5248B	LOGO	24	8B
1N5247B	LOGO	24	9B
1N5250B	LOGO	25	0B
1N5251B	LOGO	25	1B
1N5252B	LOGO	25	2B
1N5253B	LOGO	25	3B
1N5254B	LOGO	25	4B
1N5255B	LOGO	25	5B
1N5256B	LOGO	25	6B
1N5257B	LOGO	25	7B
1N5258B	LOGO	25	8B
1N5259B	LOGO	25	9B
1N5260B	LOGO	26	0B
1N5261B	LOGO	26	1B
1N5262B	LOGO	26	2B
1N5263B	LOGO	26	3B

Top Mark Information (Continued)

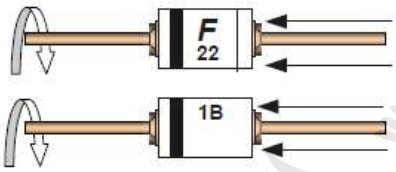

1st line: F - Fairchild Logo

2nd line: Device Name - 4th to 5th characters of the device name.
or 5th to 6th characters for BZXyy series

3rd line: Device Name - 6th to 7th characters of the device name.
or Voltage rating for BZXyy series

General Requirements:

1.0 Cathode Band

2.0 First Line: F - Fairchild Logo

3.0 Second Line: Device name - For 1Nxx series: 4th to 5th characters of the device name.
For BZxx series: 5th to 6th characters of the device name.

4.0 Third Line: Device name - For 1Nxx series: 6th to 7th characters of the device name.
For BZXyy series: Voltage rating

5.0 Devices shall be marked as required in the device specification (PID or FSC Test Spec).

6.0 Maximum no. of marking lines: 3

7.0 Maximum no. of digits per line: 2

8.0 FSC logo must be 20 % taller than the alphanumeric marking and should occupy the 2 characters of the specified line.

9.0 Marking Font: Arial (Except FSC Logo)

10.0 First character of each marking line must be aligned vertically.

11.0 All device markings must be based on Fairchild device specification.

FAIRCHILD
SEMICONDUCTOR®

TRADEMARKS

The following are registered and unregistered trademarks Fairchild Semiconductor owns or is authorized to use and is not intended to be an exhaustive list of all such trademarks.

ACEx™
Across the board. Around the world.™
ActiveArray™
Bottomless™
Build it Now™
CoolFET™
CROSSVOLT™
CTL™
Current Transfer Logic™
DOME™
E^2CMOS™
EcoSPARK®
EnSigna™
FACT Quiet Series™
FACT®
FAST®
FASTr™
FPS™
FRFET™
GlobalOptoisolator™
GTO™
HiSeC™
i-Lo™
ImpliedDisconnect™
IntelliMAX™
ISOPLANAR™
MICROCOUPLER™
MicroPak™
MICROWIRE™
MSX™
MSXPro™
OCX™
OCXPro™
OPTOLOGIC®
OPTOPLANAR™®
PACMAN™
POP™
Power220®
Power247®
PowerEdge™
PowerSaver™
PowerTrench®
Programmable Active Droop™
QFET®
QS™
QT Optoelectronics™
Quiet Series™
RapidConfigure™
RapidConnect™
ScalarPump™
SMART START™
SPM™
SuperFET™
SuperSOT™-3
SuperSOT™-6
SuperSOT™-8
TCM™
The Power Franchise®
TinyBoost™
TinyBuck™
TinyLogic®
TINYOPTO™
TinyPower™
TinyWire™
TruTranslation™
μSerDes™
UHC®
UniFET™
VCX™
Wire™

DISCLAIMER

FAIRCHILD SEMICONDUCTOR RESERVES THE RIGHT TO MAKE CHANGES WITHOUT FURTHER NOTICE TO ANY PRODUCTS HEREIN TO IMPROVE RELIABILITY, FUNCTION OR DESIGN. FAIRCHILD DOES NOT ASSUME ANY LIABILITY ARISING OUT OF THE APPLICATION OR USE OF ANY PRODUCT OR CIRCUIT DESCRIBED HEREIN;NEITHER DOES IT CONVEY ANY LICENSE UNDER ITS PATENT RIGHTS, NOR THE RIGHTS OF OTHERS. THESE SPECIFICATIONS DO NOT EXPAND THE TERMS OF FAIRCHILD'S WORLDWIDE TERMS AND CONDITIONS, SPECIFICALLY THE WARRANTY THEREIN, WHICH COVERS THESE PRODUCTS.

LIFE SUPPORT POLICY

FAIRCHILD'S PRODUCTS ARE NOT AUTHORIZED FOR USE AS CRITICAL COMPONENTS IN LIFE SUPPORT DEVICES OR SYSTEMS WITHOUT THE EXPRESS WRITTEN APPROVAL OF FAIRCHILD SEMICONDUCTOR CORPORATION.

As used herein:

1. Life support devices or systems are devices or systems which, (a) are intended for surgical implant into the body, or (b) support or sustain life, or (c) whose failure to perform when properly used in accordance with instructions for use provided in the labeling, can be reasonably expected to result in significant injury to the user.

2. A critical component is any component of a life support device or system whose failure to perform can be reasonably expected to cause the failure of the life support device or system, or to affect its safety or effectiveness.

PRODUCT STATUS DEFINITIONS

Definition of Terms

Datasheet Identification	Product Status	Definition
Advance Information	Formative or In Design	This datasheet contains the design specifications for product development. Specifications may change in any manner without notice.
Preliminary	First Production	This datasheet contains preliminary data, and supplementary data will be published at a later date.Fairchild Semiconductor reserves the right to make changes at any time without notice in order to improve design.
No Identification Needed	Full Production	This datasheet contains final specifications. Fairchild Semiconductor reserves the right to make changes at any time without notice in order to improve design.
Obsolete	Not In Production	This datasheet contains specifications on a product that has been discontinued by Fairchild semiconductor.The datasheet is printed for reference information only.

Rev. I23

A.2. CURRENT SENSOR

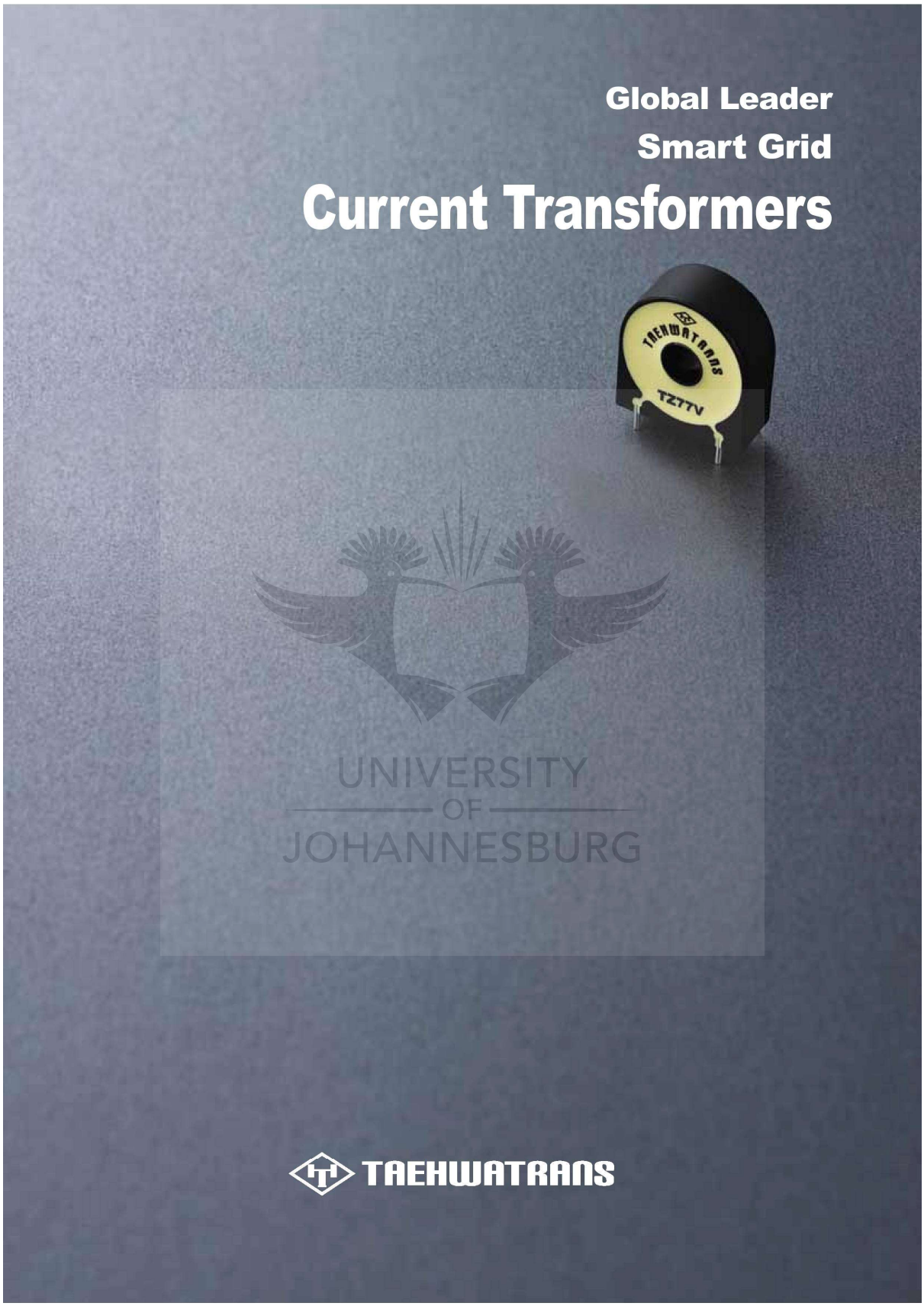

Global Leader & Strong Partnership

Company Footstep

2009	Selected as a Frontier Company by Provincial Government
2008	ISO14001 Certified
2007	Established Taehwatrans America Inc. in Chicago
2006	RoHS compliance for all the products
2003	TUV Certified
2002	ISO9001 Certified
	CE Certified
2001	Introduction of ERP System
2000	UL Certified
	Designated as a IBK family company by industrial bank of korea
1999	Opening website www.taehwatrans.com and www.taehwatrans.co.kr
	Selected as Korean best product by Samsung Global Mall
	Designated as supreme performance company by industrial bank of Korea
1998	Selected as export promising company by government institution
	& small business corporation
1993	Acquiring an award & export achievement merit from Korea trade association
1990	Started overseas sales promotion
1986	Initiating overseas sales
1985	Incorporated Taehwatrans Co., Ltd
1980	Founded by the name of Taehwa Industry

CONTENTS

High Precision Current Transformer

Application

- Accuracy power monitoring
- High-end digital protection relay
- Power transducer
- High-end UPS periphery relay
- High-end industrial power sensor
- Inverter controlling
- Precision motor protection relay

Features

- High precision & Stability
- High saturation induction
- Excellent linearity
- Excellent thermal properties
- High potential voltage of 2.5KV-4.0KV/min
- RoHS compliant

Standard Accuracy : 3.0 Class

Model & Specification

(f=50Hz, Rb=1Ω, PF=1.0, unit : percent / minute)

Model No	Current Ratio	DCR ±6%	Im Rb=1Ω	Im Rb=20Ω	Im Rb=500Ω	Rnv Rb=0, 1-20A	Pnv Rb=0, 1-20A	Phase Shift at 1V
TC1V TC1L	1000 : 1	74Ω	76A	60A	9A	1.5%	190′	106′
TC148V TC148L	2000 : 1	98Ω	225A	190A	38A	0.7%	75′	29′
TC149V TC149L	1500 : 1	46Ω	370A	260A	31A	1.0%	50′	24′
TC150V TC150L	2000 : 1	40Ω	870A	590A	69A	2.0%	85′	39′

Definition of Terms

Im : Max rated current Rnv : Nominal variation of ratio error at the mentioned primary current range Pnv : Nominal variation of phase error at the mentioned primary current range Rb : Burden resistance PF : Power factor DCR : DC Resistance of secondary winding

Remark : The data of maximum current, ratio and phase error on 60Hz testing would be around 20% better than those of above 50Hz

High Precision Current Transformer

Model & Specification

(f=50Hz, Rb=1Ω, PF=1.0, unit : percent / minute)

Model No	Current Ratio	DCR ±6%	Im Rb=1Ω	Im Rb=20Ω	Im Rb=500Ω	Rnv 1-20A, Rb=0	Pnv 1-20A, Rb=0	Phase Shift at 1V
TC140V/L	1000 : 1	34Ω	125A	82A	8A	1.2%	70′	88′
TC141V/L	1000 : 1	29Ω	250A	156A	14A	0.7%	60′	65′
TC142V/L	1000 : 1	19Ω	460A	230A	17A	2.2%	90′	34′
TC143V/L	4000 : 1	154Ω	940A	840A	210A	1.5%	86′	13′

(f=50Hz, Rb=1Ω, PF=1.0, unit : percent / minute)

Model No	Current Ratio	DCR ±6%	Im Rb=1Ω	Im Rb=20Ω	Im Rb=500Ω	Rnv 1-20A, Rb=0	Pnv 1-20A Rb=0	Phase Shift at 1V
TC172V/L	2500 : 1	129Ω	210A	170A	45A	1.0%	55′	62′
TC173V/L	2500 : 1	187Ω	260A	240A	70A	1.2%	62′	28′
TC174V/L	2500 : 1	51Ω	〉1000A	790A	100A	1.3%	100′	13′
TC175V/L	2000 : 1	26Ω	〉1000A	790A	67A	1.4%	95′	11′

Definition of Terms

Im : Max rated current Rnv : Nominal variation of ratio error at the mentioned primary current range Pnv : Nominal variation of phase error at the mentioned primary current range Rb : Burden resistance PF : Power factor DCR : DC Resistance of secondary winding
Remark : The data of maximum current, ratio and phase error on 60Hz testing would be around 20% better than those of above 50Hz

(f=50Hz, Rb=1Ω, PF=1.0, unit : percent / minute)

Model No	Current Ratio	DCR(±6%)	Tolerance	Imax		
				Rb=1Ω	Rb=20Ω	Rb=500Ω
TC1PV	1000 : 1	62Ω	±3%	54A	42A	5A
TC2V/L	1000 : 1	41Ω		60A	44A	5A
TC3L	1000 : 1	33Ω		142A	95A	9A
TC4V/L	1000 : 1	19Ω		460A	230A	17A
TC5V/L	1000 : 1	12Ω		660A	260A	16A

Drawing

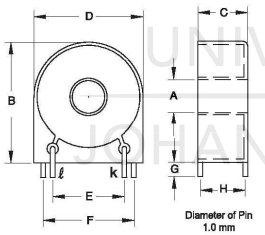

PCB Mountable Type

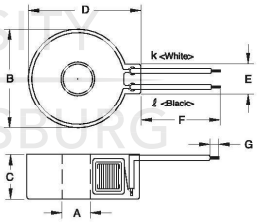

Wire Lead Type

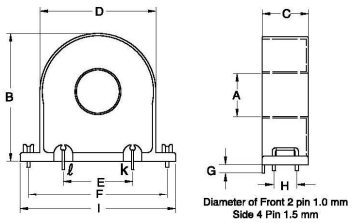

TC175V & TC5V

Dimension

PCB Mountable type (unit : mm/inch)

Model No	A(min)	B(max)	C(max)	D(max)	E(±0.3)	F(±0.3)	G(±0.5)	H(±0.3)	I(max)
TC1PV	5.7 0.224"	19.5 0.768"	8.6 0.339"	19.2 0.756"	12.7 0.500"	16.0 0.630"	3.0 0.118"	7.5 0.295"	
TC1V TC140V TC148V TC172V	6.8 0.268"	25.0 0.984"	11.0 0.433"	23.5 0.925"	15.1 0.594"	19.1 0.752"	3.0 0.118"	9.1 0.358"	
TC2V TC141V TC149V TC173V	8.9 0.350"	27.5 1.083"	17.0 0.670"	25.3 0.996"	15.1 0.594"	19.1 0.752"	3.0 0.118"	15.1 0.594"	
TC4V TC142V TC143V TC150V TC174V	12.9 0.508"	39.3 1.547"	14.0 0.551"	38.0 1.496"	25.2 0.992"	32.8 1.291"	3.0 0.118"	12.1 0.476"	
TC5V TC175V	18.4 0.744"	55.5 2.185"	20.3 0.799"	50.5 1.988"	30.0 1.181"	60.0 2.362"	4.0 0.157"	10.0 0.394"	67.6 2.661"

Wire lead type (unit : mm/inch)

Model No	A(min)	B(max)	C(max)	D(max)	E(max)	F(±3.0)	G(±1.0)
TC1L	8.9 0.350"	22.0 0.866"	9.0 0.354"	25.0 0.984"	7.0 0.276"	73.0 2.874"	3.0 0.118"
TC2L	9.9 0.390"	24.0 0.945"	9.0 0.354"	27.0 1.063"	6.0 0.236"	120.0 4.724"	5.0 0.197"
TC3L	15.6 0.614"	30.25 1.191"	9.1 0.358"	33.8 1.331"	6.3 0.248"	122.0 4.803"	5.0 0.197"
TC172L	6.9 0.272"	23.6 0.930"	11.0 0.433"	26.8 1.055"	7.1 0.280"	71.0 2.795"	3.0 0.118"
TC140L TC148L	6.9 0.272"	23.6 0.930"	11.0 0.433"	26.8 1.055"	7.1 0.280"	81.0 3.189"	3.0 0.118"
TC141L TC149L	8.9 0.350"	24.8 0.976"	17.0 0.669"	28.4 1.118"	7.6 0.299"	73.0 2.874"	3.0 0.118"
TC173I	8.9 0.350"	24.8 0.976"	17.0 0.669"	28.4 1.118"	7.6 0.299"	65.0 2.559"	3.0 0.118"
TC150L	12.9 0.508"	37.5 1.476"	14.0 0.551"	41.3 1.626"	10.3 0.406"	77.0 3.031"	3.0 0.118"
TC4L TC142L TC143L TC174L	12.9 0.508"	37.5 1.476"	14.0 0.551"	41.3 1.626"	10.3 0.406"	68.0 2.677"	3.0 0.118"
TC175L	19.6 0.772"	48.2 1.898"	19.2 0.756"	52.0 2.047"	13.2 0.520"	110.0 4.331"	5.0 0.197"
TC5L	19.6 0.772"	48.2 1.898"	19.2 0.756"	52.0 2.047"	13.2 0.520"	130.0 5.118"	5.0 0.197"

Specialty Transformer for Bidet & Leakage Protection

Application & Feature

- Instantaneous water heater
- Bidet (Monitoring & Leakage protection)
- Refrigerator

Drawing

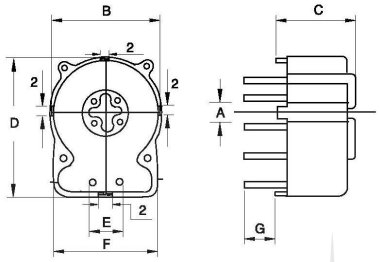

TZ1PH

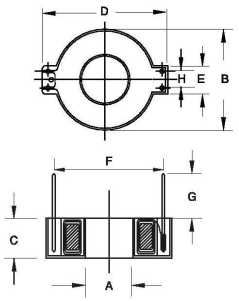

TC153H

Dimension

Horizontal type

(unit : mm/inch)

Model No	A(min)	B(max)	C(max)	D(max)	E	F	G	H	Rdc
TZ1PH	5.0 0.197″	19.0 0.748″	11.0 0.433″	21.5 0.846″	5.0 0.197″	18.5 0.728″	4.2 0.165″		22.5– 28.5Ω
TC153H	10.5 0.413″	23.5 0.925″	10.0 0.394″	29.7 1.170″	7.1 0.280″	25.0 0.984″	5.5 0.217″	3.0 0.118″	22.5– 27.5Ω

Secondary Burden & Output Voltage Graph

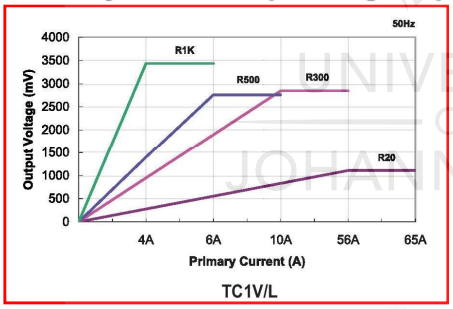

TC1V/L

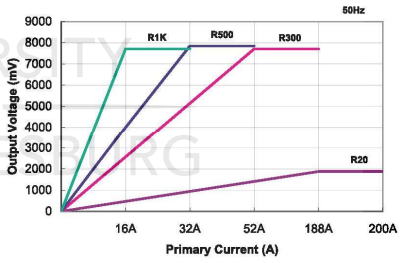

TC148V/L

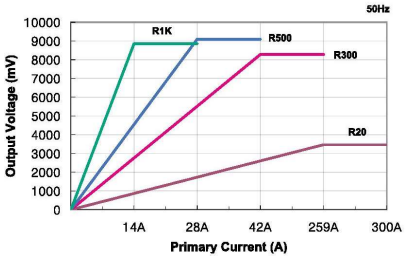

TC149V/L

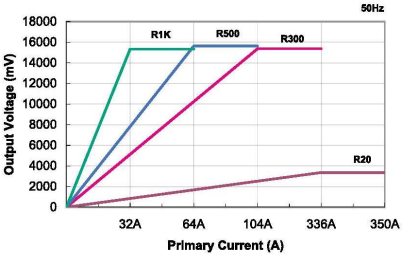

TC150V/L

TAEHWATRANS

HEAD OFFICE & FACTORY
288-2, Misan-Dong, Siheung-Si,
Gyeonggi-Do, Korea, 429-822
TEL : 82-31-315-8161~4 FAX : 82-31-315-8165
http : //www.taehwatrans.com
E-mail : sales@taehwatrans.com

Taehwatrans America Inc
8700 Waukegan Road, ste114, Morton Grove, IL, 60053
TEL : 847-299-5182 FAX : 847-965-3336
http : //www.taehwatrans.com
E-mail : salesusa@taehwatrans.com

2011-9

A.3. ARDUINO MICROCONTROLLER

Arduino MEGA 2560

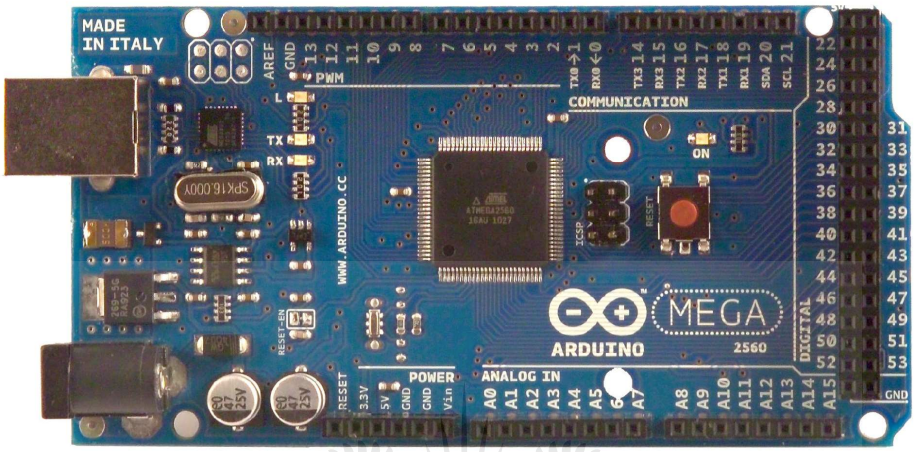

CE

Product Overview

The Arduino Mega 2560 is a microcontroller board based on the ATmega2560 (datasheet). It has 54 digital input/output pins (of which 14 can be used as PWM outputs), 16 analog inputs, 4 UARTs (hardware serial ports), a 16 MHz crystal oscillator, a USB connection, a power jack, an ICSP header, and a reset button. It contains everything needed to support the microcontroller; simply connect it to a computer with a USB cable or power it with a AC-to-DC adapter or battery to get started. The Mega is compatible with most shields designed for the Arduino Duemilanove or Diecimila.

Index

Technical Specification

EAGLE files: arduino-mega2560-reference-design.zip Schematic: arduino-mega2560-schematic.pdf

Summary

Microcontroller	ATmega2560
Operating Voltage	5V
Input Voltage (recommended)	7-12V
Input Voltage (limits)	6-20V
Digital I/O Pins	54 (of which 14 provide PWM output)
Analog Input Pins	16
DC Current per I/O Pin	40 mA
DC Current for 3.3V Pin	50 mA
Flash Memory	256 KB of which 8 KB used by bootloader
SRAM	8 KB
EEPROM	4 KB
Clock Speed	16 MHz

the board

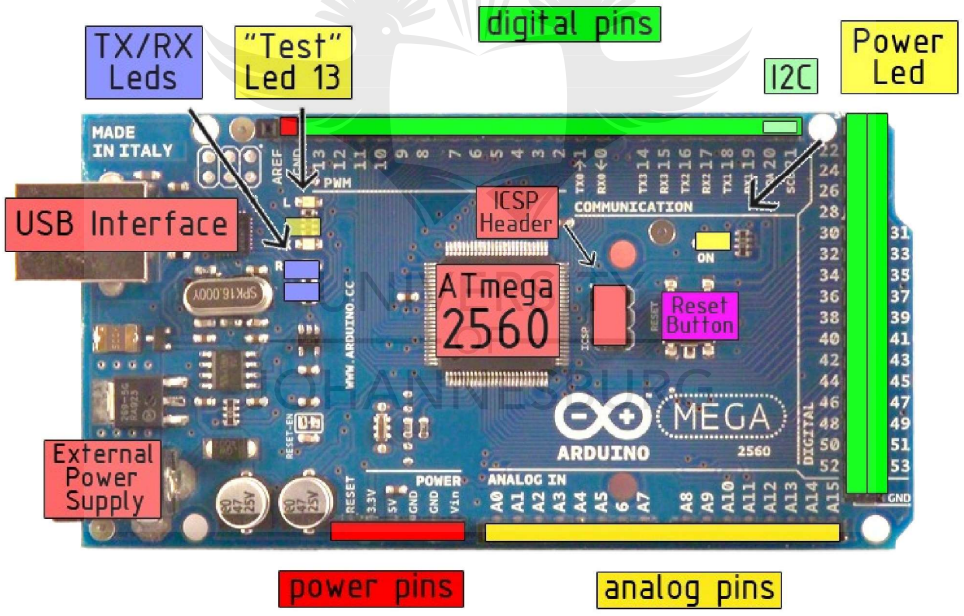

Power

The Arduino Mega2560 can be powered via the USB connection or with an external power supply. The power source is selected automatically. External (non-USB) power can come either from an AC-to-DC adapter (wall-wart) or battery. The adapter can be connected by plugging a 2.1mm center-positive plug into the board's power jack. Leads from a battery can be inserted in the Gnd and Vin pin headers of the POWER connector.

The board can operate on an external supply of 6 to 20 volts. If supplied with less than 7V, however, the 5V pin may supply less than five volts and the board may be unstable. If using more than 12V, the voltage regulator may overheat and damage the board. The recommended range is 7 to 12 volts.

The Mega2560 differs from all preceding boards in that it does not use the FTDI USB-to-serial driver chip. Instead, it features the Atmega8U2 programmed as a USB-to-serial converter.

The power pins are as follows:

- **VIN.** The input voltage to the Arduino board when it's using an external power source (as opposed to 5 volts from the USB connection or other regulated power source). You can supply voltage through this pin, or, if supplying voltage via the power jack, access it through this pin.
- **5V.** The regulated power supply used to power the microcontroller and other components on the board. This can come either from VIN via an on-board regulator, or be supplied by USB or another regulated 5V supply.
- **3V3.** A 3.3 volt supply generated by the on-board regulator. Maximum current draw is 50 mA.
- **GND.** Ground pins.

Memory

The ATmega2560 has 256 KB of flash memory for storing code (of which 8 KB is used for the bootloader), 8 KB of SRAM and 4 KB of EEPROM (which can be read and written with the EEPROM library).

Input and Output

Each of the 54 digital pins on the Mega can be used as an input or output, using pinMode(), digitalWrite(), and digitalRead() functions. They operate at 5 volts. Each pin can provide or receive a maximum of 40 mA and has an internal pull-up resistor (disconnected by default) of 20-50 kOhms. In addition, some pins have specialized functions:

- **Serial: 0 (RX) and 1 (TX); Serial 1: 19 (RX) and 18 (TX); Serial 2: 17 (RX) and 16 (TX); Serial 3: 15 (RX) and 14 (TX).** Used to receive (RX) and transmit (TX) TTL serial data. Pins 0 and 1 are also connected to the corresponding pins of the ATmega8U2 USB-to-TTL Serial chip .
- **External Interrupts: 2 (interrupt 0), 3 (interrupt 1), 18 (interrupt 5), 19 (interrupt 4), 20 (interrupt 3), and 21 (interrupt 2).** These pins can be configured to trigger an interrupt on a low value, a rising or falling edge, or a change in value. See the attachInterrupt() function for details.
- **PWM: 0 to 13.** Provide 8-bit PWM output with the analogWrite() function.
- **SPI: 50 (MISO), 51 (MOSI), 52 (SCK), 53 (SS).** These pins support SPI communication, which, although provided by the underlying hardware, is not currently included in the Arduino language. The SPI pins are also broken out on the ICSP header, which is physically compatible with the Duemilanove and Diecimila.
- **LED: 13.** There is a built-in LED connected to digital pin 13. When the pin is HIGH value, the LED is on, when the pin is LOW, it's off.
- **I^2C: 20 (SDA) and 21 (SCL).** Support I^2C (TWI) communication using the Wire library (documentation on the Wiring website). Note that these pins are not in the same location as the I^2C pins on the Duemilanove.

The Mega2560 has 16 analog inputs, each of which provide 10 bits of resolution (i.e. 1024 different values). By default they measure from ground to 5 volts, though is it possible to change the upper end of their range using the AREF pin and analogReference() function.

There are a couple of other pins on the board:

- **AREF.** Reference voltage for the analog inputs. Used with analogReference().
- **Reset.** Bring this line LOW to reset the microcontroller. Typically used to add a reset button to shields which block the one on the board.

Communication

The Arduino Mega2560 has a number of facilities for communicating with a computer, another Arduino, or other microcontrollers. The ATmega2560 provides four hardware UARTs for TTL (5V) serial communication. An ATmega8U2 on the board channels one of these over USB and provides a virtual com port to software on the computer (Windows machines will need a .inf file, but OSX and Linux machines will recognize the board as a COM port automatically. The Arduino software includes a serial monitor which allows simple textual data to be sent to and from the board. The RX and TX LEDs on the board will flash when data is being transmitted via the ATmega8U2 chip and USB connection to the computer (but not for serial communication on pins 0 and 1).

A SoftwareSerial library allows for serial communication on any of the Mega's digital pins.

The ATmega2560 also supports I2C (TWI) and SPI communication. The Arduino software includes a Wire library to simplify use of the I2C bus; see the documentation on the Wiring website for details. To use the SPI communication, please see the ATmega2560 datasheet.

Programming

The Arduino Mega2560 can be programmed with the Arduino software (download). For details, see the reference and tutorials.

The Atmega2560 on the Arduino Mega comes preburned with a bootloader that allows you to upload new code to it without the use of an external hardware programmer. It communicates using the original STK500 protocol (reference, C header files).

You can also bypass the bootloader and program the microcontroller through the ICSP (In-Circuit Serial Programming) header; see these instructions for details.

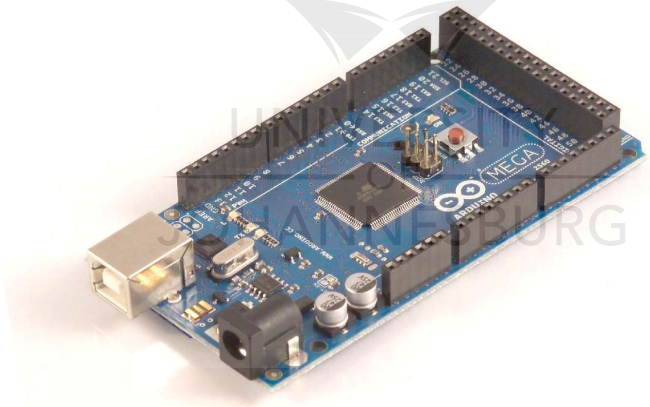

Automatic (Software) Reset

Rather then requiring a physical press of the reset button before an upload, the Arduino Mega2560 is designed in a way that allows it to be reset by software running on a connected computer. One of the hardware flow control lines (DTR) of the ATmega8U2 is connected to the reset line of the ATmega2560 via a 100 nanofarad capacitor. When this line is asserted (taken low), the reset line drops long enough to reset the chip. The Arduino software uses this capability to allow you to upload code by simply pressing the upload button in the Arduino environment. This means that the bootloader can have a shorter timeout, as the lowering of DTR can be well-coordinated with the start of the upload.

This setup has other implications. When the Mega2560 is connected to either a computer running Mac OS X or Linux, it resets each time a connection is made to it from software (via USB). For the following half-second or so, the bootloader is running on the Mega2560. While it is programmed to ignore malformed data (i.e. anything besides an upload of new code), it will intercept the first few bytes of data sent to the board after a connection is opened. If a sketch running on the board receives one-time configuration or other data when it first starts, make sure that the software with which it communicates waits a second after opening the connection and before sending this data.

The Mega contains a trace that can be cut to disable the auto-reset. The pads on either side of the trace can be soldered together to re-enable it. It's labeled "RESET-EN". You may also be able to disable the auto-reset by connecting a 110 ohm resistor from 5V to the reset line; see this forum thread for details.

USB Overcurrent Protection

The Arduino Mega has a resettable polyfuse that protects your computer's USB ports from shorts and overcurrent. Although most computers provide their own internal protection, the fuse provides an extra layer of protection. If more than 500 mA is applied to the USB port, the fuse will automatically break the connection until the short or overload is removed.

Physical Characteristics and Shield Compatibility

The maximum length and width of the Mega PCB are 4 and 2.1 inches respectively, with the USB connector and power jack extending beyond the former dimension. Three screw holes allow the board to be attached to a surface or case. Note that the distance between digital pins 7 and 8 is 160 mil (0.16"), not an even multiple of the 100 mil spacing of the other pins.

The Mega is designed to be compatible with most shields designed for the Diecimila or Duemilanove. Digital pins 0 to 13 (and the adjacent AREF and GND pins), analog inputs 0 to 5, the power header, and ICSP header are all in equivalent locations. Further the main UART (serial port) is located on the same pins (0 and 1), as are external interrupts 0 and 1 (pins 2 and 3 respectively). SPI is available through the ICSP header on both the Mega and Duemilanove / Diecimila. **Please note that I^2C is not located on the same pins on the Mega (20 and 21) as the Duemilanove / Diecimila (analog inputs 4 and 5).**

How to use Arduino

Arduino can sense the environment by receiving input from a variety of sensors and can affect its surroundings by controlling lights, motors, and other actuators. The microcontroller on the board is programmed using the Arduino programming language (based on Wiring) and the Arduino development environment (based on Processing). Arduino projects can be stand-alone or they can communicate with software on running on a computer (e.g. Flash, Processing, MaxMSP).

Arduino is a cross-platoform program. You'll have to follow different instructions for your personal OS. Check on the Arduino site for the latest instructions. *http://arduino.cc/en/Guide/HomePage*

Linux Install Windows Install Mac Install

Once you have downloaded/unzipped the arduino IDE, you can Plug the Arduino to your PC via USB cable.

Blink led

Now you're actually ready to "burn" your first program on the arduino board. To select "blink led", the physical translation of the well known programming "hello world", select

File>Sketchbook>
Arduino-0017>Examples>
Digital>Blink

Once you have your skecth you'll see something very close to the screenshot on the right.

In **Tools>Board** select MEGA

Now you have to go to
Tools>SerialPort
and select the right serial port, the one arduino is attached to.

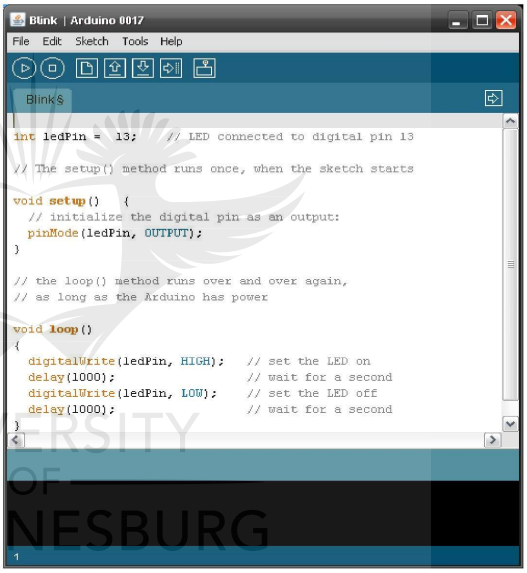

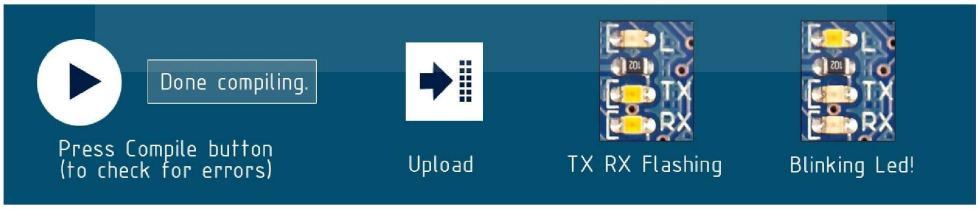

Dimensioned Drawing

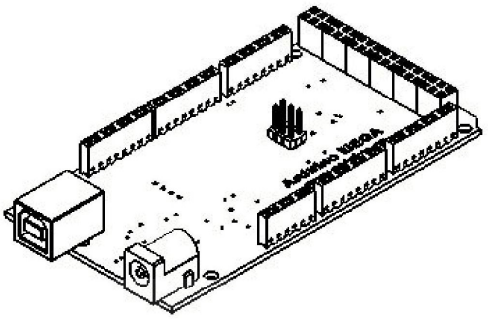

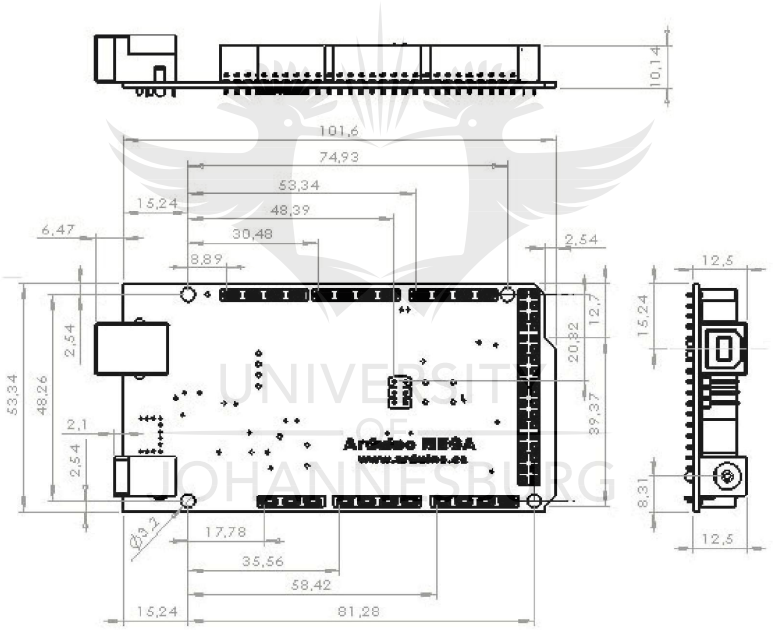

Terms & Conditions

1. Warranties

1.1 The producer warrants that its products will conform to the Specifications. This warranty lasts for one (1) years from the date of the sale. The producer shall not be liable for any defects that are caused by neglect, misuse or mistreatment by the Customer, including improper installation or testing, or for any products that have been altered or modified in any way by a Customer. Moreover, The producer shall not be liable for any defects that result from Customer's design, specifications or instructions for such products. Testing and other quality control techniques are used to the extent the producer deems necessary.

1.2 If any products fail to conform to the warranty set forth above, the producer's sole liability shall be to replace such products. The producer's liability shall be limited to products that are determined by the producer not to conform to such warranty. If the producer elects to replace such products, the producer shall have a reasonable time to replacements. Replaced products shall be warranted for a new full warranty period.

1.3 EXCEPT AS SET FORTH ABOVE, PRODUCTS ARE PROVIDED "AS IS" AND "WITH ALL FAULTS." THE PRODUCER DISCLAIMS ALL OTHER WARRANTIES, EXPRESS OR IMPLIED, REGARDING PRODUCTS, INCLUDING BUT NOT LIMITED TO, ANY IMPLIED WARRANTIES OF MERCHANTABILITY OR FITNESS FOR A PARTICULAR PURPOSE

1.4 Customer agrees that prior to using any systems that include the producer products, Customer will test such systems and the functionality of the products as used in such systems. The producer may provide technical, applications or design advice, quality characterization, reliability data or other services. Customer acknowledges and agrees that providing these services shall not expand or otherwise alter the producer's warranties, as set forth above, and no additional obligations or liabilities shall arise from the producer providing such services.

1.5 The Arduino™ products are not authorized for use in safety-critical applications where a failure of the product would reasonably be expected to cause severe personal injury or death. Safety-Critical Applications include, without limitation, life support devices and systems, equipment or systems for the operation of nuclear facilities and weapons systems. Arduino™ products are neither designed nor intended for use in military or aerospace applications or environments and for automotive applications or environment. Customer acknowledges and agrees that any such use of Arduino™ products which is solely at the Customer's risk, and that Customer is solely responsible for compliance with all legal and regulatory requirements in connection with such use.

1.6 Customer acknowledges and agrees that it is solely responsible for compliance with all legal, regulatory and safety-related requirements concerning its products and any use of Arduino™ products in Customer's applications, notwithstanding any applications-related information or support that may be provided by the producer.

2. Indemnification

The Customer acknowledges and agrees to defend, indemnify and hold harmless the producer from and against any and all third-party losses, damages, liabilities and expenses it incurs to the extent directly caused by: (i) an actual breach by a Customer of the representation and warranties made under this terms and conditions or (ii) the gross negligence or willful misconduct by the Customer.

3. Consequential Damages Waiver

In no event the producer shall be liable to the Customer or any third parties for any special, collateral, indirect, punitive, incidental, consequential or exemplary damages in connection with or arising out of the products provided hereunder, regardless of whether the producer has been advised of the possibility of such damages. This section will survive the termination of the warranty period.

4. Changes to specifications

The producer may make changes to specifications and product descriptions at any time, without notice. The Customer must not rely on the absence or characteristics of any features or instructions marked "reserved" or "undefined." The producer reserves these for future definition and shall have no responsibility whatsoever for conflicts or incompatibilities arising from future changes to them. The product information on the Web Site or Materials is subject to change without notice. Do not finalize a design with this information.

Enviromental Policies

The producer of Arduino™ has joined the Impatto Zero® policy of LifeGate.it. For each Arduino board produced is created / looked after half squared Km of Costa Rica's forest's.

A.4. OPTOCOUPLER

TOSHIBA Photocoupler GaAℓAs Ired & Photo-IC

TLP250

Industrial Inverter
Inverter For Air Conditioner
IGBT Gate Drive
Power MOS FET Gate Drive

The TOSHIBA TLP250 consists of a GaAlAs light emitting diode and a integrated photodetector.
This unit is 8-lead DIP package.
TLP250 is suitable for gate driving circuit of IGBT or power MOS FET.

- Input threshold current: 5mA(max)
- Supply current : 11mA(max)
- Supply voltage : 10-35V
- Output current : ±1.5A (max)
- Switching time (t_{pLH}/t_{pHL}): 0.5μs(max)
- Isolation voltage: 2500V_{rms}(min)
- UL recognized: UL1577, file No.E67349
- c-UL approved : CSA Component Acceptance Service No. 5A, File No.E67349
- Option(D4)
  VDE Approved : EN60747-5- 5
  Note: When a EN60747-5-5 approved type is needed, Please designate "Option(D4)"

Unit: mm

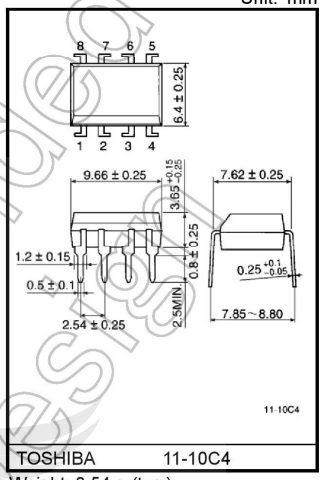

TOSHIBA 11-10C4

Weight: 0.54 g (typ.)

Truth Table

		Tr1	Tr2
Input LED	On	On	Off
	Off	Off	On

Pin Configuration (top view)

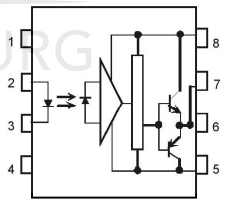

1 : N.C.
2 : Anode
3 : Cathode
4 : N.C.
5 : GND
6 : V_O (Output)
7 : V_O
8 : V_{CC}

Schmatic

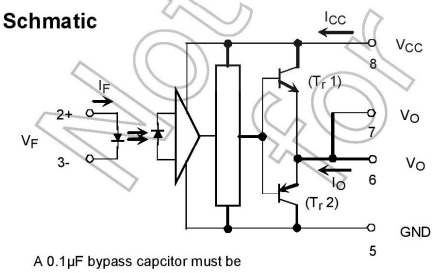

A 0.1μF bypass capcitor must be connected between pin 8 and 5

Start of commercial production
1990-11

Absolute Maximum Ratings (Ta = 25°C)

Characteristic			Symbol	Rating	Unit
LED	Forward current		I_F	20	mA
	Forward current derating (Ta ≥ 70°C)		ΔI_F / ΔTa	-0.36	mA / °C
	Peak transient forward curent	(Note 1)	I_{FPT}	1	A
	Reverse voltage		V_R	5	V
	Diode power dissipation		P_D	40	mW
	Diode power dissipation derating (Ta≥70°C)		ΔP_D /°C	-0.72	mW / °C
	Junction temperature		Tj	125	°C
Detector	"H"peak output current (P_W ≤ 2.5μs,f ≤ 15kHz)	(Note 2)	I_{OPH}	-1.5	A
	"L"peak output current (P_W ≤ 2.5μs,f ≤ 15kHz)	(Note 2)	I_{OPL}	+1.5	A
	Output voltage	(Ta ≤ 70°C)	V_O	35	V
		(Ta ≤ 85°C)		24	
	Supply voltage	(Ta ≤ 70°C)	V_{CC}	35	V
		(Ta ≤ 85°C)		24	
	Output voltage derating (Ta ≥ 70°C)		ΔV_O / ΔTa	-0.73	V / °C
	Supply voltage derating (Ta ≥ 70°C)		ΔV_{CC} / ΔTa	-0.73	V / °C
	Power dissipation		P_C	800	mW
	Power dissipation derating (Ta ≥ 70°C)		ΔP_C / °C	-14.5	mW / °C
	Junction temperature		Tj	125	°C
Operating frequency		(Note 3)	f	25	kHz
Operating temperature range			T_{opr}	-20 to 85	°C
Storage temperature range			T_{stg}	-55 to 125	°C
Lead soldering temperature (10 s)			T_{sol}	260	°C
Isolation voltage (AC, 60 s., R.H.≤ 60%)		(Note 4)	BV_S	2500	Vrms

Note: Using continuously under heavy loads (e.g. the application of high temperature/current/voltage and the significant change in temperature, etc.) may cause this product to decrease in the reliability significantly even if the operating conditions (i.e. operating temperature/current/voltage, etc.) are within the absolute maximum ratings.
Please design the appropriate reliability upon reviewing the Toshiba Semiconductor Reliability Handbook ("Handling Precautions"/"Derating Concept and Methods") and individual reliability data (i.e. reliability test report and estimated failure rate, etc).

Note 1: Pulse width P_W ≤ 1μs, 300pps

Note 2: Exporenential wavefom

Note 3: Exporenential wavefom, I_{OPH} ≤ -1.0A(≤ 2.5μs), I_{OPL} ≤ +1.0A(≤ 2.5μs)

Note 4: Device considerd a two terminal device: Pins 1, 2, 3 and 4 shorted together, and pins 5, 6, 7 and 8 shorted together.

Recommended Operating Conditions

Characteristic	Symbol	Min	Typ.	Max	Unit
Input current, on	$I_{F(ON)}$	7	8	10	mA
Input voltage, off	$V_{F(OFF)}$	0	—	0.8	V
Supply voltage	V_{CC}	15	—	30	V
Peak output current	I_{OPH}/I_{OPL}	—	—	±0.5	A
Operating temperature	T_{opr}	-20	25	85	°C

Note: Recommended operating conditions are given as a design guideline to obtain expected performance of the device. Additionally, each item is an independent guideline respectively. In developing designs using this product, please confirm specified characteristics shown in this document.

Note : A ceramic capacitor(0.1μF) should be connected from pin 8 to pin 5 to stabilize the operation of the high gain linear amplifier. Failure to provide the bypassing may impair the switching proparty. The total lead length between capacitor and coupler should not exceed 1cm.

Note : Input signal rise time(fall time)<0.5μs.

Electrical Characteristics (Ta = -20 to 70°C, unless otherwise specified)

Characteristic		Symbol	Test Circuit	Test Condition		Min	Typ.*	Max	Unit
Input forward voltage		V_F	—	I_F = 10 mA, Ta = 25°C		—	1.6	1.8	V
Temperature coefficient of forward voltage		$\Delta V_F / \Delta Ta$	—	I_F = 10 mA		—	-2.0	—	mV / °C
Input reverse current		I_R	—	V_R = 5V, Ta = 25°C		—	—	10	μA
Input capacitance		C_T	—	V = 0 V, f = 1MHz , Ta = 25°C		—	45	250	pF
Output current	"H" level	I_{OPH}	1	V_{CC} = 30V (Note 1)	I_F = 10 mA V_{8-6} = 4V	-0.5	-1.5	—	A
	"L" level	I_{OPL}	2		I_F = 0 mA V_{6-5} = 2.5V	0.5	2	—	
Output voltage	"H" level	V_{OH}	3	V_{CC1} = +15V, V_{EE1} = -15V R_L = 200Ω, I_F = 5mA		11	12.8	—	V
	"L" level	V_{OL}	4	V_{CC1} = +15V, V_{EE1} = -15V R_L = 200Ω, V_F = 0.8V		—	-14.2	-12.5	
Supply current	"H" level	I_{CCH}	—	V_{CC} = 30V, I_F = 10mA Ta = 25°C		—	7	—	mA
				V_{CC} = 30V, I_F = 10mA		—	—	11	
	"L" level	I_{CCL}	—	V_{CC} = 30V, I_F = 0mA Ta = 25°C		—	7.5	—	
				V_{CC} = 30V, I_F = 0mA		—	—	11	
Threshold input current	"Output L→H"	I_{FLH}	—	V_{CC1} = +15V, V_{EE1} = -15V R_L = 200Ω, V_O > 0V		—	1.2	5	mA
Threshold input voltage	"Output H→L"	V_{FHL}	—	V_{CC1} = +15V, V_{EE1} = -15V R_L = 200Ω, V_O < 0V		0.8	—	—	V
Supply voltage		V_{CC}	—	—		10	—	35	V
Capacitance (input-output)		C_S	—	V_S = 0 V, f = 1MHz Ta = 25°C		—	1.0	2.0	pF
Resistance(input-output)		R_S	—	V_S = 500V , Ta = 25°C R.H.≤ 60%		1×10^{12}	10^{14}	—	Ω

* All typical values are at Ta = 25°C

Note 1: Duration of I_O time ≤ 50μs

Switching Characteristics (Ta = -20 to 70°C, unless otherwise specified)

Characteristic		Symbol	Test Cir-cuit	Test Condition	Min	Typ.	Max	Unit
Propagation delay time	L→H	t_{pLH}	5	I_F = 8mA V_{CC1} = +15V, V_{EE1} = -15V R_L = 200Ω	—	0.15	0.5	μs
	H→L	t_{pHL}			—	0.15	0.5	
Common mode transient immunity at high level output		CM_H	6	V_{CM} = 600V, I_F = 8mA V_{CC} = 30V, Ta = 25°C	-5000	—	—	V / μs
Common mode transient immunity at low level output		CM_L		V_{CM} = 600V, I_F = 0mA V_{CC} = 30V, Ta = 25°C	5000	—	—	V / μs

Note: All typical values are at Ta = 25°C

Test Circuit 1 : I_{OPH}

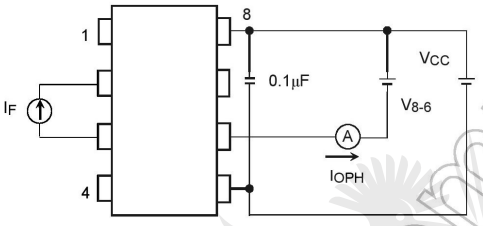

Test Circuit 2 : I_{OPL}

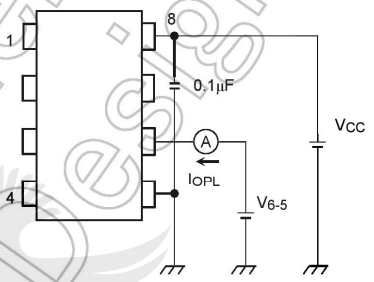

Test Circuit 3 : V_{OH}

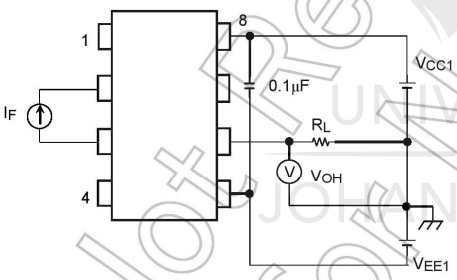

Test Circuit 4 : V_{OL}

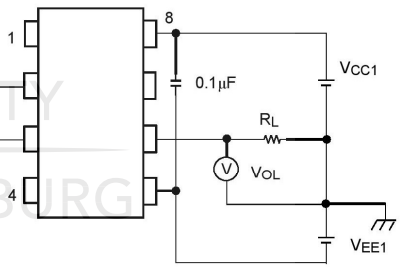

Test Circuit 5: t_{pLH}, t_{pHL}, t_r t_f

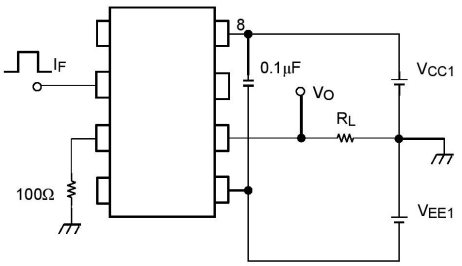

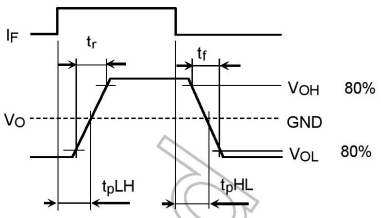

Test Circuit 6: CM_H, CM_L

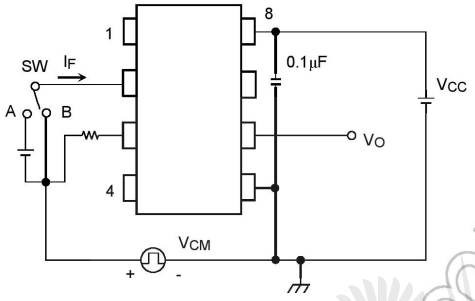

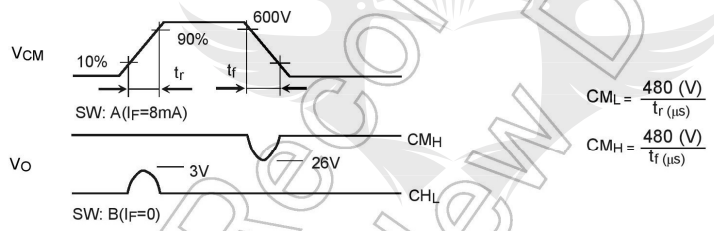

$$CM_L = \frac{480\ (V)}{t_{r\ (\mu s)}}$$

$$CM_H = \frac{480\ (V)}{t_{f\ (\mu s)}}$$

CM_L(CM_H) is the maximum rate of rise (fall) of the common mode voltage that can be sustained with the output voltage in the low (high) state.

$I_F - V_F$

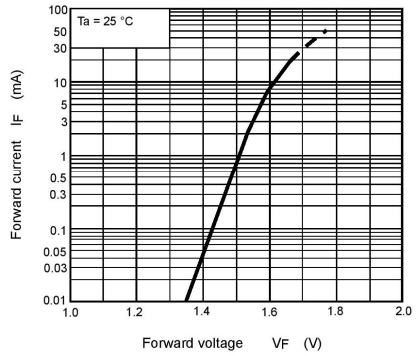

$\Delta V_F / \Delta Ta - I_F$

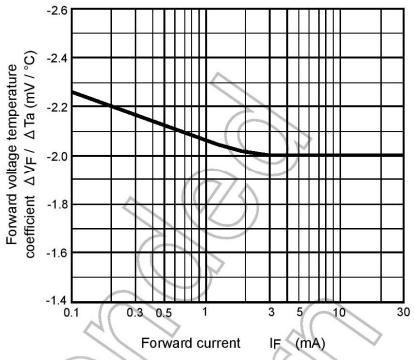

$I_F - Ta$

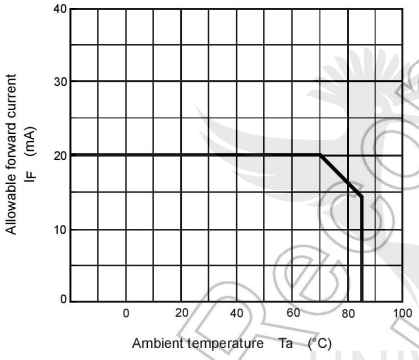

$V_{CC} - Ta$

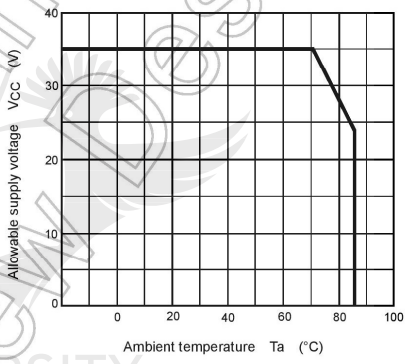

$I_{OPH}, I_{OPL} - Ta$

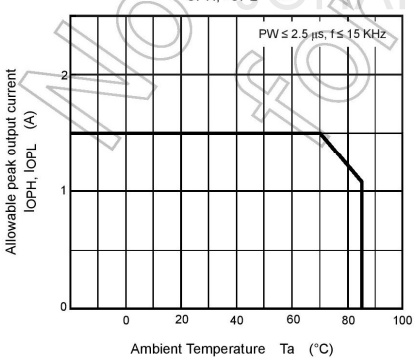

RESTRICTIONS ON PRODUCT USE

- Toshiba Corporation, and its subsidiaries and affiliates (collectively "TOSHIBA"), reserve the right to make changes to the information in this document, and related hardware, software and systems (collectively "Product") without notice.
- This document and any information herein may not be reproduced without prior written permission from TOSHIBA. Even with TOSHIBA's written permission, reproduction is permissible only if reproduction is without alteration/omission.
- Though TOSHIBA works continually to improve Product's quality and reliability, Product can malfunction or fail. Customers are responsible for complying with safety standards and for providing adequate designs and safeguards for their hardware, software and systems which minimize risk and avoid situations in which a malfunction or failure of Product could cause loss of human life, bodily injury or damage to property, including data loss or corruption. Before customers use the Product, create designs including the Product, or incorporate the Product into their own applications, customers must also refer to and comply with (a) the latest versions of all relevant TOSHIBA information, including without limitation, this document, the specifications, the data sheets and application notes for Product and the precautions and conditions set forth in the "TOSHIBA Semiconductor Reliability Handbook" and (b) the instructions for the application with which the Product will be used with or for. Customers are solely responsible for all aspects of their own product design or applications, including but not limited to (a) determining the appropriateness of the use of this Product in such design or applications; (b) evaluating and determining the applicability of any information contained in this document, or in charts, diagrams, programs, algorithms, sample application circuits, or any other referenced documents; and (c) validating all operating parameters for such designs and applications. **TOSHIBA ASSUMES NO LIABILITY FOR CUSTOMERS' PRODUCT DESIGN OR APPLICATIONS.**
- **PRODUCT IS NEITHER INTENDED NOR WARRANTED FOR USE IN EQUIPMENTS OR SYSTEMS THAT REQUIRE EXTRAORDINARILY HIGH LEVELS OF QUALITY AND/OR RELIABILITY, AND/OR A MALFUNCTION OR FAILURE OF WHICH MAY CAUSE LOSS OF HUMAN LIFE, BODILY INJURY, SERIOUS PROPERTY DAMAGE AND/OR SERIOUS PUBLIC IMPACT ("UNINTENDED USE").** Except for specific applications as expressly stated in this document, Unintended Use includes, without limitation, equipment used in nuclear facilities, equipment used in the aerospace industry, medical equipment, equipment used for automobiles, trains, ships and other transportation, traffic signaling equipment, equipment used to control combustions or explosions, safety devices, elevators and escalators, devices related to electric power, and equipment used in finance-related fields. **IF YOU USE PRODUCT FOR UNINTENDED USE, TOSHIBA ASSUMES NO LIABILITY FOR PRODUCT.** For details, please contact your TOSHIBA sales representative.
- Do not disassemble, analyze, reverse-engineer, alter, modify, translate or copy Product, whether in whole or in part.
- Product shall not be used for or incorporated into any products or systems whose manufacture, use, or sale is prohibited under any applicable laws or regulations.
- The information contained herein is presented only as guidance for Product use. No responsibility is assumed by TOSHIBA for any infringement of patents or any other intellectual property rights of third parties that may result from the use of Product. No license to any intellectual property right is granted by this document, whether express or implied, by estoppel or otherwise.
- **ABSENT A WRITTEN SIGNED AGREEMENT, EXCEPT AS PROVIDED IN THE RELEVANT TERMS AND CONDITIONS OF SALE FOR PRODUCT, AND TO THE MAXIMUM EXTENT ALLOWABLE BY LAW, TOSHIBA (1) ASSUMES NO LIABILITY WHATSOEVER, INCLUDING WITHOUT LIMITATION, INDIRECT, CONSEQUENTIAL, SPECIAL, OR INCIDENTAL DAMAGES OR LOSS, INCLUDING WITHOUT LIMITATION, LOSS OF PROFITS, LOSS OF OPPORTUNITIES, BUSINESS INTERRUPTION AND LOSS OF DATA, AND (2) DISCLAIMS ANY AND ALL EXPRESS OR IMPLIED WARRANTIES AND CONDITIONS RELATED TO SALE, USE OF PRODUCT, OR INFORMATION, INCLUDING WARRANTIES OR CONDITIONS OF MERCHANTABILITY, FITNESS FOR A PARTICULAR PURPOSE, ACCURACY OF INFORMATION, OR NONINFRINGEMENT.**
- GaAs (Gallium Arsenide) is used in Product. GaAs is harmful to humans if consumed or absorbed, whether in the form of dust or vapor. Handle with care and do not break, cut, crush, grind, dissolve chemically or otherwise expose GaAs in Product.
- Do not use or otherwise make available Product or related software or technology for any military purposes, including without limitation, for the design, development, use, stockpiling or manufacturing of nuclear, chemical, or biological weapons or missile technology products (mass destruction weapons). Product and related software and technology may be controlled under the applicable export laws and regulations including, without limitation, the Japanese Foreign Exchange and Foreign Trade Law and the U.S. Export Administration Regulations. Export and re-export of Product or related software or technology are strictly prohibited except in compliance with all applicable export laws and regulations.
- Please contact your TOSHIBA sales representative for details as to environmental matters such as the RoHS compatibility of Product. Please use Product in compliance with all applicable laws and regulations that regulate the inclusion or use of controlled substances, including without limitation, the EU RoHS Directive. **TOSHIBA ASSUMES NO LIABILITY FOR DAMAGES OR LOSSES OCCURRING AS A RESULT OF NONCOMPLIANCE WITH APPLICABLE LAWS AND REGULATIONS.**

A.5. INSULATED-GATE BIPOLAR TRANSISTOR (IGBT)

STGW20NC60VD

N-CHANNEL 30A - 600V TO-247
Very Fast PowerMESH™ IGBT

Table 1: General Features

TYPE	V_{CES}	$V_{CE(sat)}$ (Max) @25°C	I_C @100°C
STGW20NC60VD	600 V	< 2.5 V	30 A

- OFF LOSSES INCLUDE TAIL CURRENT
- LOSSES INCLUDE DIODE RECOVERY ENERGY
- HIGH CURRENT CAPABILITY
- HIGH FREQUENCY OPERATION UP TO 50 KHz
- VERY SOFT ULTRA FAST RECOVERY ANTIPARALLEL DIODE
- LOWER C_{RES} /C_{IES} RATIO
- NEW GENERATION PRODUCTS WITH TIGHTER PARAMETER DISTRIBUTION

Figure 1: Package

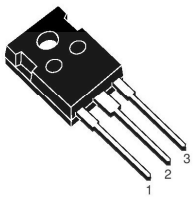

TO-247

Weight: 4.41gr ± 0.01
Max Clip Pressure: 150 N/mm^2

DESCRIPTION

Using the latest high voltage technology based on a patented strip layout, STMicroelectronics has designed an advanced family of IGBTs, the PowerMESH™ IGBTs, with outstanding performances. The suffix "V" identifies a family optimized for high frequency applications.

Figure 2: Internal Schematic Diagram

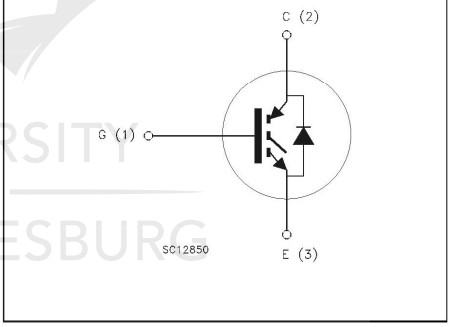

APPLICATIONS

- HIGH FREQUENCY INVERTERS
- SMPS and PFC IN BOTH HARD SWITCH AND RESONANT TOPOLOGIES
- UPS
- MOTOR DRIVERS

Table 2: Order Codes

SALES TYPE	MARKING	PACKAGE	PACKAGING
STGW20NC60VD	GW20NC60VD	TO-247	TUBE

Rev. 4

July 2004 1/11

Table 3: Absolute Maximum ratings

Symbol	Parameter	Value	Symbol
V_{CES}	Collector-Emitter Voltage (V_{GS} = 0)	600	V
V_{ECR}	Reverse Battery Protection	20	V
V_{GE}	Gate-Emitter Voltage	± 20	V
I_C	Collector Current (continuous) at 25°C (#)	60	A
I_C	Collector Current (continuous) at 100°C (#)	30	A
I_{CM} (1)	Collector Current (pulsed)	100	A
I_f	Diode RMS Forward Current at T_C = 25°C	30	A
P_{TOT}	Total Dissipation at T_C = 25°C	200	W
	Derating Factor	1.6	W/°C
T_{stg}	Storage Temperature	– 55 to 150	°C
T_j	Operating Junction Temperature		

(1)Pulse width limited by max. junction temperature.

Table 4: Thermal Data

		Min.	Typ.	Max.	
Rthj-case	Thermal Resistance Junction-case (IGBT)	--	--	0.625	°C/W
Rthj-case	Thermal Resistance Junction-case (Diode)	--	--	1.5	°C/W
Rthj-amb	Thermal Resistance Junction-ambient	--	--	50	°C/W
T_L	Maximum Lead Temperature for Soldering Purpose (1.6 mm from case, for 10 sec.)		300		°C

ELECTRICAL CHARACTERISTICS (T_{CASE} =25°C UNLESS OTHERWISE SPECIFIED)

Table 5: Off

Symbol	Parameter	Test Conditions	Min.	Typ.	Max.	Unit
$V_{BR(CES)}$	Collectro-Emitter Breakdown Voltage	I_C = 1 mA, V_{GE} = 0	600			V
I_{CES}	Collector-Emitter Leakage Current (V_{CE} = 0)	V_{GE} = Max Rating Tc=25°C Tc=125°C			10 1	µA mA
I_{GES}	Gate-Emitter Leakage Current (V_{CE} = 0)	V_{GE} = ± 20 V , V_{CE} = 0			± 100	nA

Table 6: On

Symbol	Parameter	Test Conditions	Min.	Typ.	Max.	Unit
$V_{GE(th)}$	Gate Threshold Voltage	V_{CE}= V_{GE}, I_C= 250 µA	3.75		5.75	V
$V_{CE(SAT)}$	Collector-Emitter Saturation Voltage	V_{GE}= 15 V, I_C= 20A, Tj= 25°C V_{GE}= 15 V, I_C= 20A, Tj= 125°C		1.8 1.7	2.5	V V

(#) Calculated according to the iterative formula:

$$I_C(T_C) = \frac{T_{JMAX} - T_C}{R_{THJ-C} \times V_{CESAT(MAX)}(T_C, I_C)}$$

ELECTRICAL CHARACTERISTICS (CONTINUED)

Table 7: Dynamic

Symbol	Parameter	Test Conditions	Min.	Typ.	Max.	Unit
g_{fs}(1)	Forward Transconductance	V_{CE} = 15 V, I_C= 20 A		15		S
C_{ies} C_{oes} C_{res}	Input Capacitance Output Capacitance Reverse Transfer Capacitance	V_{CE} = 25V, f = 1 MHz, V_{GE} = 0		2200 225 50		pF pF pF
Q_g Q_{ge} Q_{gc}	Total Gate Charge Gate-Emitter Charge Gate-Collector Charge	V_{CE} = 390 V, I_C = 20 A, V_{GE} = 15V, (see Figure 21)		100 16 45	140	nC nC nC
I_{CL}	Turn-Off SOA Minimum Current	V_{clamp} = 480 V , Tj = 150°C R_G = 10 Ω, V_{GE}= 15V	100			A

Table 8: Switching On

Symbol	Parameter	Test Conditions	Min.	Typ.	Max.	Unit
$t_{d(on)}$ t_r $(di/dt)_{on}$ Eon (2)	Turn-on Delay Time Current Rise Time Turn-on Current Slope Turn-on Switching Losses	V_{CC} = 390 V, I_C = 20 A R_G= 3.3Ω, V_{GE}= 15V, Tj= 25°C (see Figure 19)		31 11 1600 220	 300	ns ns A/µs µJ
$t_{d(on)}$ t_r $(di/dt)_{on}$ Eon (2)	Turn-on Delay Time Current Rise Time Turn-on Current Slope Turn-on Switching Losses	V_{CC} = 390 V, I_C = 20 A R_G= 3.3Ω, V_{GE}= 15V, Tj= 125°C (see Figure 19)		31 11.5 1500 450		ns ns A/µs µJ

2) Eon is the turn-on losses when a typical diode is used in the test circuit in figure 2. If the IGBT is offered in a package with a co-pack diode, the co-pack diode is used as external diode. IGBTs & DIODE are at the same temperature (25°C and 125°C)

Table 9: Switching Off

Symbol	Parameter	Test Conditions	Min.	Typ.	Max.	Unit
$t_r(V_{off})$	Off Voltage Rise Time	V_{cc} = 390 V, I_C = 20 A, R_{GE} = 3.3 Ω , V_{GE} = 15 V T_J = 25 °C (see Figure 19)		28		ns
$t_{d(off)}$	Turn-off Delay Time			100		ns
t_f	Current Fall Time			75		ns
E_{off} (3)	Turn-off Switching Loss			330	450	µJ
E_{ts}	Total Switching Loss			550	750	µJ
$t_r(V_{off})$	Off Voltage Rise Time	V_{cc} = 390 V, I_C = 20 A, R_{GE} = 3.3 Ω , V_{GE} = 15 V Tj = 125 °C (see Figure 19)		66		ns
$t_{d(off)}$	Turn-off Delay Time			150		ns
t_f	Current Fall Time			130		ns
E_{off} (3)	Turn-off Switching Loss			770		µJ
E_{ts}	Total Switching Loss			1220		µJ

(3)Turn-off losses include also the tail of the collector current.

Table 10: Collector-Emitter Diode

Symbol	Parameter	Test Conditions	Min.	Typ.	Max.	Unit
V_f	Forward On-Voltage	I_f = 10 A I_f = 10 A, Tj = 125 °C		1.3 1	2.0	V V
t_{rr} t_a Q_{rr} I_{rrm} S	Reverse Recovery Time Reverse Recovery Charge Reverse Recovery Current Softness factor of the diode	I_f = 20 A ,V_R = 40 V, Tj = 25°C, di/dt = 100 A/µs (see Figure 22)		44 32 66 3 0.375		ns ns nC A
t_{rr} t_a Q_{rr} I_{rrm} S	Reverse Recovery Time Reverse Recovery Charge Reverse Recovery Current Softness factor of the diode	I_f = 20 A ,V_R = 40 V, Tj =125°C, di/dt = 100 A/µs (see Figure 22)		88 56 237 5.4 0.57		ns ns nC A

Figure 3: Output Characteristics

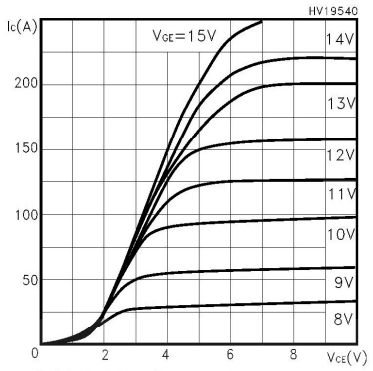

Figure 4: Transconductance

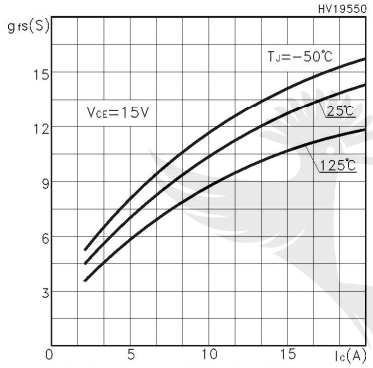

Figure 5: Collector-Emitter On Voltage vs Collector Current

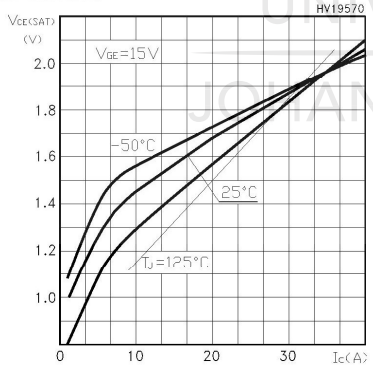

Figure 6: Transfer Characteristics

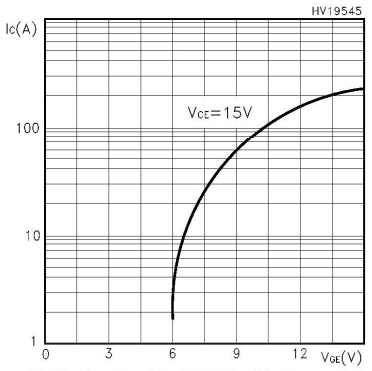

Figure 7: Collector-Emitter On Voltage vs Temperature

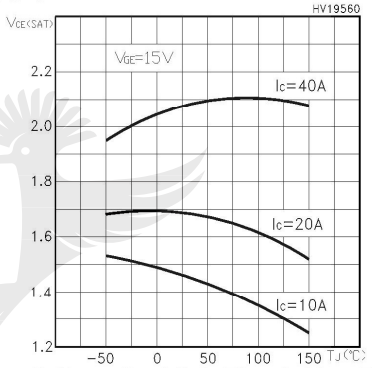

Figure 8: Normalized Gate Threshold vs Temperature

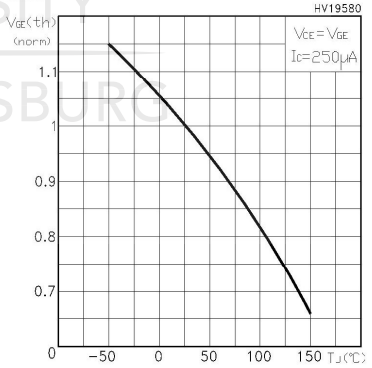

Figure 9: Normalized Breakdown Voltage vs Temperature

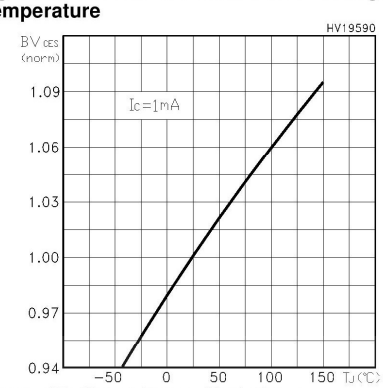

Figure 10: Capacitance Variations

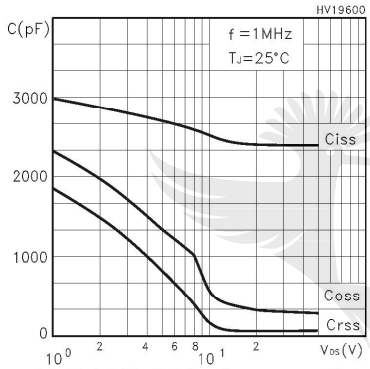

Figure 11: Total Switching Losses vs Gate Resistance

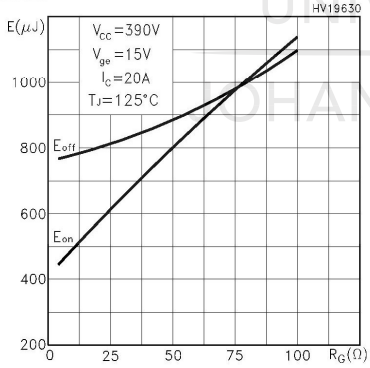

Figure 12: Gate Charge vs Gate-Emitter Voltage

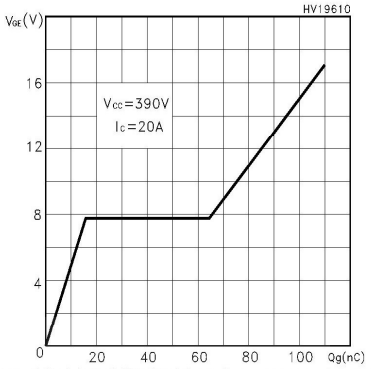

Figure 13: Total Switching Losses vs Temperature

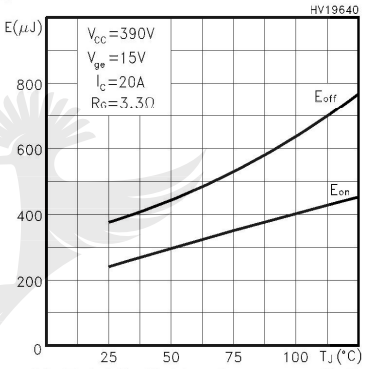

Figure 14: Total Switching Losses vs Collector Current

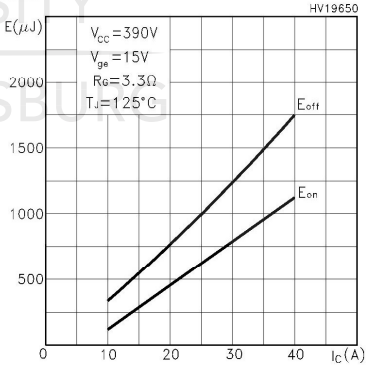

Figure 15: Thermal Impedance

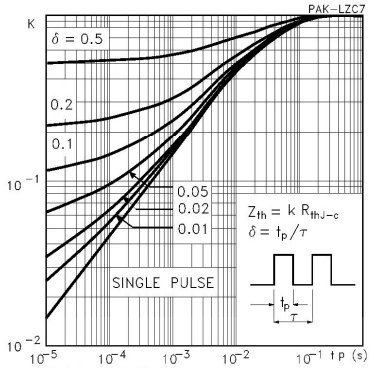

Figure 16: Turn-Off SOA

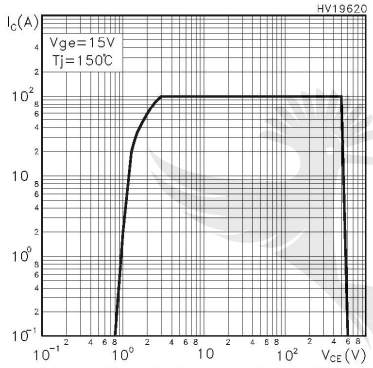

Figure 17: Emitter-Collector Diode Characteristics

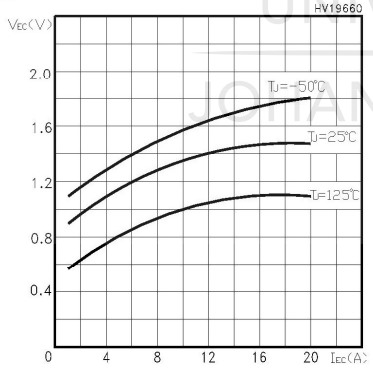

Figure 18: Ic vs Frequency

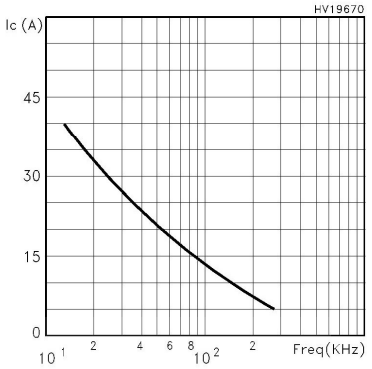

For a fast IGBT suitable for high frequency applications, the typical collector current vs. maximum operating frequency curve is reported. That frequency is defined as follows:

$$f_{MAX} = (P_D - P_C) / (E_{ON} + E_{OFF})$$

1) The maximum power dissipation is limited by maximum junction to case thermal resistance:

$$P_D = \Delta T / R_{THJ\text{-}C}$$

considering $\Delta T = T_J - T_C = 125\ ℃ - 75\ ℃ = 50℃$

2) The conduction losses are:

$$P_C = I_C * V_{CE(SAT)} * \delta$$

with 50% of duty cycle, V_{CESAT} typical value @125℃.

3) Power dissipation during ON & OFF commutations is due to the switching frequency:

$$P_{SW} = (E_{ON} + E_{OFF}) * freq.$$

4) Typical values @ 125℃ for switching losses are used (test conditions: V_{CE} = 390V, V_{GE} = 15V, R_G = 3.3 Ohm). Furthermore, diode recovery energy is included in the E_{ON} (see note 2), while the tail of the collector current is included in the E_{OFF} measurements (see note 3).

Figure 19: Test Circuit for Inductive Load Switching

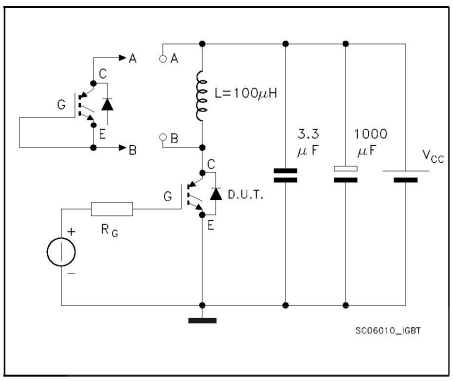

Figure 20: Switching Waveforms

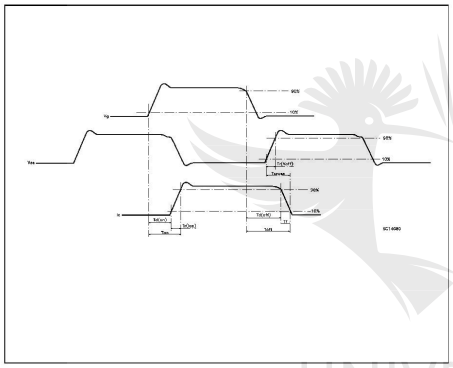

Figure 21: Gate Charge Test Circuit

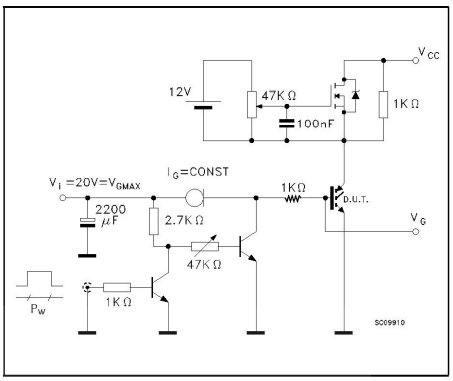

Figure 22: Diode Recovery Times Waveform

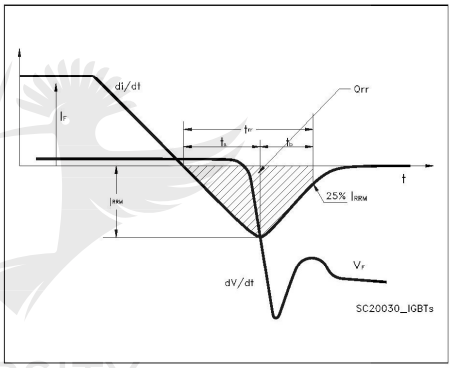

Table 11: Revision History

Date	Revision	Description of Changes
12-July-2004	4	Stylesheet update. Added Max Values see Table 8 and 9 Added Figure 22

TO-247 MECHANICAL DATA

DIM.	mm.			inch		
	MIN.	TYP	MAX.	MIN.	TYP.	MAX.
A	4.85		5.15	0.19		0.20
A1	2.20		2.60	0.086		0.102
b	1.0		1.40	0.039		0.055
b1	2.0		2.40	0.079		0.094
b2	3.0		3.40	0.118		0.134
c	0.40		0.80	0.015		0.03
D	19.85		20.15	0.781		0.793
E	15.45		15.75	0.608		0.620
e		5.45			0.214	
L	14.20		14.80	0.560		0.582
L1	3.70		4.30	0.14		0.17
L2		18.50			0.728	
øP	3.55		3.65	0.140		0.143
øR	4.50		5.50	0.177		0.216
S		5.50			0.216